AD-A035 147 MICHIGAN STATE UNIV EAST LANSING DIV OF ENGINEERING --ETC F/G 20/11
MEASUREMENT OF RESIDUAL STRAINS AROUND COLDWORKED FASTENER HOLE--ETC(U)
APR 76 W N SHARPE AF-AFOSR-2817-75

UNCLASSIFIED AFOSR-TR-77-0020 NL

1 OF 1
AD-A
035 147

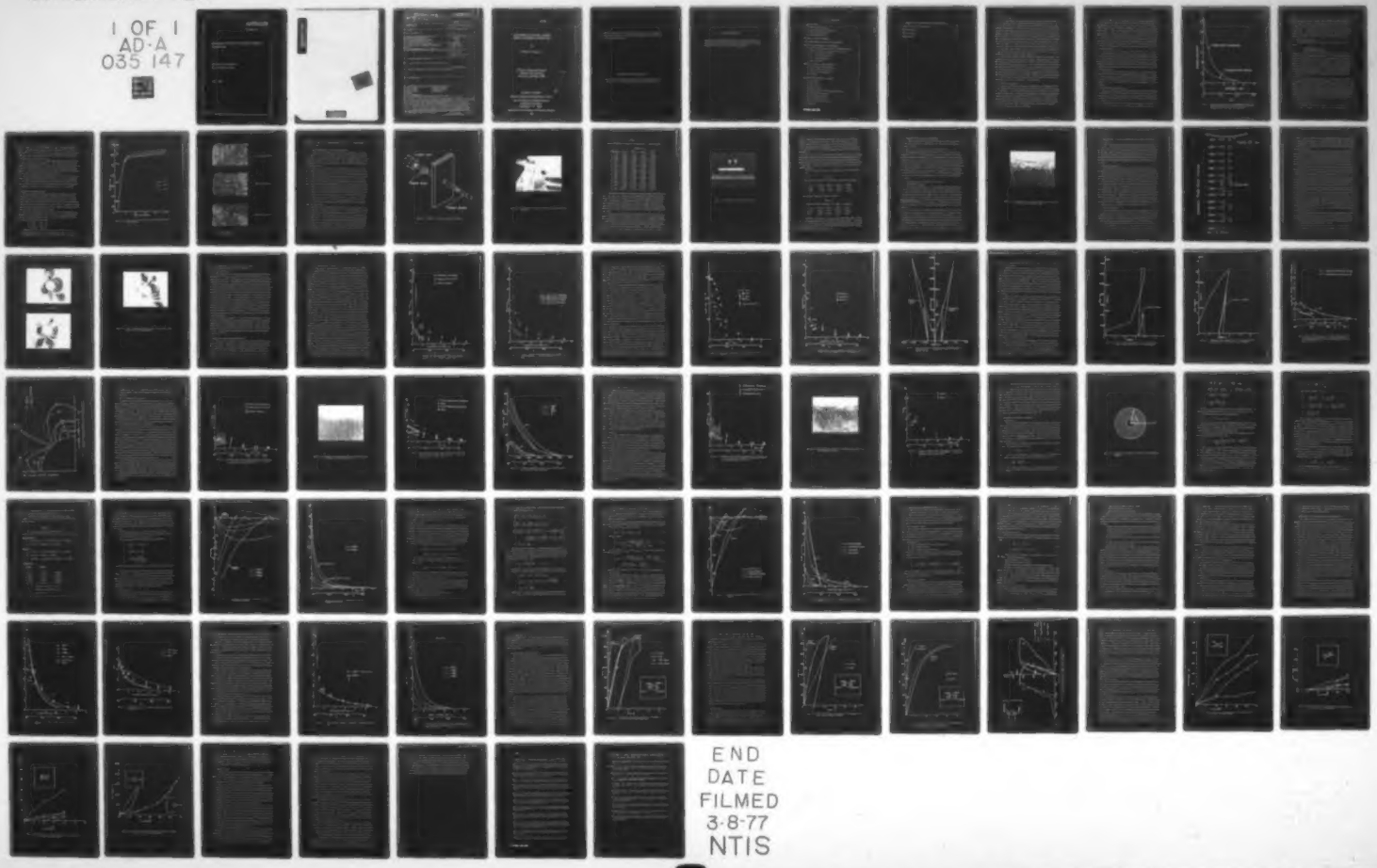

END
DATE
FILMED
3-8-77
NTIS

MEASUREMENT OF RESIDUAL STRAINS AROUND COLDWORKED FASTENER HOLES

MICHIGAN STATE UNIVERSITY
EAST LANSING, MICHIGAN

APRIL 1976

UNCLASSIFIED

SECURITY CLASSIFICATION OF THIS PAGE (When Date Entered)

REPORT DOCUMENTATION PAGE		READ INSTRUCTIONS BEFORE COMPLETING FORM
1. REPORT NUMBER AFOSR - TR - 77 - 0020	2. GOVT ACCESSION NO.	3. RECIPIENT'S CATALOG NUMBER -
4. TITLE (and Subtitle) MEASUREMENT OF RESIDUAL STRAINS AROUND COLDWORKED FASTENER HOLES		5. TYPE OF REPORT & PERIOD COVERED INTERIM March 1975 - March 1976 6. PERFORMING ORG. REPORT NUMBER
7. AUTHOR(s) WILLIAM N SHARPE, JR		8. CONTRACT OR GRANT NUMBER(s) AFOSR 75-2817
9. PERFORMING ORGANIZATION NAME AND ADDRESS MICHIGAN STATE UNIVERSITY DIVISION OF ENGINEERING RESEARCH EAST LANSING, MICHIGAN 48824		10. PROGRAM ELEMENT, PROJECT, TASK AREA & WORK UNIT NUMBERS 681307 9782-05 61102F
11. CONTROLLING OFFICE NAME AND ADDRESS AIR FORCE OFFICE OF SCIENTIFIC RESEARCH/NA BLDG 410 BOLLING AIR FORCE BASE, D C 20332		12. REPORT DATE April 1976 13. NUMBER OF PAGES 86
14. MONITORING AGENCY NAME & ADDRESS(if different from Controlling Office)		15. SECURITY CLASS. (of this report) UNCLASSIFIED 15a. DECLASSIFICATION/ DOWNGRADING SCHEDULE

16. DISTRIBUTION STATEMENT (of this Report)

Approved for public release; distribution unlimited.

17. DISTRIBUTION STATEMENT (of the abstract entered in Block 20, if different from Report)

18. SUPPLEMENTARY NOTES

19. KEY WORDS (Continue on reverse side if necessary and identify by block number)

COLDWORKED HOLES	STRAIN MEASUREMENT
RESIDUAL STRESS	PLASTICITY THEORY
RESIDUAL STRAIN	FATIGUE LIFE
FASTENERS	
PLASTIC DEFORMATION	

20. ABSTRACT (Continue on reverse side if necessary and identify by block number)

Coldworking a fastener hole by pulling an oversize mandrel through it can improve its fatigue life because of the residual stresses generated around the hole. This report describes an experimental study of the residual strains around the hole and compares the results with existing theories. An industrial coldworking process is studied, and strains are determined close to the hole by measuring the distance between fiducial marks with an X-Y microscope and by the moire method. The strains near the hole are large (on the order of 5-10 percent) and inhomogeneous. None of the theories predict the strains well, though better agreement is obtained for thinner test specimens at positions away from the hole edge.

DD FORM 1 JAN 73 1473 EDITION OF 1 NOV 65 IS OBSOLETE

UNCLASSIFIED

SECURITY CLASSIFICATION OF THIS PAGE (When Date Entered)

AFOSR-

MEASUREMENT OF RESIDUAL STRAINS AROUND COLDWORKED FASTENER HOLES

by

William N. Sharpe, Jr.

Division of Engineering Research
Michigan State University
East Lansing, Michigan 48824

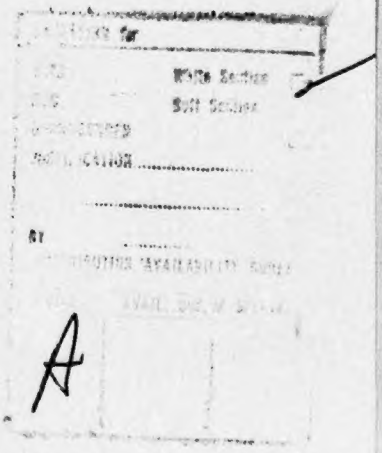

SCIENTIFIC REPORT

Research Sponsored by AFOSR Grant 75-2817

Air Force Office of Scientific Research
Bolling Air Force Base
Washington, D. C. 20332

ia

Qualified requestors may obtain additional copies from the Defense Documentation Center. All others should apply to the National Technical Information Service.

ACKNOWLEDGMENT

The author would like to acknowledge the very capable assistance of the students who worked on this project: David Hafelin, Nopporn Chandawanich, Saravut Poolsuk, and Susan Emery.

TABLE OF CONTENTS

1. INTRODUCTION

The operational lives of many Air Force systems have been limited by flaws which initiate at fastener holes and propagate to failure. One means of improving the fatigue life of the structure is to inhibit the growth of flaws emanating from the holes by prestressing the metal around the hole either by coldworking with an oversized mandrel or using interference-fit fasteners. Successful design improvement of fasteners or processing techniques requires an understanding of the residual stress state around the hole and the change in this stress state with static or fatigue loading. Grandt [1] has shown that, given this stress state, the stress intensity factor can be readily calculated for radial cracks. Once this factor is known, the influence of the flaw can be evaluated and the maximum allowable crack size for a material can be prescribed. The Air Force's damage tolerant design procedure [2] requires the consideration of cracks at fasteners, as well as the traditional static and fatigue design requirements.

Basic understanding of the complicated nonlinear stress state around prestressed holes subjected to various loading configurations will come from theoretical and experimental studies of representative problems. Analytical and finite-element techniques have been used to predict the residual stresses and strains around a prestressed hole, but validation of these theories with experimental results has been extremely limited. In many cases, e.g., a pin-loaded prestressed hole, it is almost impossible to model the structure properly because of the complex boundary conditions. Experimental studies are clearly needed, but the measurement of large strains and sharp strain gradients near a hole or fastener is a difficult task.

1.1. Theoretical Solutions

Several theoretical solutions to the problem of an expanding hole in a thin sheet of material exist; these are discussed in more detail in section 6 of this report. All of these theories assume that the hole is radially loaded (prescribing either pressure or displacement at the hole) so that the material near the hole is loaded above its yield stress. All of the theories assume that a state of plane stress exists everywhere in the sheet, and most of them assume that the sheet is infinite in extent. After the loading is removed at the hole edge, most theories assume that the material unloads elastically with no reverse yielding.

The theories may be classified according to their kind of solution. Analytical solutions in which expressions for the stresses and strains are given in closed form exist; this kind of solution is desirable because of its ease of application. Some numerical solutions in which the differential equation, along with its boundary conditions, is solved via a computer are also available. These numerical solutions present their results in dimensionless form, so they are also easy to use. One finite-element solution which employs an elastic-plastic finite-element computer code also exists [3]; that Air Force-sponsored research has motivated the present study. Equally as important as the form of the solution is the assumption about the material behavior in the plastic region. The constitutive behavior assumed ranges from perfectly plastic to elastic-perfectly-plastic to a two parameter power law.

A fair amount of work has been done on this residual stress problem in the past few years, and at this point almost all the power of the modern deformation theory of plasticity has been brought to bear on the problem. Any theoretical solution that gives the residual stress and strain distribution also gives the location of the elastic-plastic boundary. In this report the residual strain distributions are measured; in the future, measurement of the elastic-plastic boundary location may be used to initially evaluate the theories.

To give an idea of the measurement problem, residual strains predicted by the earliest theory (Nadai [4]) are plotted in Figure 1.1. Discussion of the theories in section 6 and comparison with the measurements in section 5 will show that this earliest theory is by no means the worst; in fact, Figure 1.1 is a reasonably good quantitative description of the residual strains.

1.2. Residual Strain Measurements

The only existing experimental stress analysis devoted specifically to this problem, i.e., coldworked holes, is that of Adler and Dupree [3]. Several other investigations in which the strain near interference-fit fasteners was measured have been performed; these will be discussed later in section 4.

Adler and Dupree [3] used the moiré technique to measure the strains around the hole both after it had been coldworked and as it was

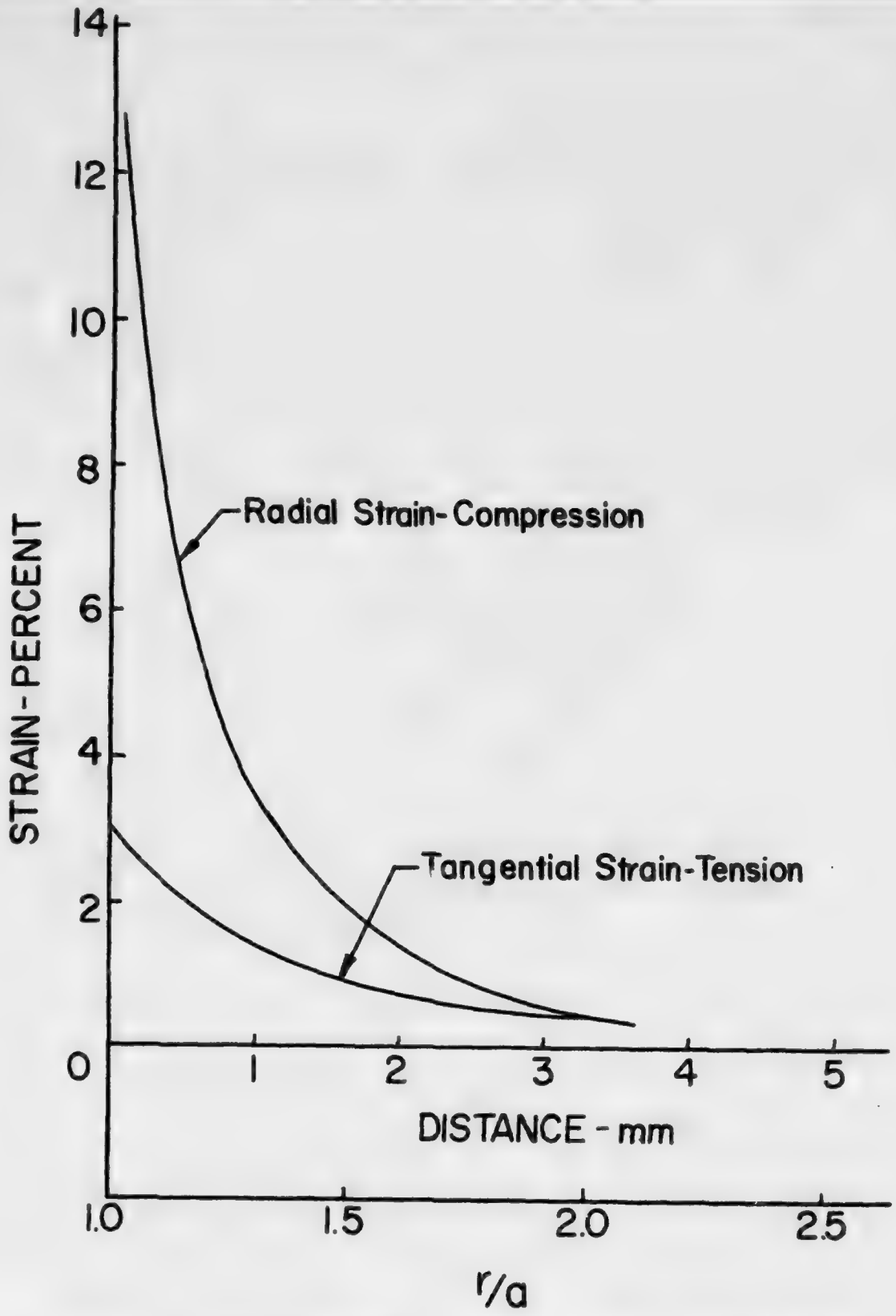

Figure 1.1 Predicted residual radial and tangential strain from Nadai's theory (4) for a 0.012 inch (0.030 mm) diametral expansion of a 0.260 inch (6.60 mm) hole.

subjected to a remote tensile load. However, when their specimens were prepared, the holes were chamfered according to standard machine shop practice. This greatly affected the strain field on the specimen surface and made comparison with the finite element solution inconclusive.

Figure 1.1 illustrates the difficulty to be expected in making strain measurements. The plastic strains are quite large, and they vary drastically over very short distances near the hole edge. Measurement of this kind of strain field is a nontrivial experimental mechanics problem.

1.3. Coldworking Procedure

The coldworking procedure studied in this report is the one developed by

J. O. King, Inc
711 Trabert Avenue, N. W.
Atlanta, Georgia 30318

in which a thin-walled sleeve is first inserted into the hole and then a tapered mandrel is pulled through the sleeve. After the mandrel has been removed, the sleeve may or may not be removed before the fastener is inserted, but usually the sleeve is left in the hole. The specific amount of expansion used in this study, 0.012 inch (0.30 mm) diametral expansion of a 0.260 inch (6.60 mm) hole, was chosen because it matched the finite-element solution of Adler-Dupree [3]. They chose it originally because it is typical of coldworking applications. The sleeve was removed for these experiments because none of the modern theories account for the presence of a sleeve.

It may be argued that if one wishes to evaluate theories of plastic radial expansion, one should match the boundary conditions as closely as possible. The approach in this report is to examine (by comparison of experiment and theory) the capability of the theories to model this one practical coldworking process. An experimental study in which one carefully generated a radial loading would be quite useful in deciding what simplifying assumptions (as to material behavior, for example) are permissible. However, the industrial process would still have to be studied to determine the theory's applicability.

1.4. Overview of Report

The material used in this research is aluminum 7075-T6; its properties are given in section 2. Care must be taken in preparing the original

hole to exact dimensions and coldworking it in a manner that is similar to the industrial process and yet controlled enough to permit reproducible tests. The procedures for preparing and coldworking the specimens are given in section 3. The difficulty of strain measurement has already been mentioned; various possible techniques are examined and those used in this report are described in section 4.

The results of a series of coldworking experiments for three specimen thicknesses are given in section 5. The existing theories are discussed at some length in section 6, and their predicted residual stress and strain distributions are plotted for the particular coldworking expansion. Section 7 is a comparison of the theories with the experimental results and as such contains the primary information of this work.

Adler and Dupree [3] studied the behavior of a test specimen under remote loading using their finite-element method. In this investigation, strains were measured with foil gages as specimens were loaded; these results are given in section 8. Some preliminary results of fatigue tests are presented in section 9, and closing comments are in section 10.

2. MATERIAL SPECIFICATIONS

The material used for these studies was aluminum type 7075-T6. Material for the 3/4 inch (6.4 mm) thick specimens was taken from the same plate of material as used in the Adler-Dupree [3] work. Material was purchased for the 1/8 inch (3.2 mm) and 1/16 inch (1.6 mm) specimens. To verify that the various thicknesses of material had essentially the same mechanical properties, stress-strain curves, hardness readings, and photographs of the microstructure were obtained.

Figure 2.1 presents the stress-strain curves and shows that there is little difference among them. These curves are only slightly different from the one obtained by Adler-Dupree. Rockwell B hardness measurements for the three thicknesses were:

1/4 inch -- $R_B = 92$
1/8 inch -- $R_B = 93$
1/16 inch -- $R_B = 92$.

Photographs of the microstructure are presented in Figure 2.2, and it is seen that the microstructure is essentially the same.

From these measurements, it is concluded that there is insignificant

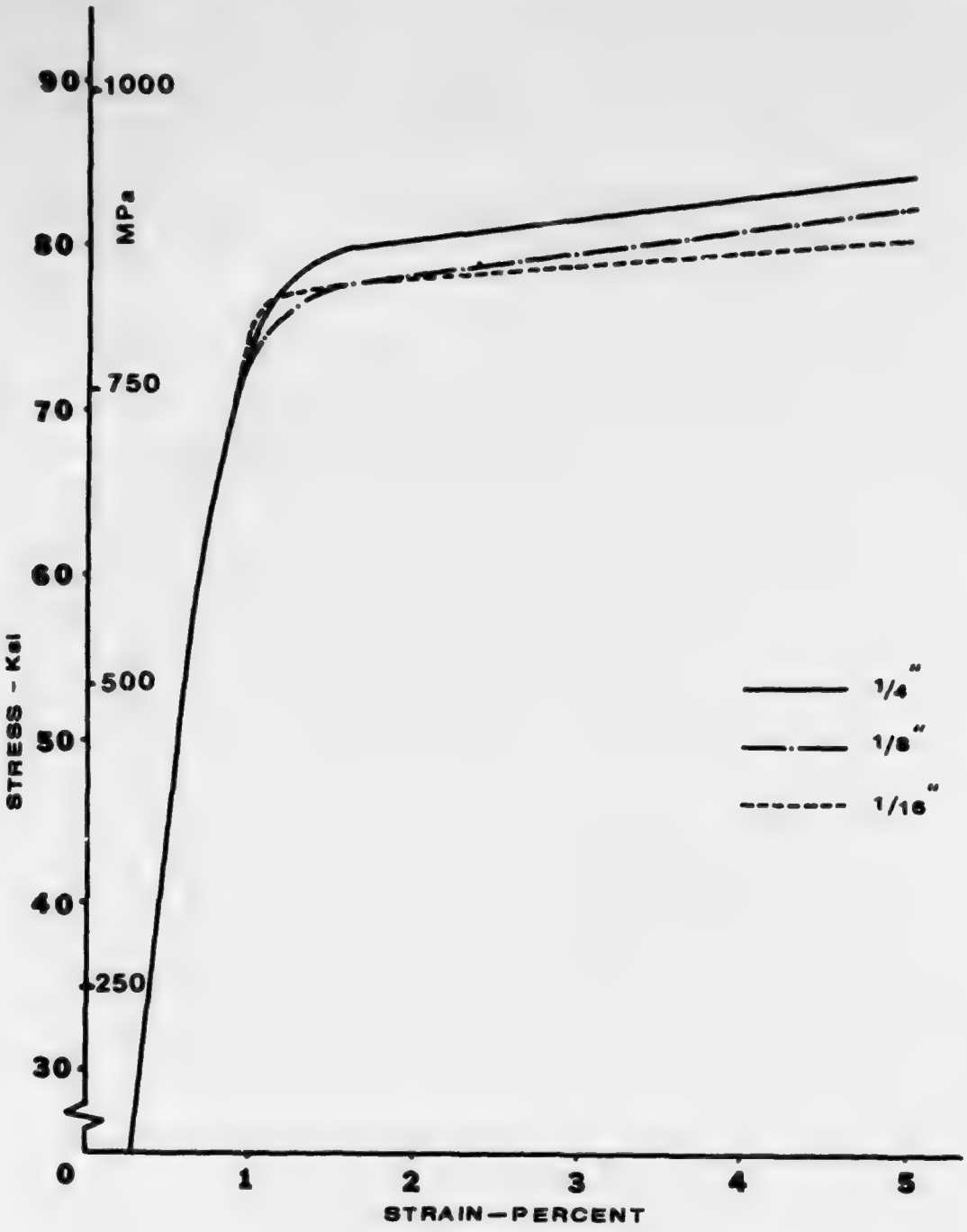

Figure 2.1 Stress-strain curves for the three different sheets of 7075-T6 aluminum.

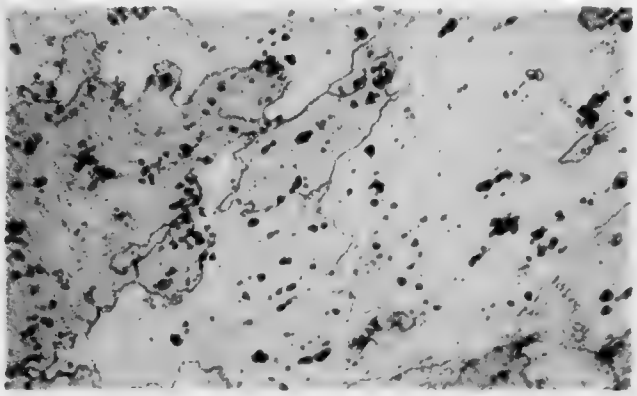

1/4 inch (6.4 mm) thick

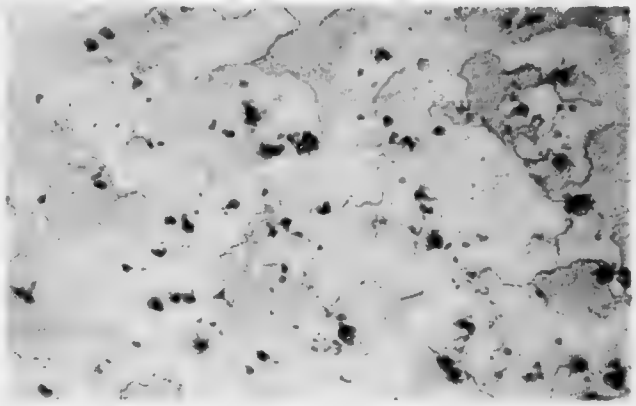

1/8 inch (3.2 mm) thick

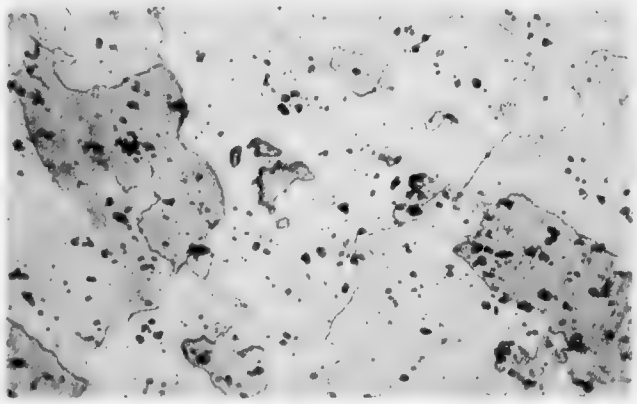

1/16 inch (1.6 mm) thick

Figure 2.2 Photomicrographs of the three different sheets of 7075-T6 aluminum (100 X).

variation in the mechanical properties of the three different sheets of specimen material.

3. HOLE PREPARATION AND COLDWORKING

It is necessary to generate round, nontapered holes to a specific dimension so that one can accurately measure the amount of coldworking deformation. A certain tolerance on the holes is required if one is to compare coldworking of various specimens. The variability in hole size and coldworking process that would be present in an industrial atmosphere cannot be permitted here.

Holes were prepared by first drilling them with a 0.25 inch (6.4 mm) drill and then using a honing machine to bring the diameter up to the nominal 0.260 ± 0.001 inch (6.60 ± .03 mm). The honing machine produced straight sides in the hole (no evidence of spiraling) and square edges of the hole. The size was determined with a plug gage with a "go" cylinder of 0.2598 inch (6.599 mm) and a "no-go" cylinder of 0.2602 inch (6.609 mm). Upon receipt from the machine shop, the holes in the specimens were measured with a microscope equipped with an x-y stage. The greatest uncertainty in this measurement is in locating the edges of the holes accurately. Measurements were made along diameters at 45° intervals, and each measurement was repeated at least three times. The variation in repeated measurements was usually less than 0.0001 inch (3 microns). Typical diameters measured for a set of six rectangular specimens are given in Table 3.1. These measurements show that the holes are of acceptable roundness and diameter.

The holes were coldworked by pulling a mandrel through them, as illustrated by the schematic in Figure 3.1. The tapered mandrel is inserted into the sleeve, and the mandrel and sleeve inserted into the hole. The washer of the sleeve is pressed against an anvil, and the mandrel pulled through the sleeve. This is the same as the industrial process specified by J. O. King, Inc. A machine incorporating a hand-operated hydraulic cylinder was constructed to pull the mandrel in the laboratory; a photograph of it is given in Figure 3.2. The tension rod linking the mandrel to the cylinder piston had been instrumented with strain gages to permit calibration of the force in terms of the pressure. The peak force was 1200-1600 pounds (5340-7120N).

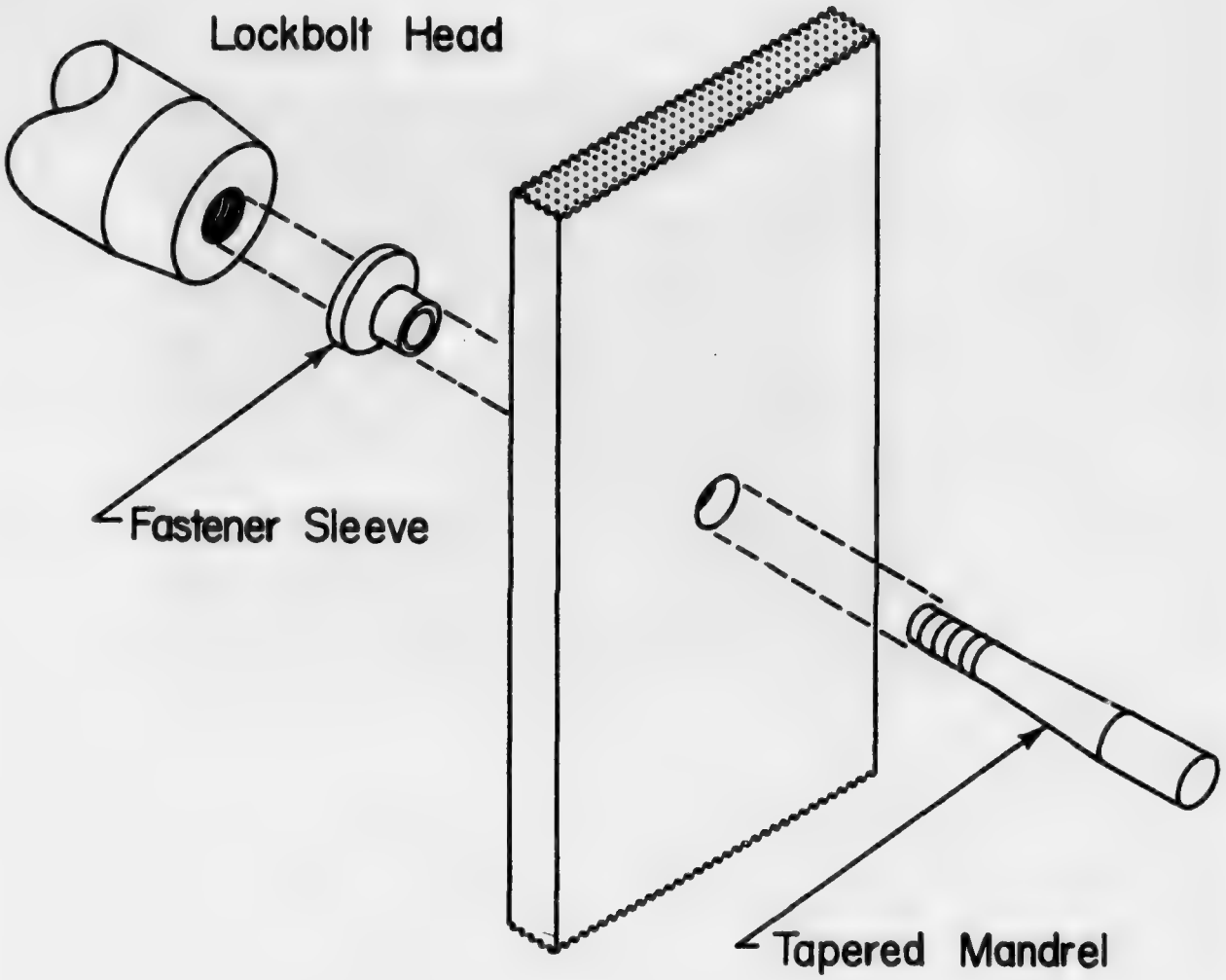

Figure 3.1 Schematic of the King coldworking process.

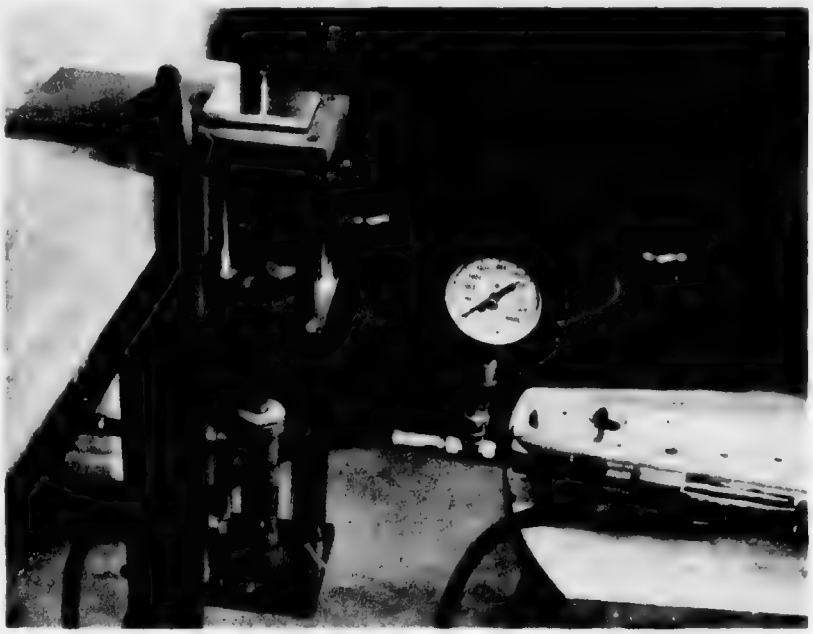

Figure 3.2 Photograph of the device for pulling the mandrel through the hole.

Table 3.1

Diameters of Holes (in inches) for Typical Set of ¼ inch Specimens

Specimen		Orientation 45°	90°	135°	180°
A	Front	0.2603	0.2600	0.2601	0.2605
	Back	0.2606	0.2605	0.2608	0.2606
B	Front	0.2603	0.2603	0.2606	0.2604
	Back	0.2601	0.2601	0.2602	0.2601
C	Front	0.2601	0.2601	0.2598	0.2600
	Back	0.2601	0.2599	0.2597	0.2596
D	Front	0.2601	0.2600	0.2599	0.2599
	Back	0.2600	0.2598	0.2600	0.2600
E	Front	0.2602	0.2602	0.2601	0.2602
	Back	0.2594	0.2598	0.2613	0.2607
F	Front	0.2598	0.2595	0.2595	0.2593
	Back	0.2601	0.2594	0.2594	0.2593

The sleeves inserted in the hole were part number JK5535C08N04L from J. O. King, Inc. These were supplied with the mild steel washer attached (see Figure 3.3), and a dry film lubricant applied to the inside and outside. The function of the mild steel washer is simply to protect the sleeve and specimen as the mandrel is pulled through; it pops off after coldworking. Several sleeves were sectioned, and the average wall thickness was found to be 0.0075 inches (0.19mm) in agreement with Adler and Dupree [3].

The 0.257 inch (6.53mm) mandrel used was J. O. King, Inc., part number JK 6540-08-257, illustrated in Figure 3.3. Note that the length of the final diameter is only 0.125 inch (3.2mm); it is not possible to uniformly expand a hole in a 0.25 inch (6.4mm) thick plate. According to the J. O. King, Inc., literature, the 0.257 inch (6.53mm) diameter mandrel will give a radial expansion of 0.007 inches (0.18mm) to a 0.260 inch (6.60mm) hole, but this is based on a sleeve thickness of 0.0085 inches (.22mm). A maximum

Figure 3.3 Photograph of the mandrel and sleeve.

radial expansion of 0.006 inches (0.15 mm) would be achieved with the 0.0075 inch (0.19 mm) thick sleeves. The radial expansion of the hole with the mandrel and sleeve inserted cannot be measured directly; it must be computed from the dimensions of the hole, mandrel, and sleeve. It is estimated that this computed expansion is accurate to ± 0.0005 inch (0.01 mm).

The 0.257 inch (6.53 mm) diameter mandrel is the largest available for nominal 1/4 inch holes, so the sleeve is very tightly wedged into the hole. To remove the sleeve, the washer end of it was surrounded by a larger washer for the anvil to react against and the mandrel pulled through a second time. The force required to pull the sleeve out was about 600 pounds (2670N).

After removal of the sleeve, the dimensions of the hole in Specimen A are:

Table 3.2

Hole Dimensions (in inches) of Specimen A After Sleeve Removal

	0°	45°	90°	135°
Front	0.2722	0.2711	0.2718	0.2710
Back	0.2710	0.2710	0.2709	0.2707

This gives radial expansions listed in Table 3.3.

Table 3.3

Residual Diametral Expansion (in inches) of Specimen A

	0°	45°	90°	135°
Front	0.0112	0.0106	0.0114	0.0102
Back	0.0100	0.0102	0.0099	0.0095

The hole is not uniform through the plate thickness after coldworking; it is slightly smaller on the back side where the washer is attached to the sleeve. The nature of the coldworking operation is to exert a force perpendicular to the specimen surface through the sleeve and thus constrain deformation of the hole on the back side.

4. STRAIN MEASUREMENT TECHNIQUES

In this section the various tools available to the experimentalist are examined and the most appropriate ones selected for measurement of the plastic strains.

4.1. Nature of Deformation around a Coldworked Hole

Some preliminary experiments were run to verify that the coldworking procedure was working properly and to get an idea of the state of deformation around a coldworked hole. Photographs of the deformed area around the holes in a 1/4 inch thick (6.4mm) specimen are given in Figure 4.1. The most notable feature is the large amount of deformation near the hole edge. Furthermore, the deformation is so great that individual grains have rotated; slip lines are easily visible in Figure 4.1. The material in the neighborhood of the hole edge cannot be considered as a homogeneous, isotropic continuum on a local scale. The large deformation, inhomogeneity of strains, and the sharp gradient make strain measurements difficult near the hole.

4.2. Techniques Used in This Research Program

4.2.1. Indentation technique

It was quickly discovered, after examining coldworked specimens such as the one shown in Figure 4.1, that a way of measuring the strain over a short gage length close to the whole was to measure the before-and-after distance between small fiducial marks. A Vicker's hardness tester was used for this kind of measurement, which will be referred to as the indentation technique. The hardness tester consists of a 100X and 400X microscope mounted above an X-Y stage. Included with the microscope head is a mechanism for making pyramidal indentations with a diamond indenter.

The procedure was to apply two indentations (each about 10 microns on a side) a nominal distance of 200 microns apart. This initial distance was measured, and then it was remeasured after coldworking. The strain was computed as the difference between the two distances divided by the initial distance. The diamond indenter makes sharp fiducial marks, and the distance between indentations can be measured to 0.1 microns (uncertainty of 0.05 microns). The uncertainty in comparing the before-and-after measurements is thus 0.2 microns, so the uncertainty of the measurement

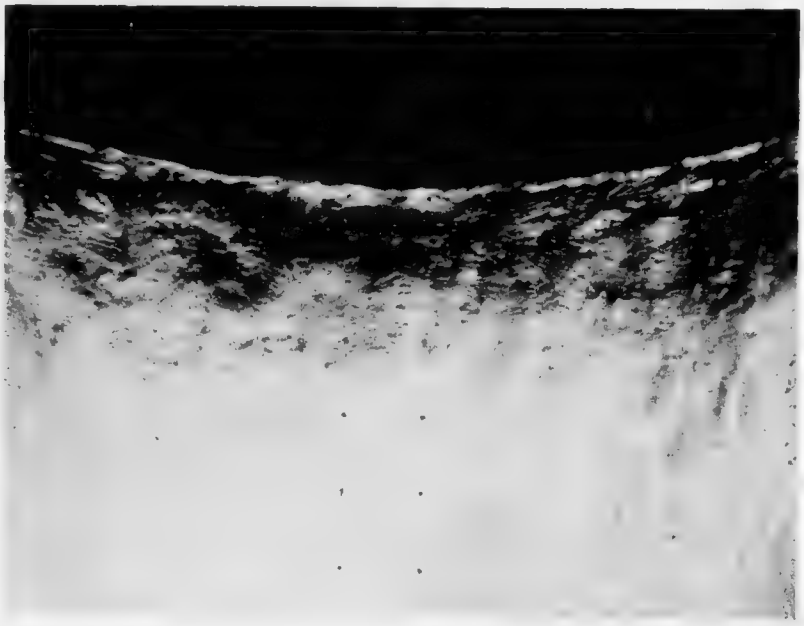

Figure 4.1 Photographs of the deformed region around the hole in a 1/4 inch (6.4 mm) specimen (100 X).

is 0.1 percent strain. This is acceptable for the larger strains of 2 percent or more.

A pattern of indentations was applied according to the scheme shown in Figure 4.2. This gives both radial and tangential strains along a radial line from the hole. The closest tangetial strain measurement is 0.05 mm from the hole and the closest radial strain is 0.15 mm. A set of indentations can be seen upon close examination of Figure 4.1. Although this is a tedious and time-consuming technique, it has proved quite useful; the bulk of the measurements in this report were made with the indentation technique.

4.2.2. Foil strain gages

The difficulty with foil gages for measurements near the hole is simply their size. Post-yield foil gages for large strain and contact adhesive give accurate readings of the plastic strain. Foil gages with gage lengths of 0.015 inch (0.38 mm) are available in the post-yield alloy. But it is difficult to attach the gages with their centerlines closer than 0.5 mm from the edge of the hole. There is some error associated with the gage length, but the variation of strain is smooth enough that it is not too severe.

Apart from their size limitations, foil gages are excellent strain measuring devices. Other researchers [5, 6, 7] have used foil gages to measure the strain near interference-fit fasteners and have been satisfied with the measurements. However, one report [7] questions the accuracy of data obtained near a fastener with short gage-length strain gages. Except for some cases where a gage was obviously damaged, no similar problems were encountered in this work. All gages were purchased from Micro-Measurements, Inc., and their M-Bond 200 adhesive was used.

4.2.3. Moiré techniques

The moiré method is an excellent one for obtaining full-field strain measurements. It was used successfully on this coldworked hole problem by Adler and Dupree. The fine work of Professor Liu and others (see for example reference 8) demonstrates that the moiré method can be used to measure large strains with sharp gradients on metal specimens.

Full field strain measurements were made on several specimens by the moiré technique, but the bulk of the data presented in section 5 was obtained by the indentation technique. Reduction of the moiré data is fairly

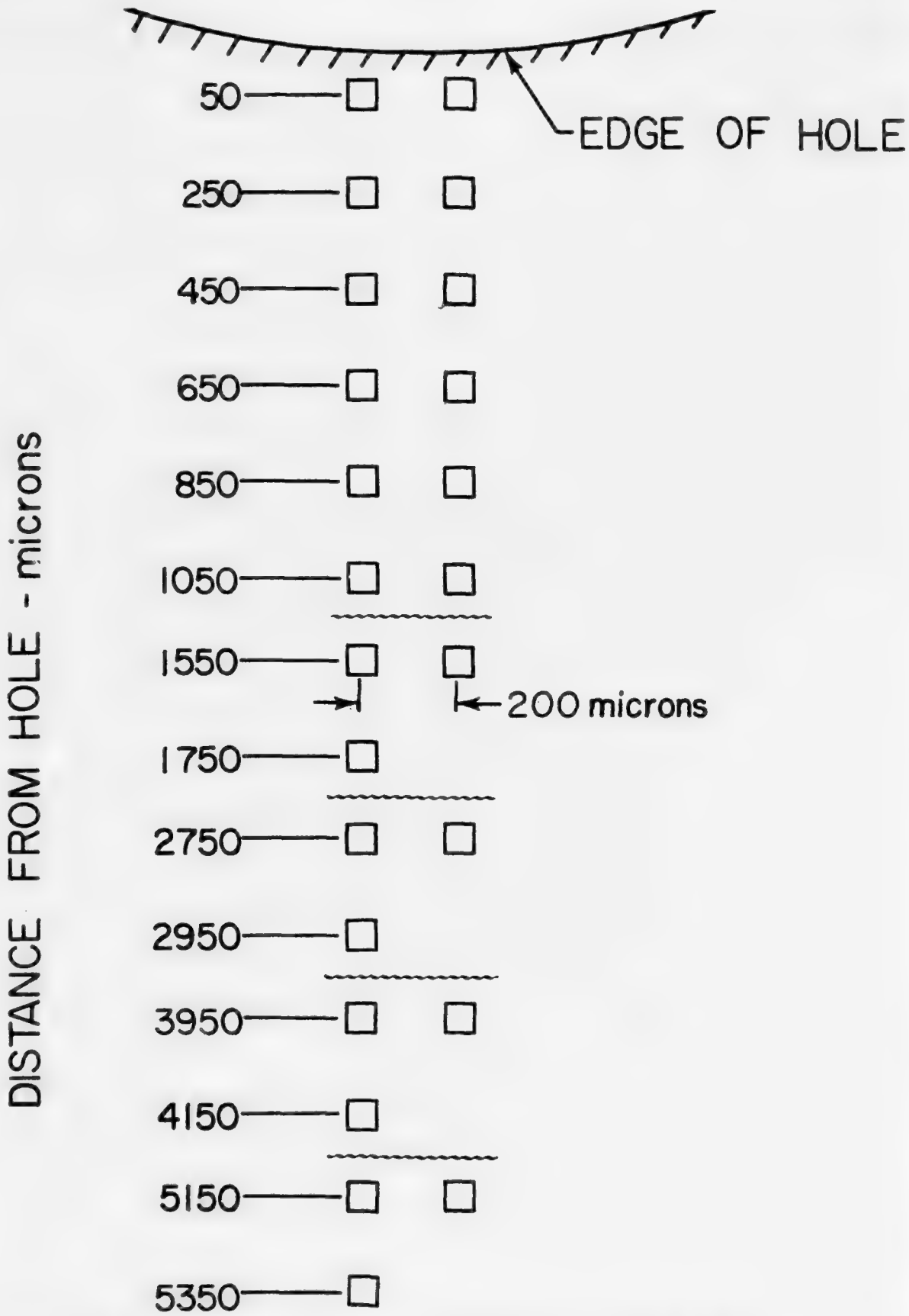

Figure 4.2 Layout of the indentation locations for radial and tangential strain measurements.

laborious. It turns out that if one counts the total time for specimen preparation and data reduction, one can probably obtain radial and tangential strains along four radial lines as quickly by the indentation procedure. The moiré technique is amenable to automation if sufficiently good fringe patterns can be obtained.

The moiré strain measurements were made with a 1000 line per inch (40 lines per mm) grille which permits strain measurement in one direction only. A master grille was purchased from Photolastic, Inc., and submasters were printed on Kodak HRP film plates by placing the master in contact with the plate and exposing it to a 200 watt mercury arc lamp filtered by a Kodak No. 74 filter for 25 seconds. The surface of the 2.5 inch (6.4mm) by 3 inch (7.6mm) specimen with a hole in the center was polished with 0.3 micron alumina and then coated by spraying AZ 1350B photoresist onto the surface with an airbrush. A submaster was placed in contact with the specimen and exposed with the mercury arc lamp.

The double-exposure moiré technique was used. First the specimen was mounted in a holder on an optical bench and a photograph taken with a high resolution camera at 1:1 magnification on Kodak HRP film. The specimen was removed, mandrelized, replaced in its holder, and photographed again. This generates the moiré fringes, as shown in Figure 4.3a. This is not sensitive enough for accurate strain measurement, but the sensitivity can be improved by Fourier processing. Photos of the second and fourth orders are given in Figures 4.3b and c. The fourth order has four times as many fringes. Data was reduced by measuring the location of the fringes, plotting the displacement curves, and then graphically differentiating. The photographs in Figure 4.3 show some asymmetry around the hole, but when strain is computed, the strain curves are nearly symmetric. The results of a whole-field moiré measurement are presented in section 5.

After the technique was developed, it was impossible to make strain measurements closer than 0.3mm to the hole edge with any confidence. Adler and Dupree [3] show measurements as close as 0.2mm on one figure, but no closer than 0.4mm on another. It is difficult to get measurements very close to the hole with the moiré technique.

Several attempts were made to use commercially available strippable moiré grids which can be glued to the specimen. It was impossible to

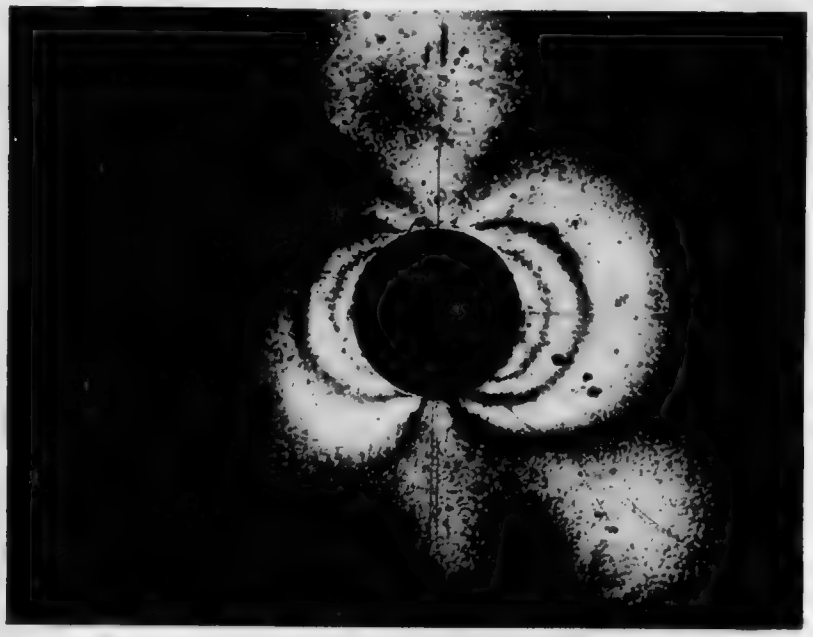

(a) First Order

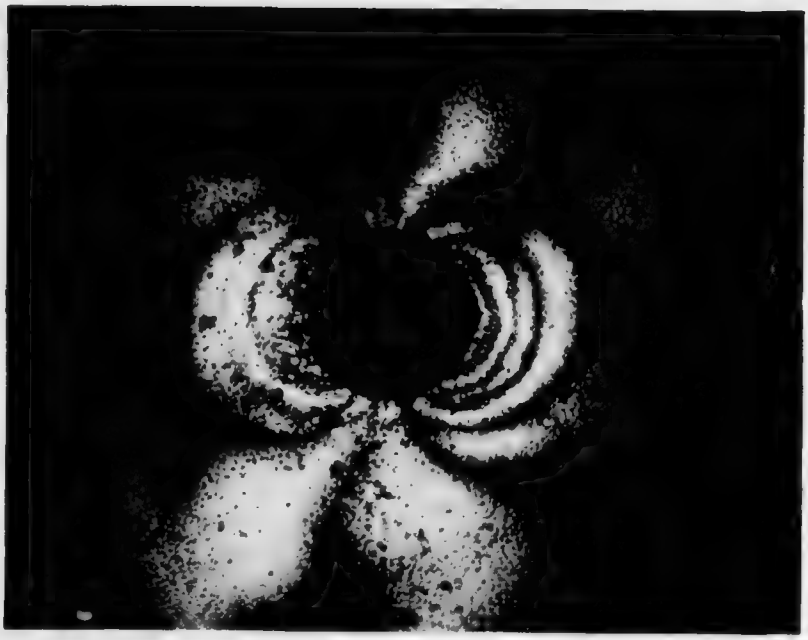

(b) Second Order

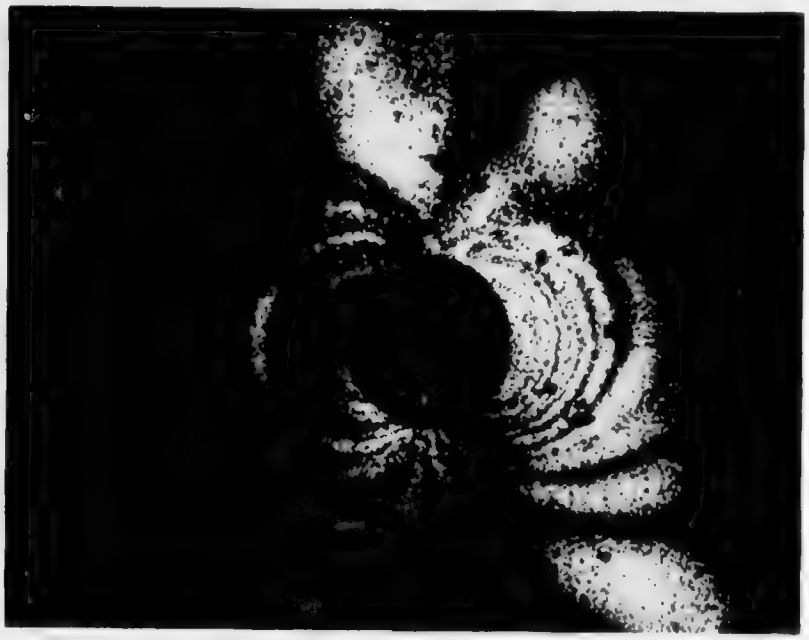

(c) Fourth Order

Figure 4.3 Moire' fringe pattern photographs of the residual strain field around the coldworked hole.

get a large percentage of the grid to bond to the specimen; even a grid applied by the manufacturer was unsatisfactory.

4.3. Other Techniques

The interferometric strain measurement technique in which laser interferometry is used to measure the relative displacement of a pair of ruled grooves was tried. The approach was to photograph the interference fringes before and after coldworking; comparison between the two patterns would produce strain data in the same manner it generated displacement data in an earlier investigation [9]. But the strain near the hole is so large that the sides of the ruled groove become deformed and the reflected laser beams from the two grooves no longer generate smooth, measurable fringes.

Speckle photography is a new technique for measuring surface displacements and thus strain. Two applications of this technique to interference fit problems [10, 7] have measured displacement as close as 1.5 mm and 2.5 mm, respectively, to the edge of the fastener. The problem was not that the fastener obscured the pattern, but that the large deformation destroyed the coherence of the pattern (essentially the same difficulty as beset the laser interferometry technique). A procedure of making incremental displacement measurements has been developed [7] and will likely resolve this problem.

Photoelastic coatings are a well-established technique, but a problem exists in using them in regions of high gradient [11, 12]. A Boeing investigation [13] used photoelastic coatings to visualize the deformation around holes, but no quantitative data is presented. Another report on interference-fit fasteners [6] attempted to use them, but found them unsatisfactory. Photoelastic coatings may be of value for measuring strains away from the hole.

5. RESIDUAL STRAIN MEASUREMENTS

In this section the results of residual strains generated by coldworking are reported. Strains were measured by the indentation procedure, moiré techniques, and foil gages. In addition, some data on surface vertical displacement are presented. Three thicknesses of specimens, 1/4 inch (6.4 mm), 1/8 inch (3.2 mm), and 1/16 inch (1.6 mm), were tested. All specimens were coldworked as described in the previous section.

5.1. 1/4 Inch Thick Specimen Data

Residual radial and tangential strains measured by the indentation procedure are plotted in Figure 5.1 for the front surface (opposite the lip of the sleeve) of two 1/4 inch specimens, A and 1. Specimen A was a 2.5 inch (6.4 cm) by 3 inch (7.6 cm) coupon, while specimen 1 was an 18 inch (46 cm) long tension specimen that was later used for loading studies. The average residual diametral expansion of specimen A was 0.0104 inches (0.264 mm) (see Table 3.3), while that of specimen 1 was 0.0102 inches (0.259 mm). The size of the standard deviations, at least for the larger strains, show that there is a great deal of variability in the results. The standard deviation in Figure 5.1 and subsequent figures is computed using the strain values measured along radial lines. In Figure 5.1, one specimen with four radial lines and one with two radial lines were used, so the standard deviations are based on six measurements. This scatter is much larger than the uncertainty associated with the measurement technique. In fact, at positions 4mm or greater from the hole edge where the residual strains are nearly elastic, the scatter is on the order of the uncertainty of measurement. It is not obvious from Figure 5.1, but the raw data show that there is no trend with radial direction or from specimen to specimen. In other words, the coldworking process produces radially symmetric residual strain fields that are reproducible from specimen to specimen.

Figure 5.2 compares the strains measured on the front and back of specimen A. The standard deviation bars are omitted, but they are very similar in magnitude to those in Figure 5.1. This shows a definite difference between front and back, particularly for the radial strain on the back near the hole edge. One must remember that the lip of the sleeve extended approximately 1 mm from the edge of the hole and thus constrained deformation close to the hole. Indeed, one can discriminate between the front and back of the specimen with the naked eye because the front has a sharp lip near the hole (see Figure 4.1a), while the back is more rounded near the hole. This difference between front and back is evidence of the complicated loading associated with pulling the mandrel and then the sleeve through the hole. That loading is clearly not a radial displacement or radial pressure that is uniform through the thickness of the specimen. Figure 5.2 indicates that there is some bending of the specimen in the plastic region.

The difference between front and back deformation is clearly pointed

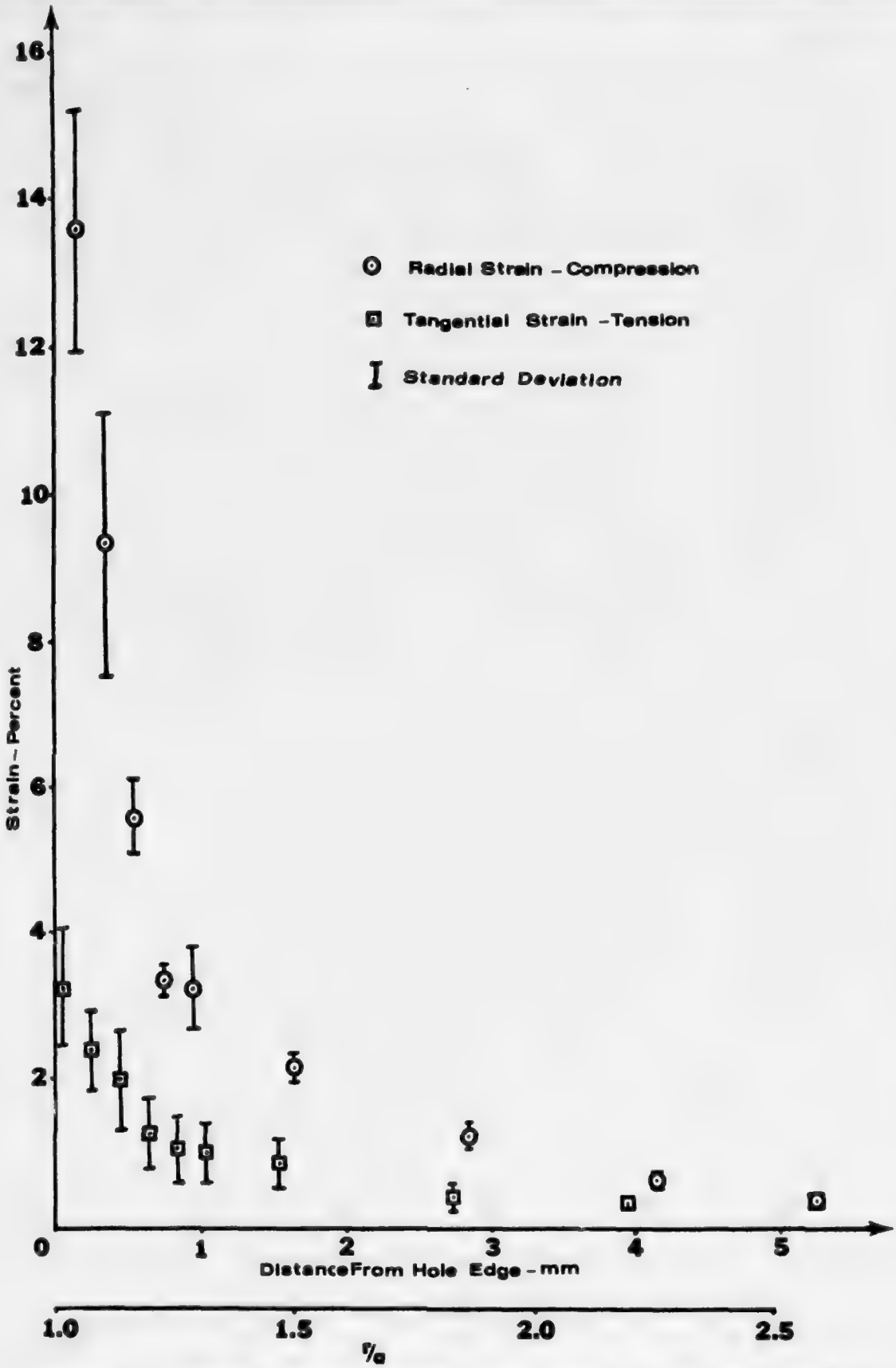

Figure 5.1 Average residual strain measurements on the front side of 1/4 inch (6.4 mm) specimens. Strain was measured on two specimens (A and 1) along 6 radial lines.

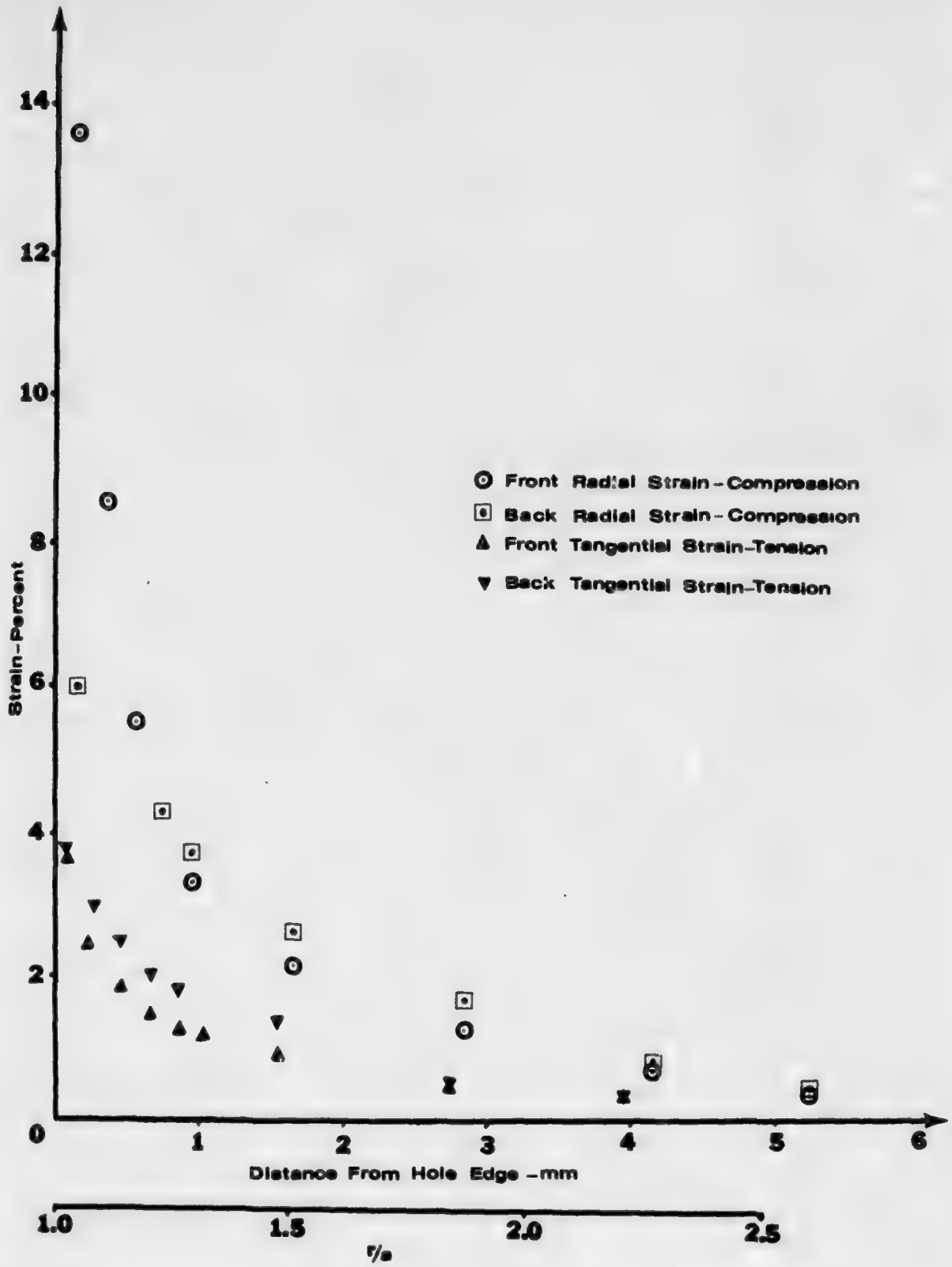

Figure 5.2 Average residual strain measurements on the front and back of specimen A. Strain was measured along 4 radial lines.

out in Figure 5.3, which is a plot of the surface displacements on both sides of specimen A. These measurements were made by focusing a 400X microscope on the specimen surface and measuring the displacement of the microscope head as it was refocused on various positions on the specimen. On the front of the specimen, the displacements are nearly identical when measured along two radial lines 180° apart. The back surface displacements are not identical and show a flattening of the curve near the hole edge caused by the constraining sleeve lip.

Figure 5.4 shows an interesting comparison between the radial strains on the front of specimen A at various stages of the coldworking process. With ideal loading, one would expect the strains to decrease from the "mandrel in" to the "mandrel out" to the "sleeve out" condition. The opposite is observed in Figure 5.4. The tangential strains (not plotted) decreased from "mandrel in" to "mandrel out," but increased to their highest value after the sleeve was removed. The "mandrel in" condition is not very satisfactory because the portion of the mandrel that is a uniform 0.257 inches (6.53 mm) diameter is not quite 1/4 inch (6.4 mm) long, so the whole thickness is not subjected to a uniform expansion at any time. In the "mandrel in" position, the end of the mandrel extends approximately 1/32 inch (0.8 mm) above the specimen. The process of pulling the sleeve out, even though it took only about one-fourth of the force required to pull the mandrel through, contributes significantly to the deformation in the specimen. This data emphasizes the fact that the coldworking process is not a uniform radial displacement.

Strains were measured with foil gages during the coldworking process. Two post-yield foil gages with gage length 0.031 inches (0.78 mm) were attached at radial positions of 5 mm from the hole edge on a tensile specimen. One gage measured strain in the radial direction and one in the tangential direction. The strains as a function of load applied to the mandrel are both plotted in Figure 5.5. As will be seen in the section discussing the various theories, when the material is elastic in a radially loaded infinite sheet, the tangential and radial strains are equal in magnitude. Furthermore, the strain at yield for this material is 0.59 percent (using the Mises-Hencky yield criterion). These strain measurements show that the deformation field within 5 mm from the hole edge is radially symmetric and that the location of the elastic-plastic interface is at approximately 5 mm.

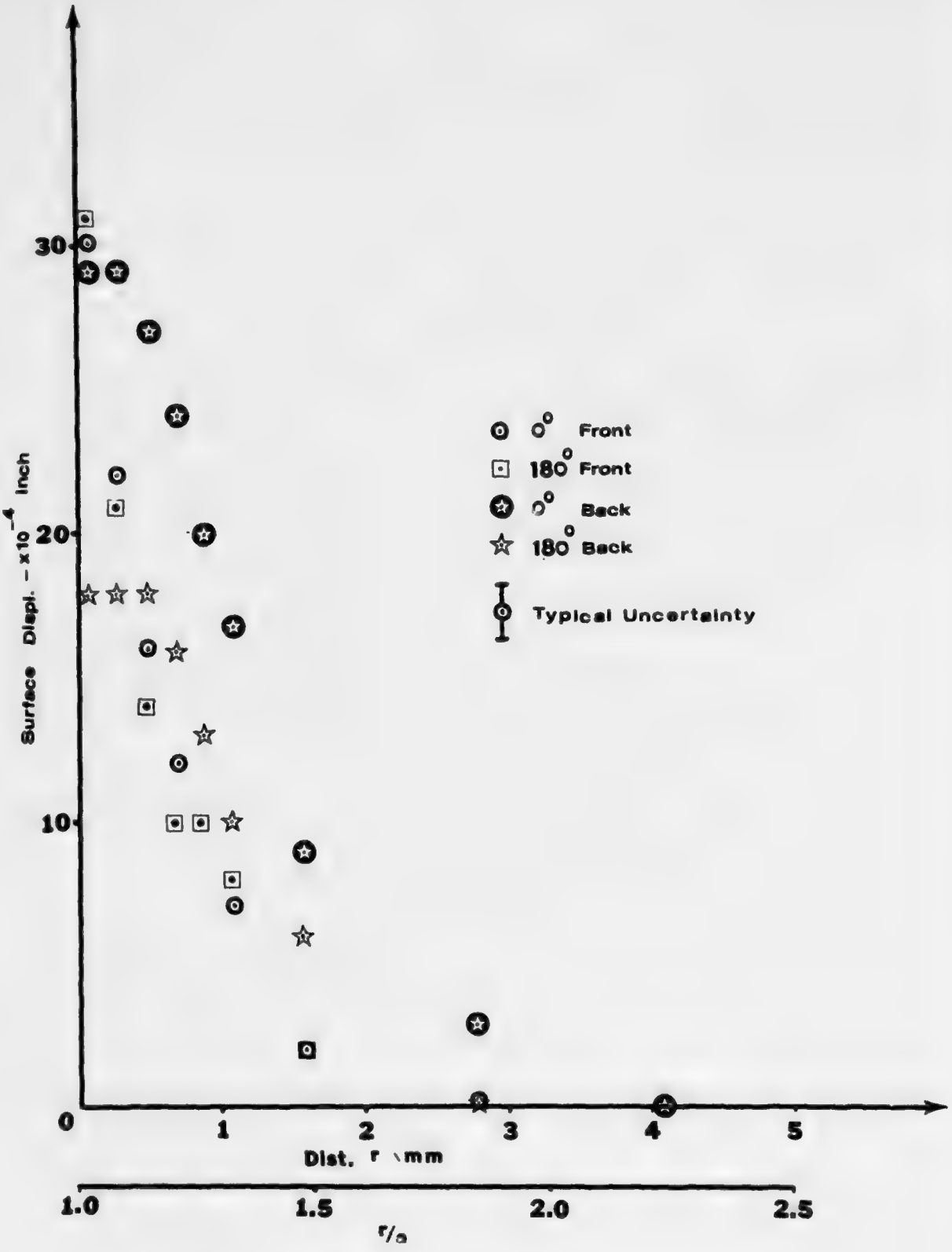

Figure 5.3 Vertical displacements of the front and back surface of specimen A.

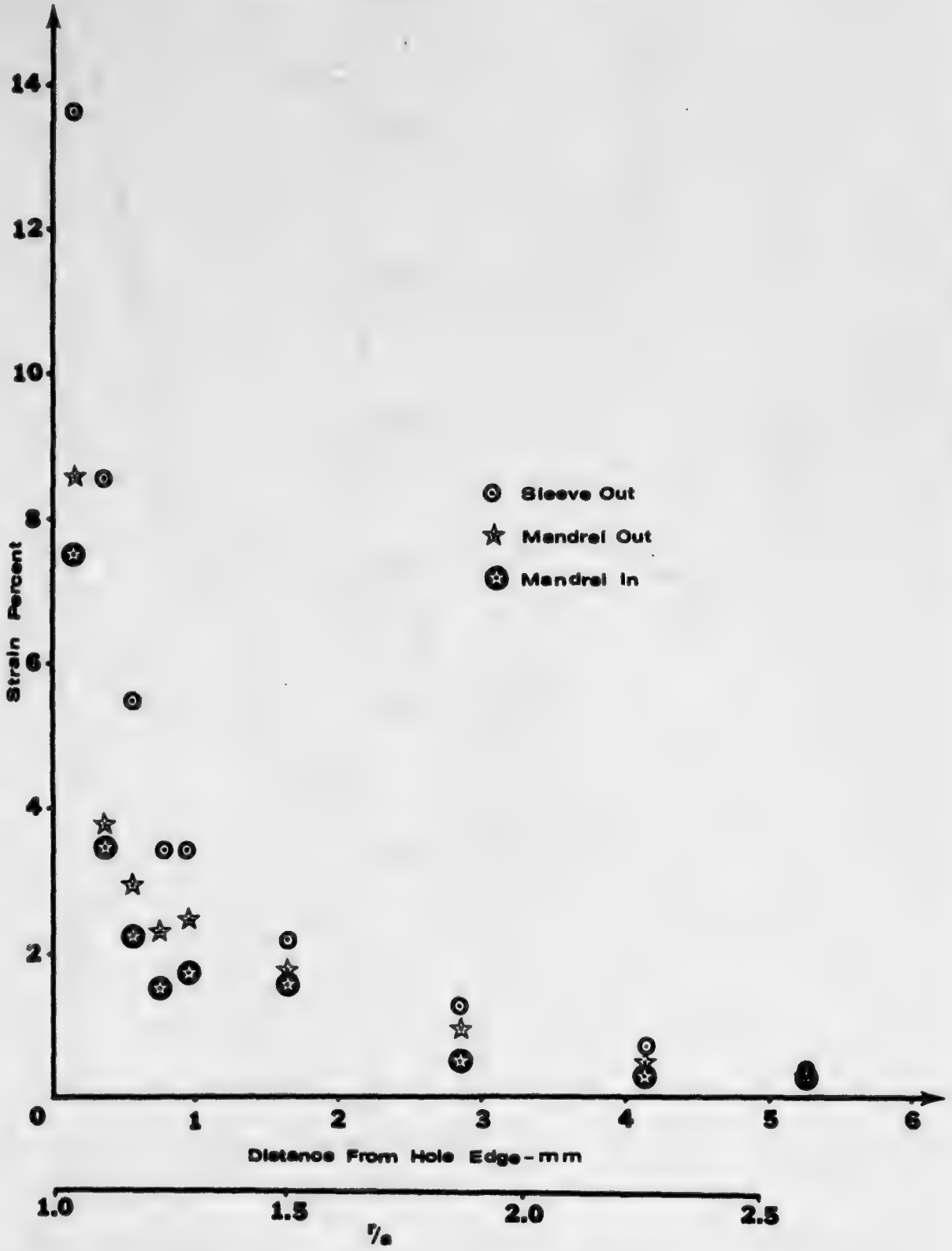

Figure 5.4 Average radial strains measured on specimen A (4 radial lines) at various stages of the coldworking process.

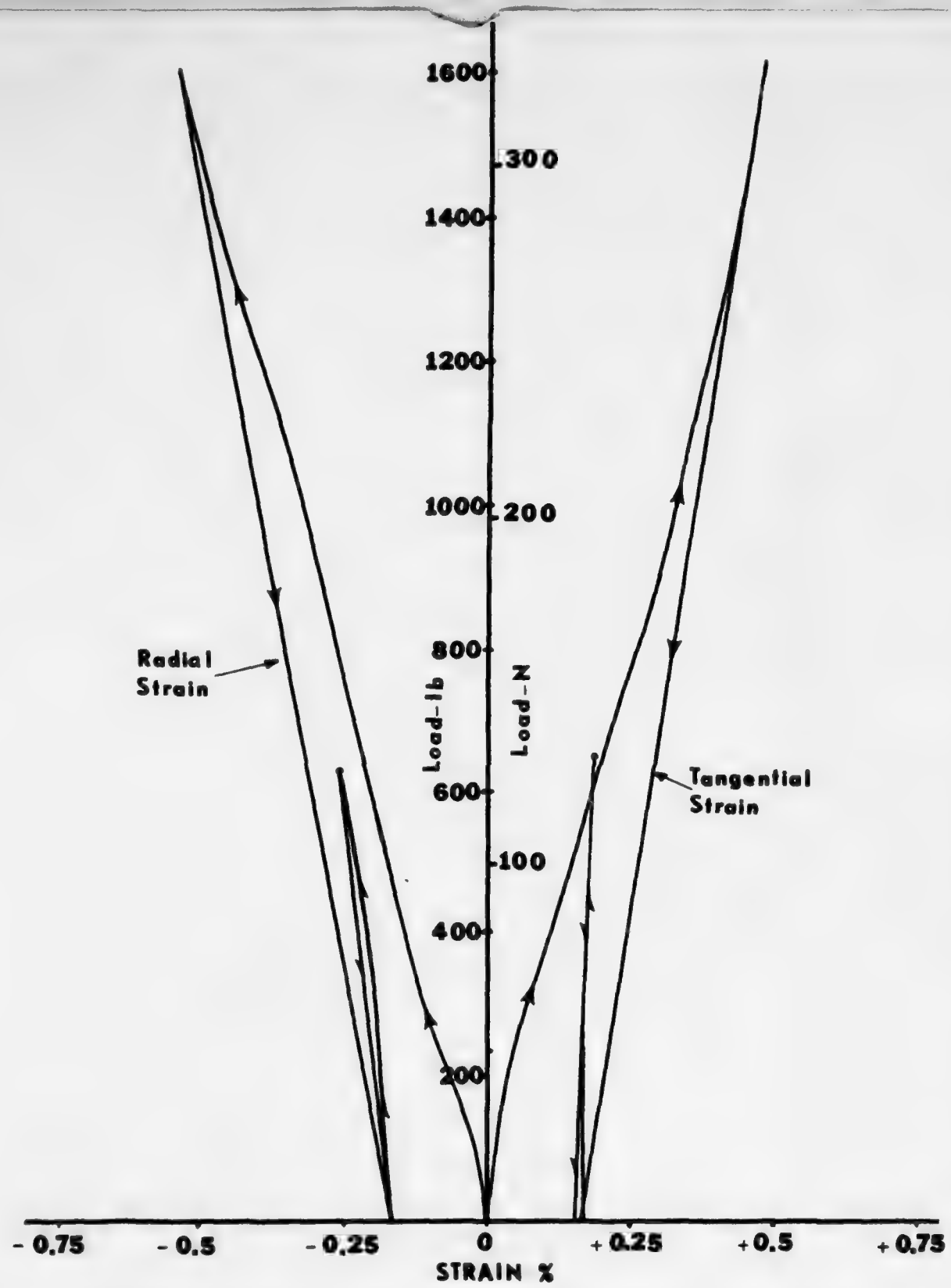

Figure 5.5 Strain measured with foil gages as the mandrel was pulled through the hole. The gages were located 5 mm from the edge of the hole.

Note also that removing the sleeve has no residual effect on the strains this far from the hole.

Measurements of strains closer to the hole with foil gages were more difficult because of the large plastic strain and large strain gradients. Measurements of radial and tangetial strain approximately 0.5 mm from the hole edge were made on different specimens and are shown in Figures 5.6 and 5.7. The complicated behavior as the mandrel is pulled through the sleeve is illustrated here. Also, the additional residual strain associated with sleeve removal is shown; this increase in strain reinforces the indentation measurements of Figure 5.4. In considering this data, one must bear in mind that these strains are measured on the surface and that the strains associated with expansion vary as the mandrel is pulled through the specimen.

Figure 5.8 shows the radial and tangential residual strain measured by the moiré technique as a function of distance from the hole. The strains here are not as large as those in Figure 5.1 because the original hole diameter was slightly larger and the residual diametral expansion was only 0.0069 inches (0.175 mm) compared to 0.0102 inches (0.264 mm). In actual practice, one cannot make measurements right up to the edge of the hole because of lack of resolution of the fringes; the radial strain was measured only to within 1/2 mm in Figure 5.8. One problem with the moiré technique was that the printed grid tended to crack for a distance about 1 mm from the edge of the hole and this caused lack of definition there. This problem could presumably be removed by curing the coating at an elevated temperature before coldworking. To assure that the moiré technique was giving the correct results, strain was measured on the specimen of Figure 5.8 by the indentation procedure. The indentations were applied, the grid printed, moiré measurements made, and then the grid dissolved off the specimen and final strain measurements made. The agreement between the strains is excellent, as shown in Figure 5.8.

Of course, one of the great advantages of the moiré technique is that it produces whole-field strains. A whole-field strain measurement (for one quadrant) is shown in Figure 5.9. This gives the strain in terms of ϵ_x and ϵ_y instead of the ϵ_r and ϵ_θ that is more conveniently used for theoretical analysis. The predicted strain field of Adler-Dupree [3] is also plotted in Figure 5.9. They predicted a residual diametral expansion

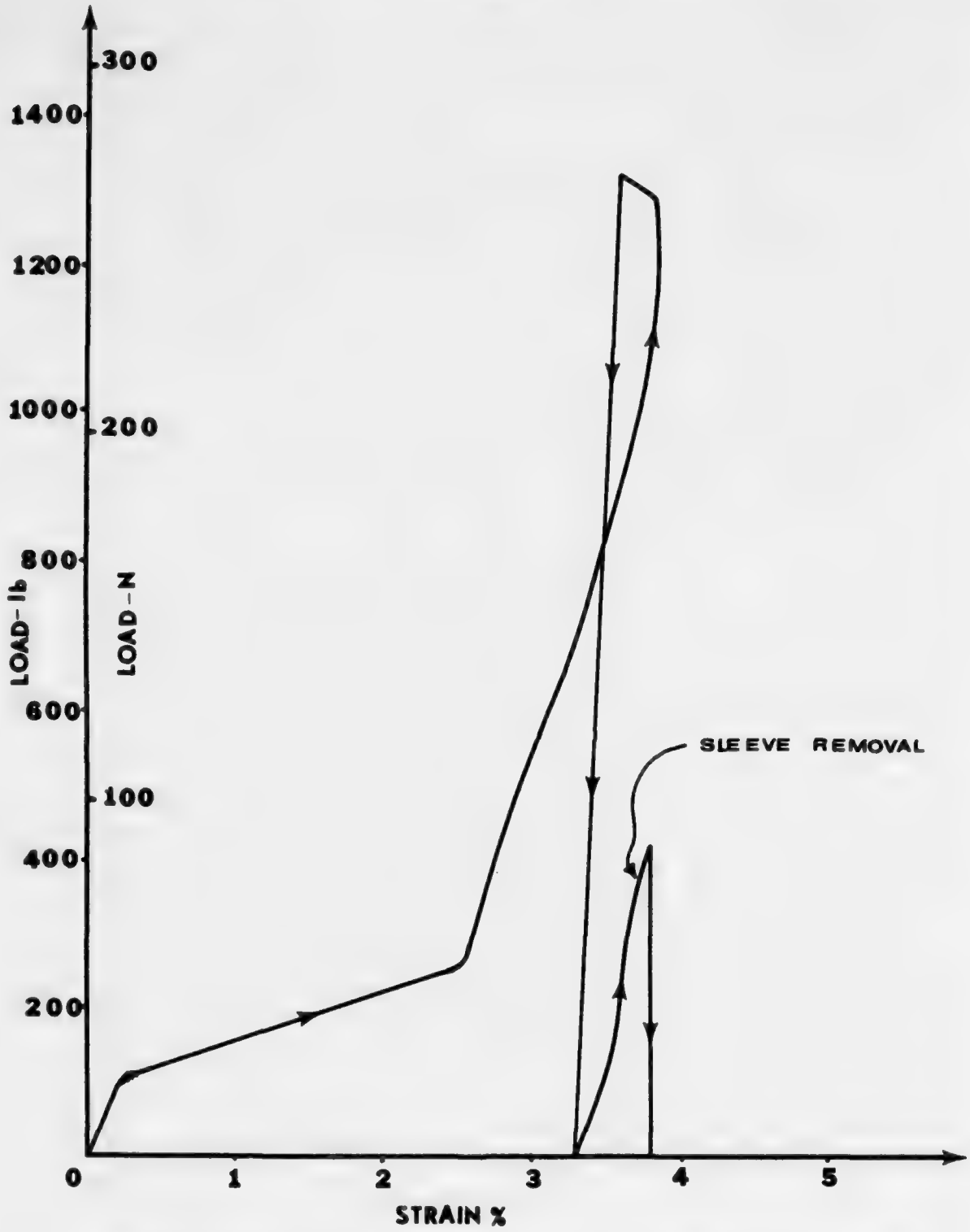

Figure 5.6 Radial strain measured with a foil gage located 0.5 mm from the edge of the hole as it was coldworked.

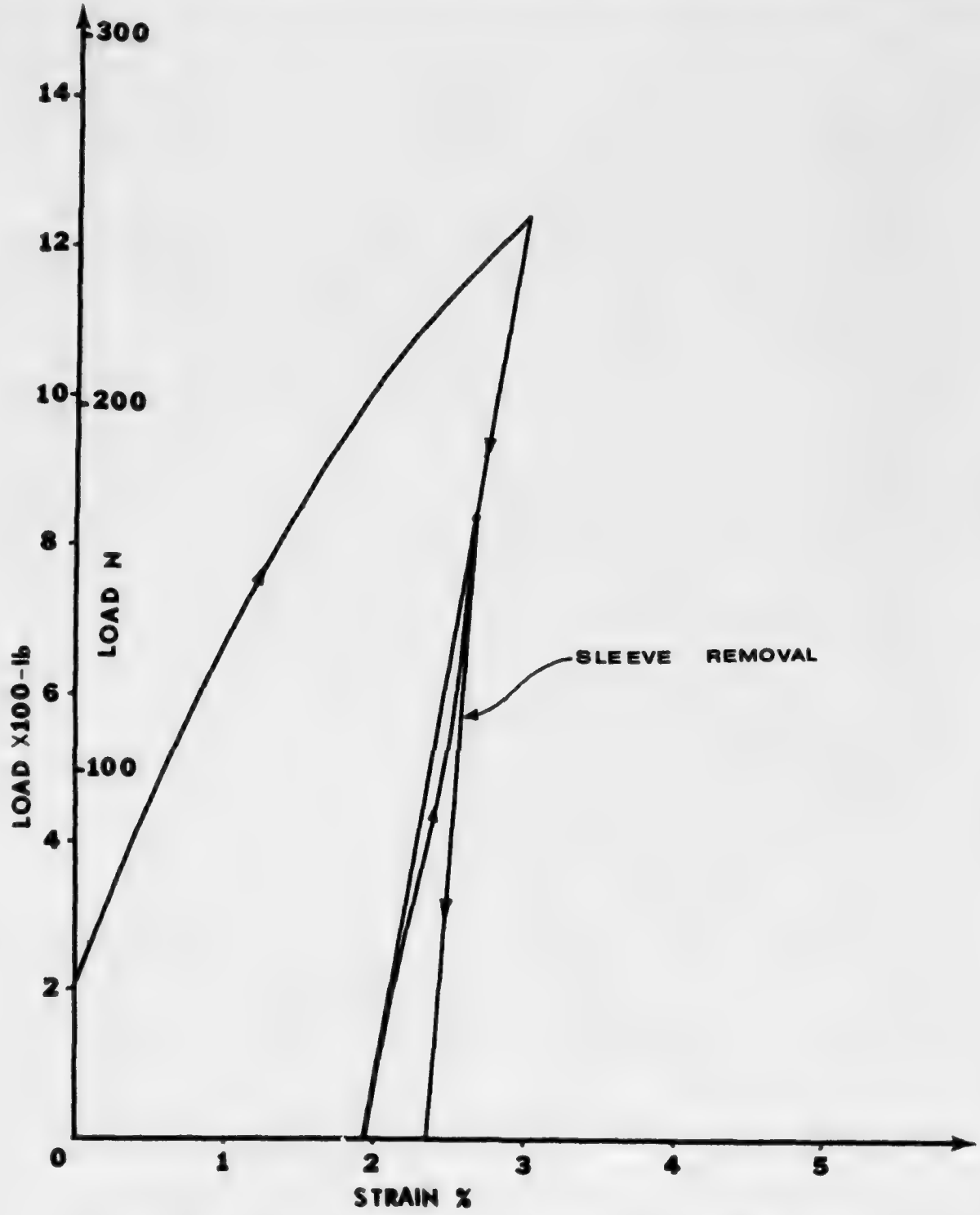

Figure 5.7 Tangential strain measured with a foil gage located 0.5 mm from the edge of the hole as it was coldworked.

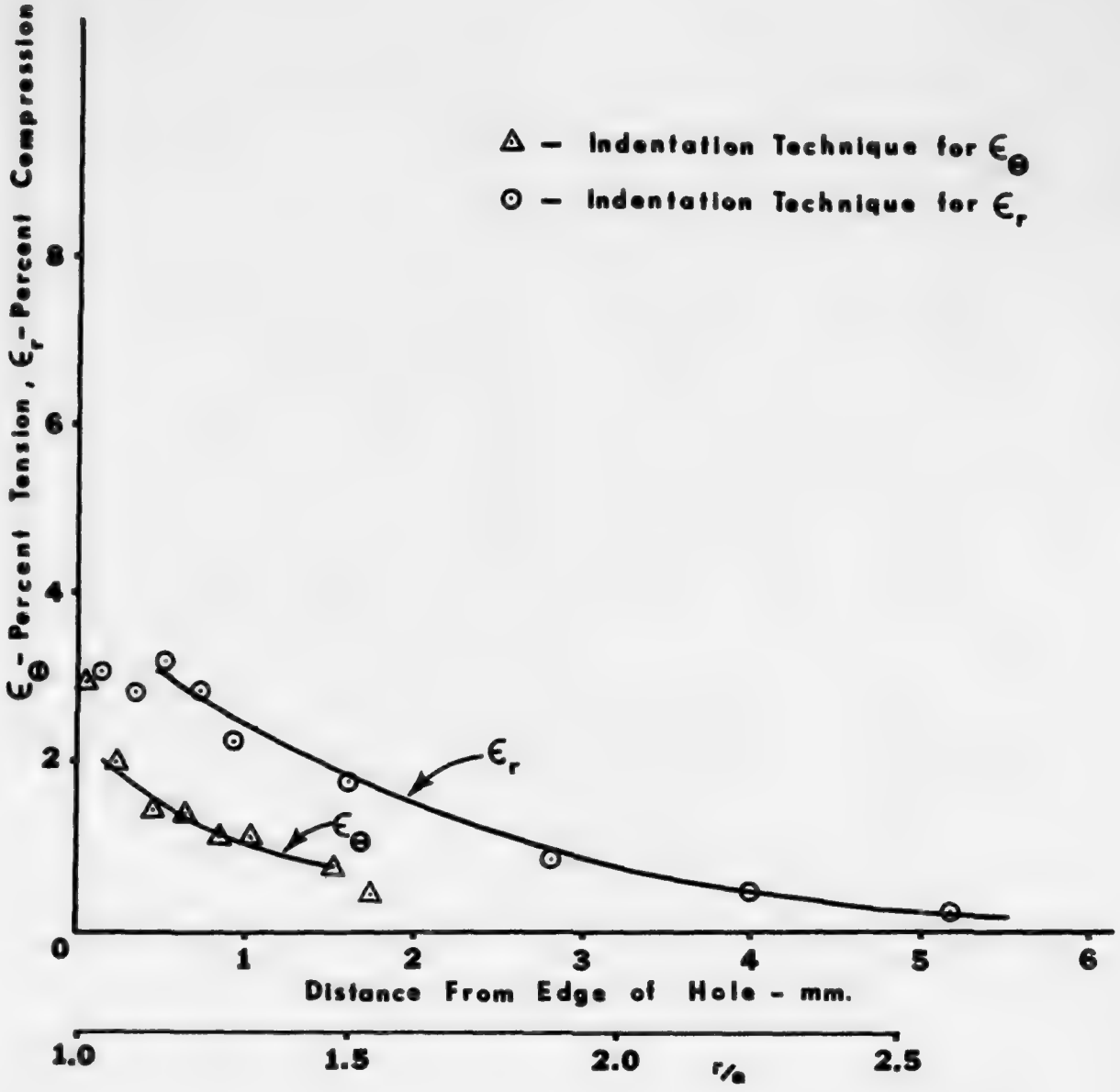

Fig. 5.8 Residual strains measured by the moire´technique for the 1/4 inch (6.4 mm) specimen LL. Diametral expansion of the originally 0.261 inch (7.63 mm) hole was only 0.0069 inches (0.175 mm).

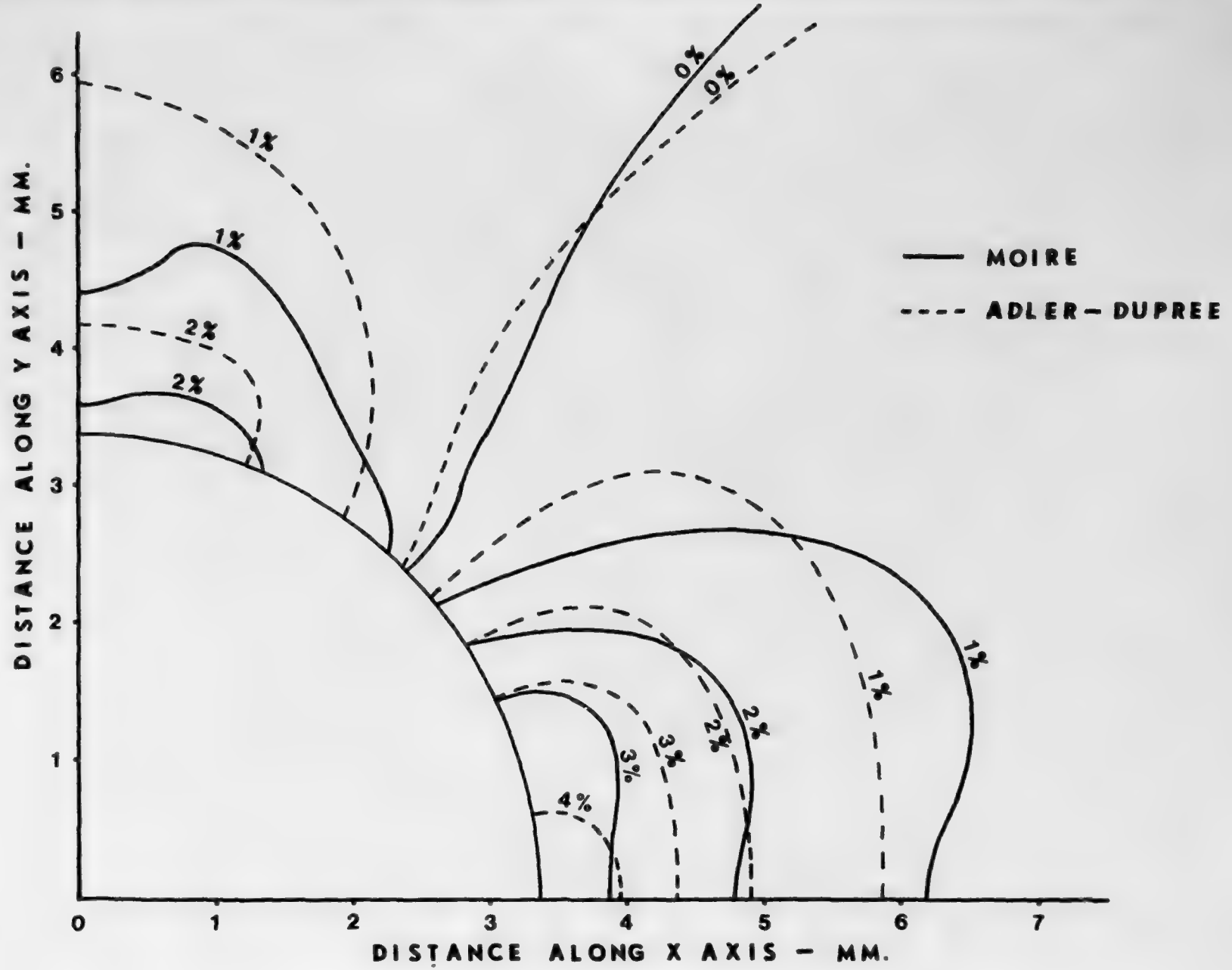

Figure 5.9 Whole-field moire measurement of the residual strain of specimen LL compared with predictions of Adler-Dupree (3).

of 0.008 inches (6.2 mm), so the experiment and theory are not exactly the same (0.0069 inches versus 0.008 inches expansion), but the strains agree reasonably well.

5.2. 1/8 Inch Thick Specimen Data

Residual strain measurements (4 on one and 2 on the other) by the indentation method from two rectangular specimens are plotted in Figure 5.10. The specimen holes were originally 0.2601 inches (6.61 mm) and 0.2604 inches (6.61 mm) in diameter and were subjected to the standard coldworking procedures. The sleeves were cut off so that they were the same length as the specimen thickness. The residual hole expansions were quite different as measured on the front and back sides. One specimen had a residual displacement of 0.0048 inches (0.12 mm) on the front and 0.0093 inches (0.24 mm) on the back; the other was 0.0064 inches (0.16 mm) on the front and 0.0098 inches (0.25 mm) on the back.

The striking feature of Figure 5.10 is the fact that the average strain does not continue to increase near the edge of the hole. This is not a result of large scatter in the data; no radial strain larger than 4.3 percent was measured. Figure 5.11 is a photograph of the area near the hole edge, and one can see the rounding of the specimen surface near the hole; compare this with Figure 4.1. A further illustration of this behavior is given in Figure 5.12, which compares the average strains on the front and back of the two specimens. This is similar to the 1/4 inch specimen data in that the strains on the back are greater than on the front at distances greater than 1 mm away from the edge, but different in that the radial strains on the back are larger near the hole. The lip of the sleeve leaves a very faint impression on the specimen surface, so it is easy to be sure that the sides of the specimen were not mislabeled.

Vertical displacements on the front and back of one of the 1/8 inch specimens are plotted in Figure 5.13. The fact that the residual deformations are so much larger on the back than on the front is consistent with these strain and displacement results. The interaction between the mandrel, sleeve, and specimen that generated such a variation in residual strain through the thickness is not at all clear. This combination of hole size, sleeve thickness, and mandrel taper is obviously not optimal for this thickness.

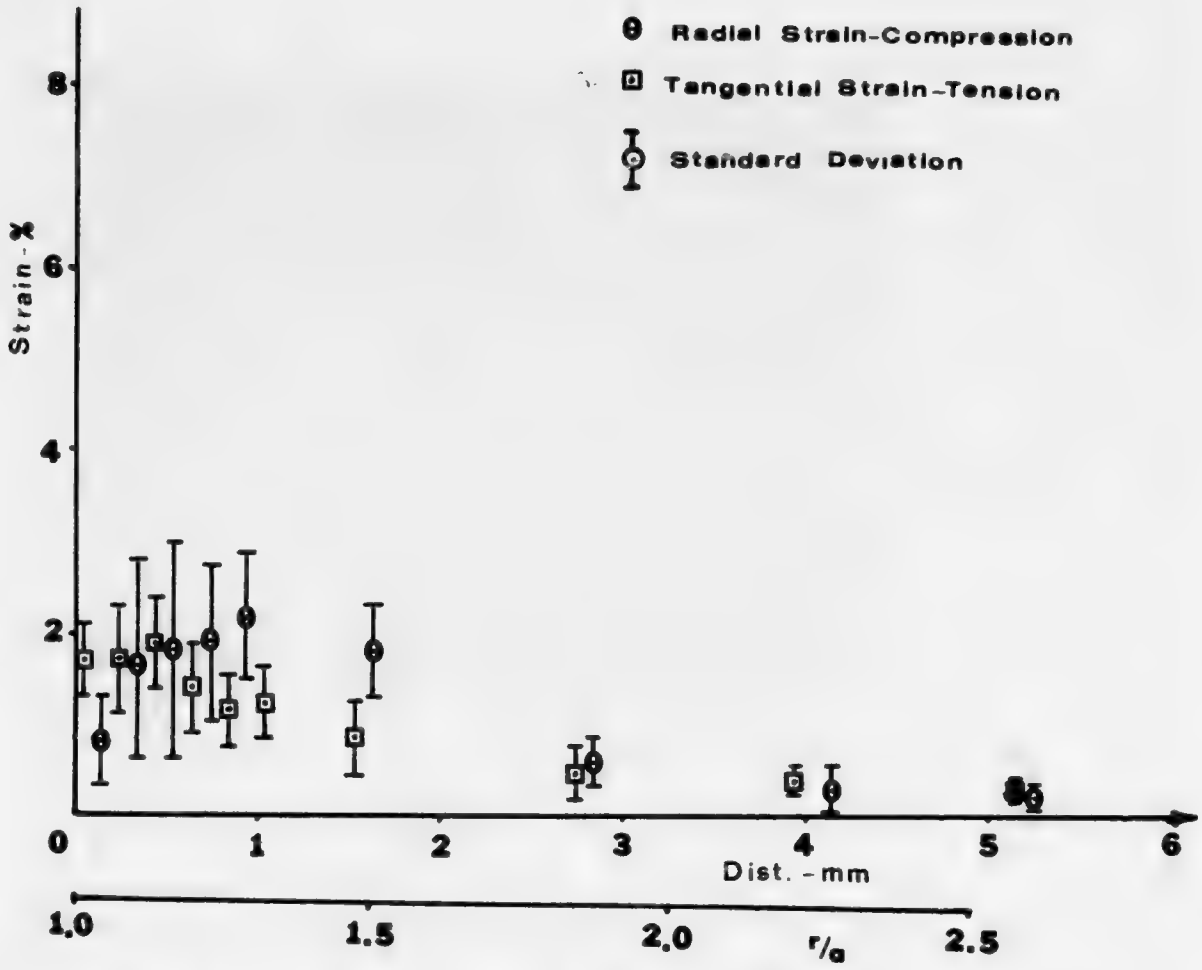

Figure 5.10 Average residual strain measurements on the front side of 1/8 inch (3.2 mm) specimens. Strain was measured on two specimens along 8 radial lines.

Figure 5.11 Photograph of the deformed region around the hole in a 1/8 inch (3.2 mm) specimen (100 X).

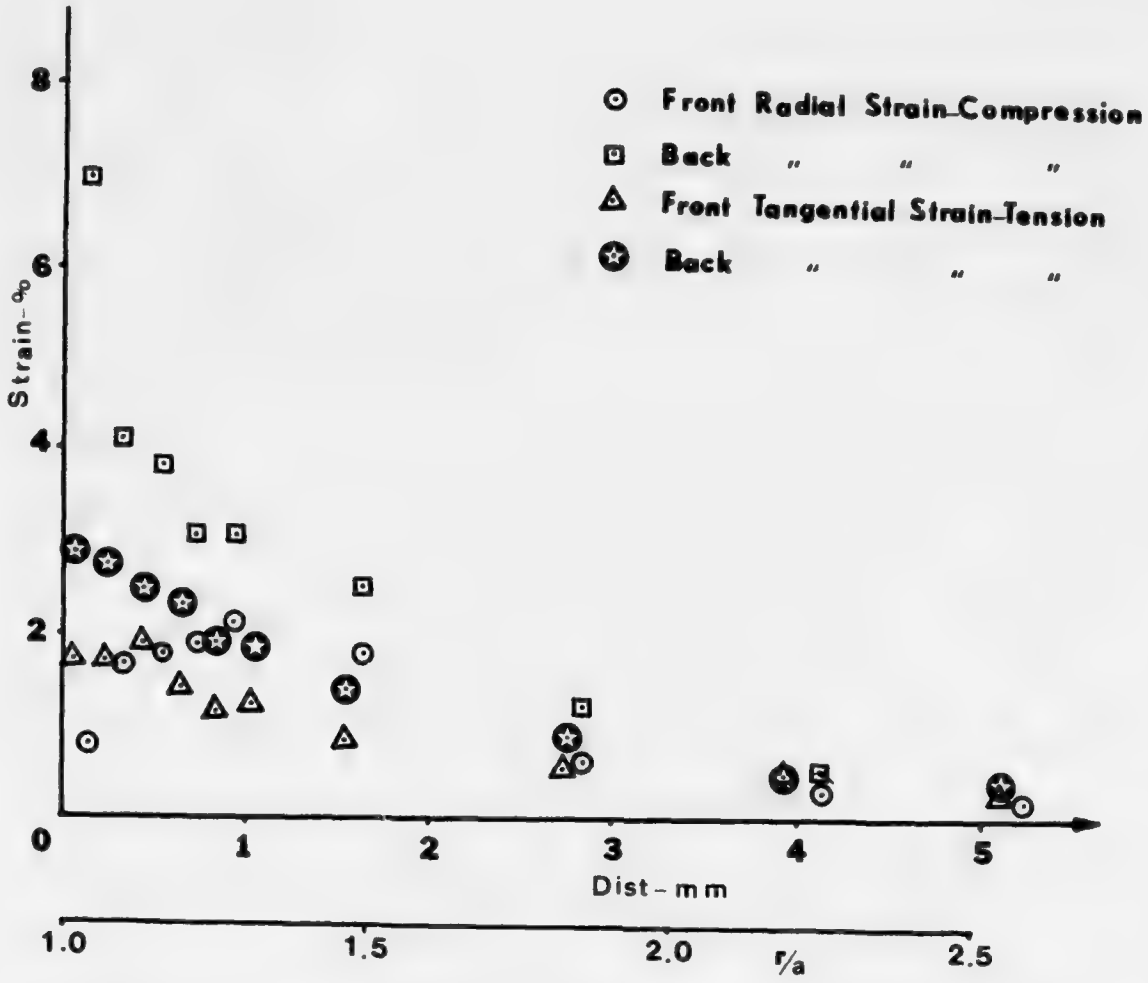

Figure 5.12 Average residual strain measurements on the front and back of two 1/8 inch (3.2 mm) specimens. Strain was measured along 4 radial lines.

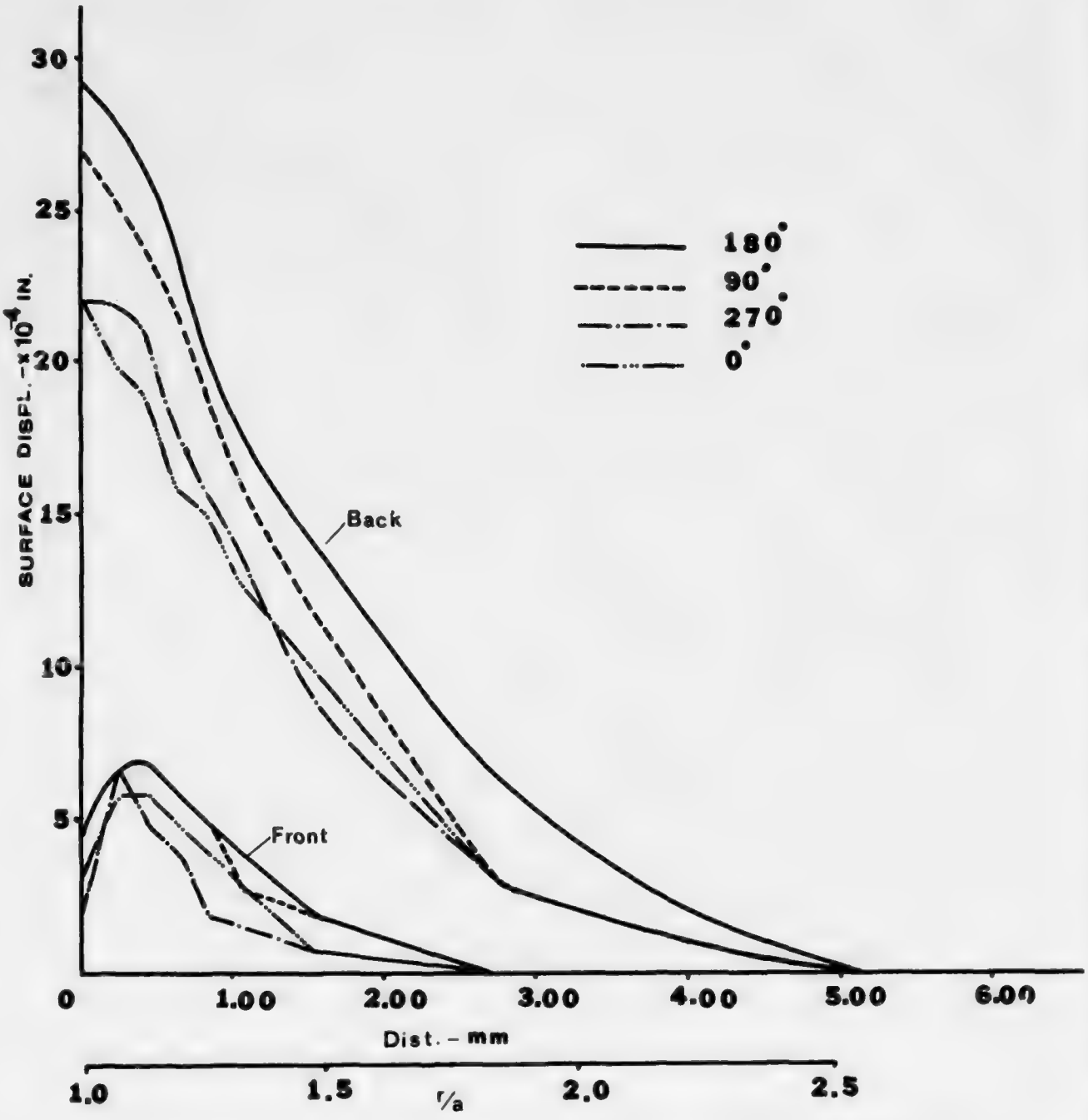

Figure 5.13 Vertical displacements of the front and back surfaces of two 1/8 inch (3.2 mm) specimens.

5.3. 1/16 Inch Thick Specimens

Residual strain measurements on coldworked 1/16 inch (1.6 mm) thick rectangular specimens (two specimens--six measurements) are plotted in Figure 5.14. The original hole diameter in these was slightly oversize, being 0.2613 inches (6.64 mm). The residual diametral expansions were 0.0085 inches (0.22 mm) and 0.0070 inches (0.18 mm). There was no significant difference between the residual expansion on the front versus the back. Here the radial strains continue to increase near the hole edge, although there is exceptionally large scatter in the data there.

Figure 5.15 is a photograph of a coldworked 1/16 inch specimen after the sleeve has been removed. All of the specimens of this thickness tended to buckle in a region of about 2 mm around the hole. The specimen is too thin to deform in the plane without buckling out of the plane.

Figure 5.16 compares the front and back average residual strain for one specimen; as should be expected, there is less difference between them. The surface displacements for such a thin specimen are really too small to measure reliably with the microscope.

5.4. Discussion

As to the techniques used to measure the strain, the indentation procedure, though tedious, is accurate and workable. Useful data can be obtained close to the hole edge that is not obtainable via other methods. Foil gages work very nicely even at these large strains and gradients and give an accurate measure of the average strain within the gage length. The moiré method is useful for obtaining whole field data. These three techniques have been shown to be consistent with each other.

The experimental results show that the deformation is radially symmetric and reproducible from specimen to specimen. This means that the coldworking process is controllable enough that it can be predicted by application of the principles of solid mechanics. However, the deformation near the hole is not uniform through the specimen thickness, so the analysis problem is complicated. It would be difficult to reduce the complicated coldworking procedure to easily-specified boundary conditions at the edge of the hole, and this makes a realistic analysis even more formidable. The inhomogeneity of the strains near the hole edge (because of the large deformation of the relatively large grains) require that strains be averaged over a number of positions.

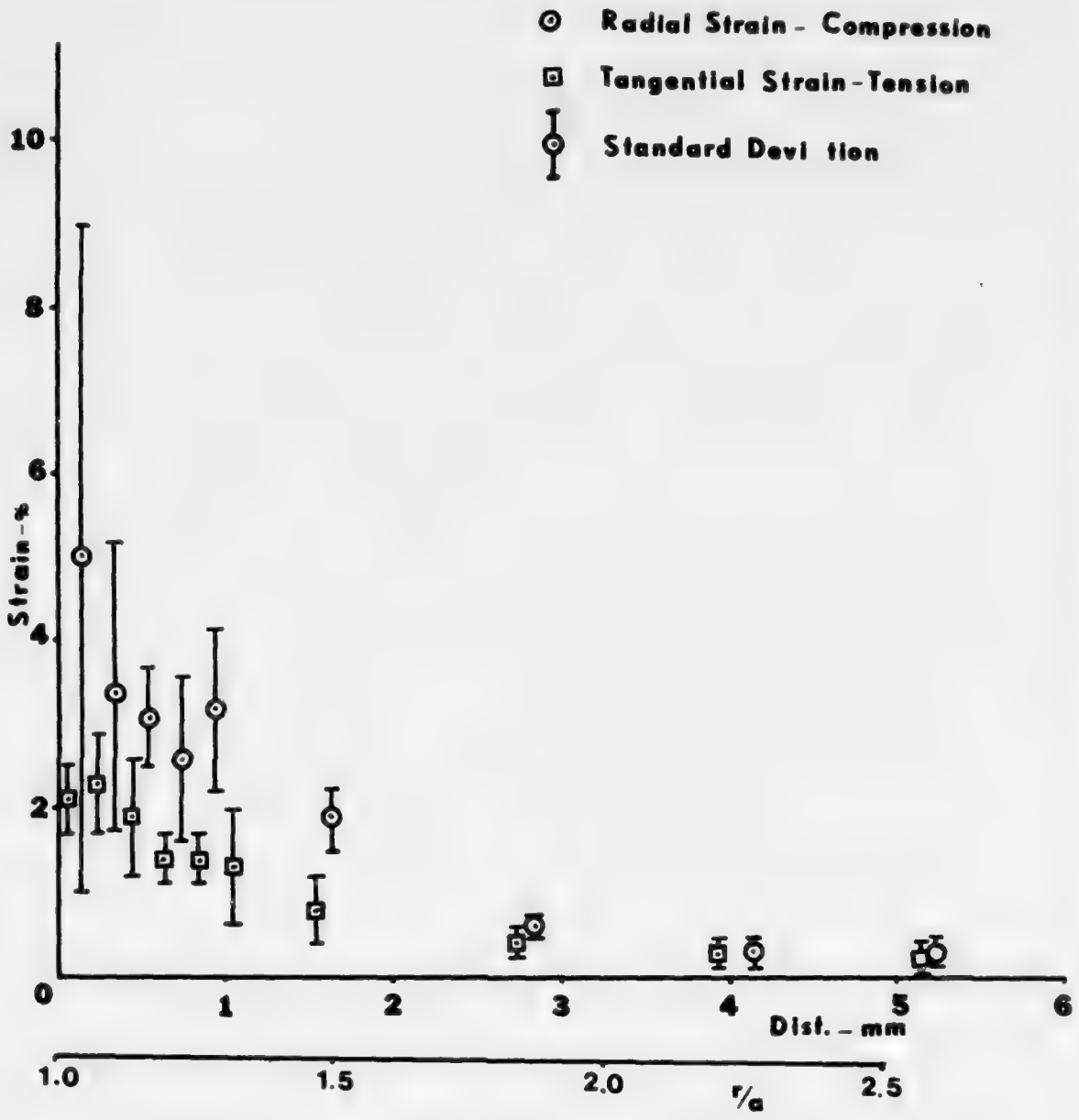

Figure 5.14 Average residual strain measurements on the front side of 1/16 inch (1.6 mm) specimens. Strain was measured on two specimens along 6 radial lines.

Figure 5.15 Photograph of a 1/16 inch (1.6 mm) specimen after it has been coldworked (100 X).

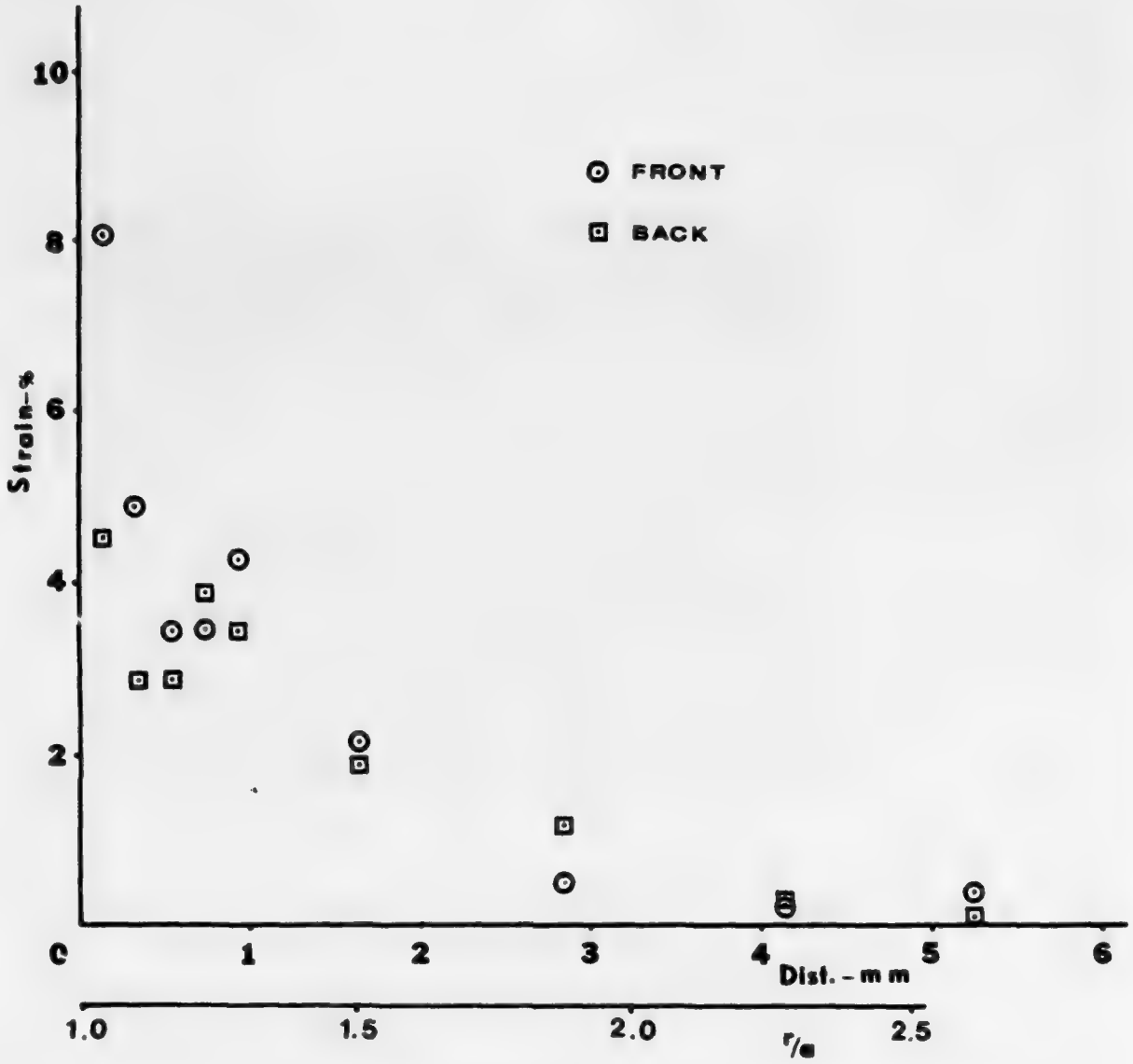

Figure 5.16 Average residual strain measurements on the front and back of a 1/16 inch (1.6 mm) specimen. Strain was measured along 2 radial lines.

The 1/4 inch (6.4mm) specimens showed the strains on the upper free surface to increase monotonically from the elastic region to the edge of the hole. This is what one would expect from the theoretical analyses, so from that point of view the 1/4 inch (6.4mm) specimens are most suitable for comparison with theories. But that data shows considerable difference between the strains on the upper and lower surfaces, indicating that the strain varies through the thickness. On the other hand, the 1/8 inch (3.2mm) and 1/16 inch (1.6mm) specimens show unexpected strains near the hole or buckling of the specimens, so they are not completely satisfactory either. Thus it is difficult to say which thickness best matches the plane stress assumptions of the theories. This coldworking process is simply not one that is easily modeled accurately.

6. THEORIES OF RESIDUAL STRAINS

6.1. Introduction

The geometrical shape under experimental and theoretical consideration is a flat circular sheet of radius "b" with a circular hole of radius "a" in the center (see Figure 6.1). Many of the theories that have been developed assume "b" to be infinitely large, but all of them assume that the thickness of the sheet is sufficiently small relative to the dimension "b" that a condition of plane stress exists. Deformation of the sheet is caused by either a uniform positive radial displacement, u_a, or a uniform negative pressure, -p, at r = a.

The problem is symmetric about the z axis because of the radial loading, so the strains are given by

$$\epsilon_r = \frac{\partial u}{\partial r} \; ; \; \epsilon_\theta = \frac{u}{r} \tag{6.1}$$

where u is the radial displacement of the material. The equilibrium equation, which must hold for either elastic or plastic stresses, is:

$$\frac{d\sigma_r}{dr} + \frac{\sigma_r - \sigma_\theta}{r} = 0 . \tag{6.2}$$

For a radial displacement, u_a, small enough that the material remains elastic everywhere, the stresses, strains, and displacements are given by (14):

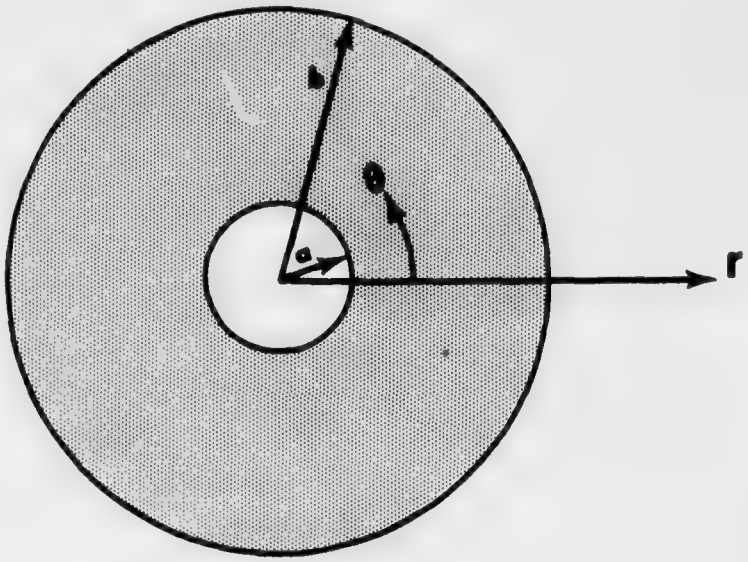

Figure 6.1 Geometry and coordinate system used in coldworked hole theories.

$$\sigma_r = A\left[-\frac{1}{r^2} + \frac{1}{b^2}\right], \quad \sigma_\theta = A\left[\frac{1}{r^2} + \frac{1}{b^2}\right]$$

$$\epsilon_r = \frac{A}{E}\left[-\frac{1+\nu}{r^2} + \frac{1-\nu}{b^2}\right], \quad \epsilon_\theta = \frac{A}{E}\left[\frac{1+\nu}{r^2} + \frac{1-\nu}{b^2}\right] \tag{6.3}$$

$$u = \frac{A}{E}\left[\frac{1+\nu}{r} + \frac{(1-\nu)r}{b^2}\right]$$

$$A = \frac{E\,u_a}{\frac{1+\nu}{a} + (1-\nu)\frac{a}{b^2}}$$

where E and ν are the modulus of elasticity and Poisson's ratio. The boundary conditions here are that $u = u_a$ at $r = a$ and $\sigma_r = 0$ at $r = b$.

The Mises-Hencky yield criterion becomes:

$$\sigma_r^2 + \sigma_\theta^2 - \sigma_r\sigma_\theta = \sigma_o^2 \tag{6.4}$$

where σ_o is the yield stress from the uniaxial stress-strain curve. Theories using an elastic-plastic stress-strain curve will take σ_o as the 0.2 percent offset yield strength, whereas those that use the actual stress-strain curve take σ_o to be the proportional limit.

The largest radial displacement that can be applied to the hole without causing plastic deformation is:

$$u_{aE} = \frac{\sigma_o}{E\left[\frac{1}{b^4} + \frac{3}{a^4}\right]^{1/2}}\left[\frac{1+\nu}{a} + \frac{(1-\nu)a}{b^2}\right]. \tag{6.5}$$

Once u_{aE} (or its equivalent pressure, p_E) is exceeded, the material in the neighborhood of "a" becomes plastically deformed and the solution of the problem is no longer easy. Denote the interface between the elastic region and the plastic region by r_p. As u_a increases, r_p increases; i. e., the elastic-plastic boundary moves out into the material. The problem in the plastic region to be solved is now one in which $u = u_a$ at $r = a$ (or $\sigma_r = -p$ at $r = a$) and the stresses, strains, and displacements match the elastic ones at $r = r_p$. If r_p is known, these elastic stresses, etc., are easily calculated because it is known that, if $b \to \infty$, $\sigma_r = -\sigma_o$, and therefore from equation (6)

$$\sigma_r \Big|_{r_p} = \frac{-\sigma_o}{\sqrt{3}} = -\sigma_\theta \Big|_{r_p} \quad . \tag{6.6}$$

In the elastic region, $r \geq r_p$:

$$\sigma_r = -\frac{\sigma_o}{\sqrt{3}}\left(\frac{r_p}{r}\right)^2 , \quad \sigma_\theta = \frac{\sigma_o}{\sqrt{3}}\left(\frac{r_p}{r}\right)^2 \tag{6.7}$$

$$\epsilon_r = -\frac{\sigma_o(1+\nu)}{E\sqrt{3}}\left(\frac{r_p}{r}\right)^2 , \quad \epsilon_\theta = \frac{\sigma_o(1+\nu)}{E\sqrt{3}}\left(\frac{r_p}{r}\right)^2 \tag{6.8}$$

$$u = \frac{\sigma_o(1+\nu)}{E\sqrt{3}}\,\frac{r_p^2}{r} \quad . \tag{6.9}$$

The problem in plasticity theory is then to find the stresses, etc., subject to the known boundary conditions at $r = a$ and $r = r_p$. An important part of the problem is the determination of the relation between loading and r_p. Various theories have been developed to predict these quantities, and they fall into three classes: analytical, numerical, and finite-element. The analytical theories produce closed-form equations based on either an elastic-perfectly-plastic stress-strain curve or a two-parameter plastic stress-strain curve. The numerical ones develop the solution in terms of incremental rings between a and b corresponding to increments on the plastic stress-strain curve. The one finite element solution uses an elastic-plastic computer code.

Once the hole has been expanded to the prescribed conditions, the loading is removed at $r = a$. This generates, because of the elastic relaxation of material outside (and inside) r_p, residual stresses. The analytical and numerical theories (except for (23)) represent this unloading by superposing an elastic stress field:

$$\sigma_r = \sigma_m\left(\frac{a}{r}\right)^2 , \quad \sigma_\theta = -\sigma_m\left(\frac{a}{r}\right)^2 \tag{6.10}$$

where σ_m is the magnitude of the radial stress generated at $r = a$ by the loading process. This guarantees that $\sigma_r = 0$ at $r = a$ after unloading.

Various theories are discussed in the following sections and

compared in the concluding section. In each case the residual stresses and strains for 7075-T6 aluminum subjected to:

$u_o = 0.006$ inches (0.15 mm) at $a = 0.13$ inches (3.3 mm)

are calculated. The stress-strain data is taken from Adler-Dupree [3] and is given in Table 1.

TABLE 1

Stress-Strain Data for 7075-T6 from [3]

Elastic-Plastic

$\sigma = 9.8 \times 10^6$ psi $\epsilon = 67.5 \times 10^3$ MPa ϵ for $\epsilon \leq 0.0080$

$\sigma = 78.2$ ksi $= 5.38$ MPa for $\epsilon \geq 0.0080$

Bilinear

$\sigma = 9.8 \times 10^6 \epsilon = 67.5 \times 10^3$ MPa ϵ for $\epsilon \leq 0.0080$

$\sigma = 78.2$ ksi $+ 195$ ksi $(\epsilon - 0.0080)$

$= 5.38$ MPa $+ 1{,}340$ MPa $(\epsilon - 0.0080)$ for $\epsilon \geq 0.0080$

Actual Data

Strain	Stress	
0	0	
0.0075	73.5 ksi	506 MPa
0.0077	75.1 ksi	517 MPa
0.0082	76.7 ksi	528 MPa
0.0090	77.9 ksi	537 MPa
0.0100	78.4 ksi	540 MPa

$\sigma = 78.4$ ksi $+ 195$ ksi $(\epsilon - 0.01)$

$= 540$ MPa $+ 1340$ MPa $(\epsilon - 0.01)$

for $\epsilon \geq 0.01$

6.2. Nadai Theory

Nadai [4] in 1943 published a theory of plastic expansion of tubes fitted into boilers. The plate of the boiler has a tube fitted into it and in the manufacturing process these tubes were expanded by a roller device to insure a leak-free fit. He considered both the plastic deformation in the steel plate and the plastic deformation of the copper alloy tubes. First, he solved the plate problem, which is the one of interest here. His assumptions were:

1) uniform pressure at the edge of the hole in the plate;
2) a linear approximation to the Mises-Hencky yield criterion;
3) perfectly plastic material response.

In the plastic zone he develops the following equations:

$$\sigma_r = \frac{\sigma_o}{\sqrt{3}}\left(-1 + 2 \ln \frac{r}{r_p}\right)$$

$$\sigma_\theta = \frac{\sigma_o}{\sqrt{3}}\left(1 + 2 \ln \frac{r}{r_p}\right) \qquad (6.11)$$

$$u = \left(\frac{3}{2}\right)^3 \frac{u_a E \frac{r}{r_p}}{\left(\frac{3}{2} + \ln \frac{r}{r_p}\right)^3} . \qquad (6.12)$$

The elastic strains and displacements are neglected in developing equation (6.12).

The residual stresses and strains after relaxation are plotted in Figures 6.2 and 6.3. For the test case computed, the theory predicts $r_p = 2.11a$. He also developed the theory for the stresses in a tube with a general stress-strain curve. This complete theory could be applied to coldworking procedures in which the sleeve remains in the hole. Nadai formulated the problem in terms of the Mises-Hencky criterion, but he linearized this criterion to obtain a closed-form solution.

6.3. Taylor Theory

G. I. Taylor [15] in 1948 published a theory of the expansion of a hole in a thin plastic sheet. He used a perfectly plastic material, developed the same expression for stresses as Nadai, and computed the thickness change. He compared the predicted variation of thickness with r

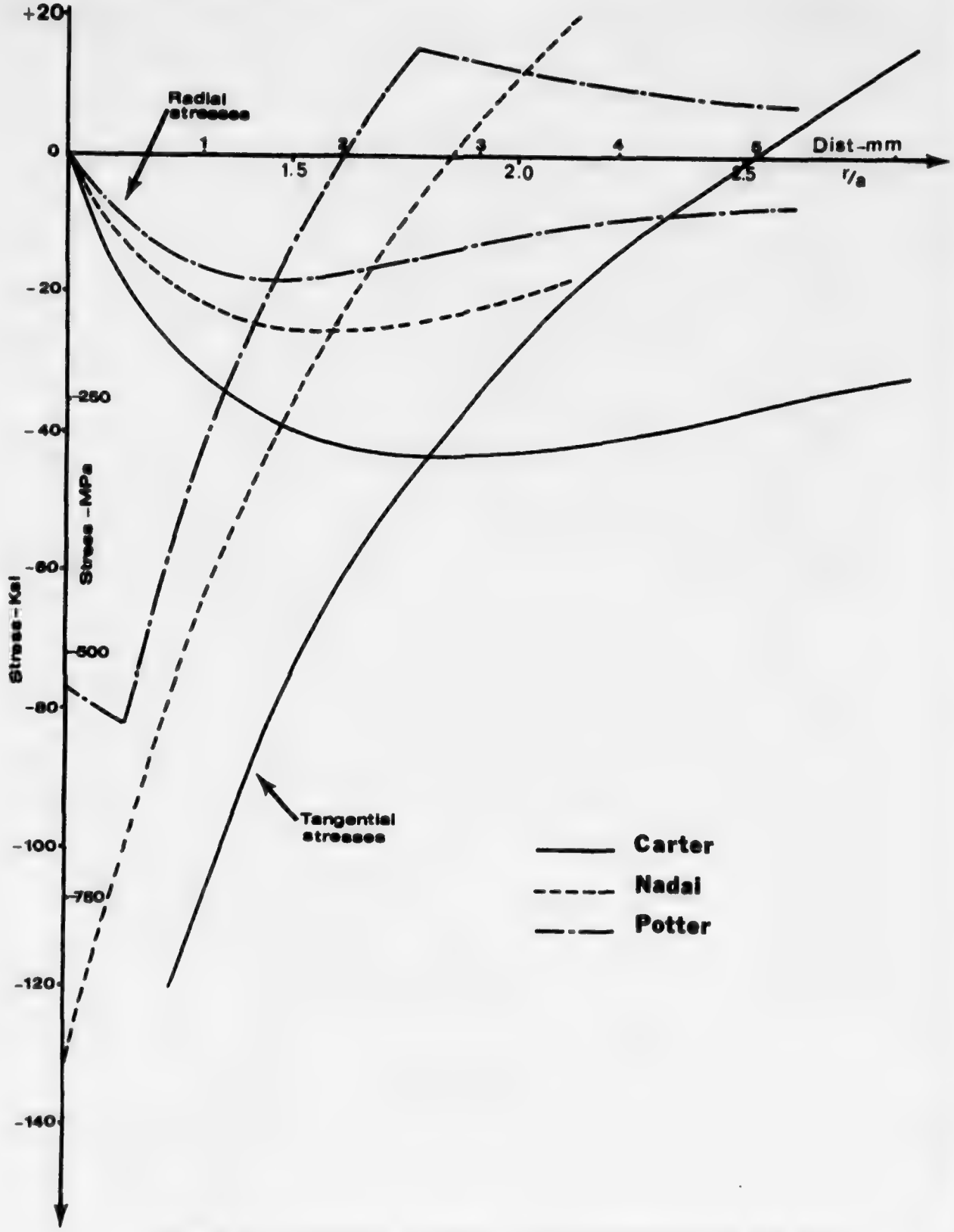

Figure 6.2 Residual stresses after coldworking for the non-workhardening theories.

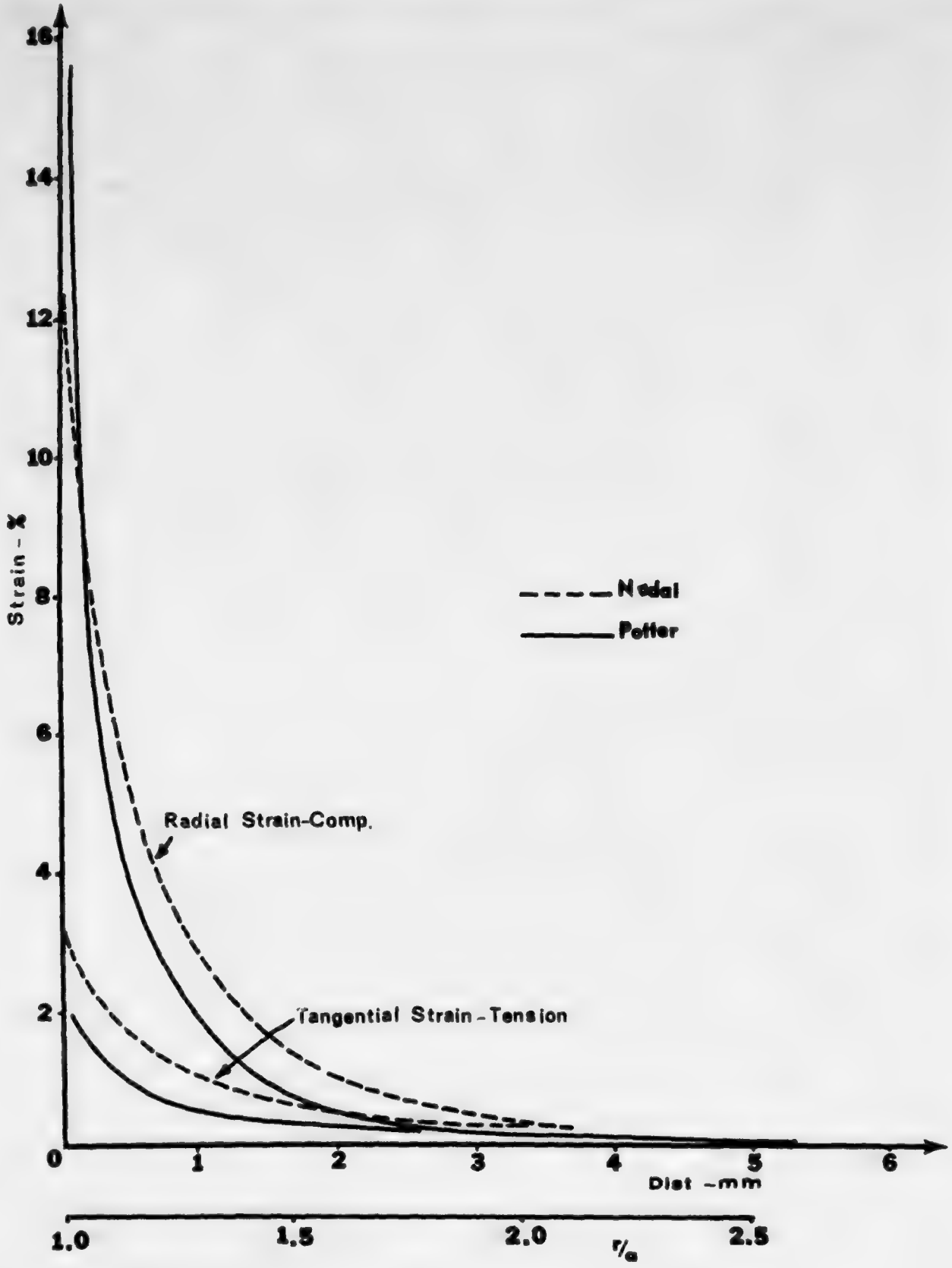

Figure 6.3 Residual strains after coldworking for the non-workhardening theories.

with experiments in which he slowly forced a rotating mandrel of very small taper into a hole in a thin lead sheet. The agreement was excellent. His stresses and strains would be the same as Nadai's in Figures 6.2 and 6.3 for the test cases if the same value of r_p was used. Taylor did not give an explicit relation between r_p and u_a.

6.4. Swainger Theory

In 1945 Swainger [16] published a theory of plasticity and calculated the stresses and residual stresses around an expanded hole to illustrate its usefulness. He founded his theory on certain observations of plastic behavior that are well-known today and treated the material as having a bilinear stress-strain curve with elastic slope E and plastic slope P. Under three-dimensional loading, the material was assumed to yield according to the Mises-Hencky theory at stresses σ_{ox}, σ_{oy}, σ_{oz}. The relation between total strain ϵ_x (for example) and the applied stresses σ_x, σ_y, σ_z is:

$$\epsilon_x = \frac{1}{P}[\sigma_x - p(\sigma_y + \sigma_z) - \sigma_{ox} + p(\sigma_{oy} + \sigma_{oz})] + p\frac{1}{E}[(p - q)(\sigma_y + \sigma_z) + \sigma_{ox} - p(\sigma_{oy} + \sigma_{oz})]. \tag{6.13}$$

Here, p = the "plastic Poisson's ratio" and q = Poisson's ratio.

This expression is really no different from that of Nadai ([17], page 383), which reads:

$$\epsilon_x = \frac{1}{E_s}[\sigma_1 - p(\sigma_2 + \sigma_3)] + \frac{1}{E}[\sigma_1 - q(\sigma_2 + \sigma_3)]. \tag{6.14}$$

The only difference is in the definition of the "plastic modulus"; P is the slope of the curve in the plastic region, and E_s is the stress of the uniaxial curve divided by the residual plastic strain.

Of course Swainger's theory allowed one to handle materials with stress-strain curves that were not simply bilinear by dividing the curve into linear increments. He illustrated this procedure by considering the problem in "Yield under Plane Stress due to Pressure in a Circular Hole in a Large Plate." His assumptions were:

1) uniform pressure on the inside of the hole;
2) Mises-Hencky yield criterion;
3) a stress-strain curve approximated by incremental straight line.

First, he solved the problem for bilinear stress-strain behavior, producing the following equations:

$$\frac{\sqrt{3}\,\sigma_r}{\sigma_o} = \left(\frac{A}{4} - 1\right)\frac{r_p^2}{r_2} + \frac{A}{2}\left(\ell n\,\frac{r}{r_p} - \frac{1}{2}\right)$$

$$\frac{\sqrt{3}\,\sigma_\theta}{\sigma_o} = -\left(\frac{A}{4} - 1\right)\left(\frac{r_p}{r}\right)^2 + \frac{A}{2}\left(\ell n\,\frac{r}{r_p} + \frac{1}{2}\right)$$

$$\frac{4}{(1+p)}\,\frac{\sqrt{3}}{\sigma_o}\,\frac{u}{r} = \frac{1}{P}\left[(A-4)\left(\frac{r_p}{r}\right)^2 + 4 - A + 2A\left(\frac{1-p}{1+p}\right)\ell n\,\frac{r}{r_p}\right] \qquad (6.15)$$

$$+\frac{1}{E}\left[\frac{p-q}{1+p}\left[-(A-4)\left(\frac{r_p}{r}\right)^2 + 2A\,\ell n\,\frac{r}{r_p} + A\right] - 4\right]$$

$$A = 2(1+p)\left(1 - \frac{P}{E}\right).$$

With this solution in hand, he considered the same problem, but for a stress-strain curve of general curvature as is observed in real materials. He divided the region inside r_p into annular strips whose thickness must be determined. He expanded the stresses, strains, and displacement in terms of D_m where

$$D_m = \frac{r_m + 1 - r_m}{r_m} \qquad m = 0, 1, 2, \ldots. \qquad (6.16)$$

r_o corresponds to r_p, the elastic-plastic boundary, and one moves inward so that D_m is always negative. The expressions for stresses are:

$$\sigma_{r(m+1)} = \sigma_{rm}(1 - D_m) + D_m\sigma_{\theta m}$$

$$\sigma_{\theta(m+1)} = \sigma_{\theta m}(1 - D_m) + D_m\sigma_{rm} + \frac{D_m A_m S_o}{\sqrt{3}} \qquad (6.17)$$

$$A_m = 3\left(1 - \frac{P_m}{E}\right).$$

These equations are assumed to adequately represent the variation in stresses σ_r and σ_θ across an incremental ring subjected to radial loading.

To solve a problem by this method, one chooses, for a given material and initial hole size, a value of r_p and follows the incremental procedure back to the initial hole diameter "a" to find out what pressure and displacement occurred at the initial hole boundary. This is an inverse of the normally stated problem.

The parameter D_m is not assigned arbitrarily; the uniaxial stress-strain curve is arbitrarily divided into linear portions and D_m computed from consideration of S_{m+s} and S_m where

$$S_m^2 = \sigma_{rm}^2 - \sigma_{rm}\sigma_{\theta m} + \sigma_{\theta m}^2 . \tag{6.18}$$

This calculation gives:

$$D_m = \frac{-\left(S_{m+1}^2 - S_m^2\right)}{3(\sigma_{rm} - \sigma_{\theta m})^2 + \frac{A_m S_o}{\sqrt{3}}(\sigma_{rm} - 2\sigma_{\theta m})} . \tag{6.19}$$

After D_m is computed, $\sigma_{r(m+1)}$ and $\sigma_{\theta(m+1)}$ are calculated and the displacement is given by:

$$u_{m+1} = u_m + \frac{D_m r_m}{1 - D_m}\left\{\frac{1}{P_m}\left[\sigma_{rm} - \frac{\sigma_{\theta m}}{2} + \frac{3}{2}\frac{S_o}{\sqrt{3}}\right] + \frac{1}{E}\left[\left(\frac{1-2q}{2}\right)\sigma_{\theta m} - \frac{3}{2}\frac{S_o}{\sqrt{3}}\right]\right\} . \tag{6.20}$$

It should be noted that equations (6.17) - (6.20) as printed in Swainger's paper are incorrect.

The residual stresses and strains are plotted in Figures 6.4 and 6.5 for two methods of calculation. In the first case, the material behavior is treated as <u>bilinear</u>. In the second case, the stress-strain curve is broken into linear regions and equations (6.17) - (6.20) used to compute the solution in an <u>incremental</u> fashion. There is little difference between the bilinear and incremental calculations because the material behaves in a nearly bilinear manner. The only difference between the two arises because of the rounding of the stress-strain curve in the neighborhood of the transition from the elastic to plastic state. Note that this theory predicts $r_p = 1.5a$, a considerably smaller value than predicted by Nadai.

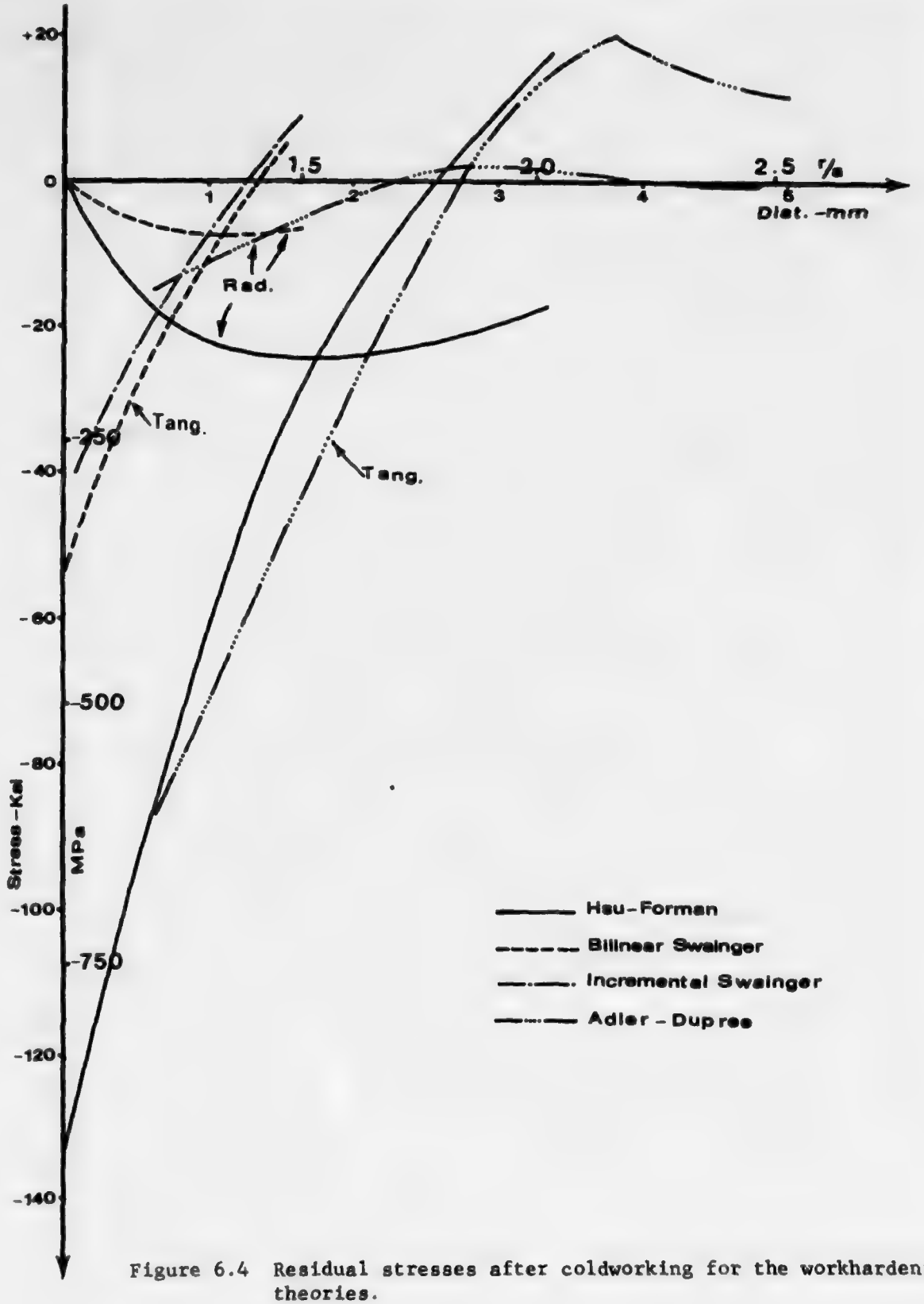

Figure 6.4 Residual stresses after coldworking for the workhardening theories.

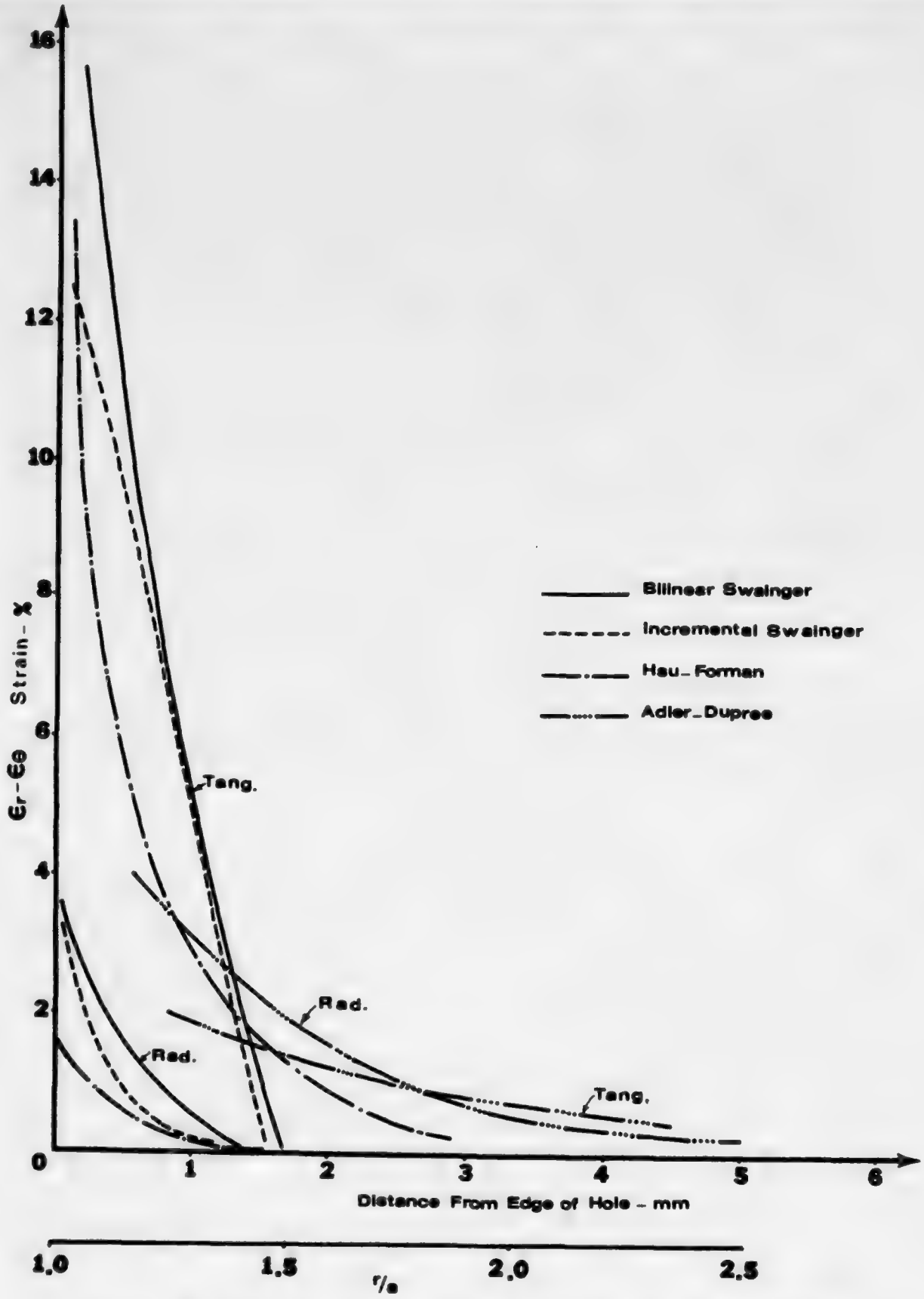

Figure 6.5 Residual strains after coldworking for the workhardening theories.

6.5. Alexander-Ford and Mangasarian Theories

Alexander and Ford [18] and Mangasarian [19] both made calculations of the stresses and strains in the plastic region in which they accounted for elastic deformation and allowed for work-hardening. The solutions in both cases were generated numerically. Mangasarian computed the solution by both the deformation theory and the incremental theory of plasticity and found little difference between the two solutions.

6.6. Carter-Hanagud Theory

Carter and Hanagud [20] in 1974 performed an experimental investigation of the stress corrosion susceptibility of coldworked holes. Their point was that the residual tensile stresses surrounding the hole could be above the threshold value for stress corrosion cracking. They used the same theory as Taylor [15], but generated a relation between u_a and r_p. Their assumptions were:

1) radial displacement at the edge of the hole;
2) Tresca yield condition;
3) elastic-plastic material response.

Their stresses were given by the same relations as Taylor's (similar to equation (6.11)). They did not compute strains, but generated the following relation between u_a and r_p:

$$u_a = u_{aE} + \frac{\sigma_o}{2E}\left\{(3-\nu)\left(\frac{a}{2}\right)\left(\frac{r_p^2}{a^2}-1\right) - 2(1-\nu)\,a\,\ell n\left(\frac{r_p}{a}\right)\right\}. \tag{6.21}$$

The elastic deformation is included in developing this equation. Their stresses are shown in Figure 6.2. Note that they predict $r_p = 3.15a$, which is larger than from other theories.

6.7. Adler-Dupree Solution

Adler and Dupree [3] performed an elastic-plastic finite element analysis of the two-dimensional stress field around a coldworked hole. They assumed plane stress and accounted for plastic behavior of the material by a Ramberg-Osgood formulation which relates the equivalent plastic strain to the nth power of the equivalent stress. The radially symmetric finite element mesh was made up of quadrilateral elements divided into two layers with two triangular elements in each layer. The specific problem

they considered was a 0.006 inch (0.15 mm) radial expansion of a 0.260 inch (6.60 mm) hole in 7075-T6 aluminum and then removal of that expansion (the same as our test case). This models the coldworking process of J. O. King, Inc., in which an oversized tapered mandrel is pulled completely through a hole. The closest they could get to the hole edge for their computation was 0.025 inches (0.64 mm). Two-dimensional plots of stresses and strains for the expanded hole, the relaxed hole, and a hole subjected to remote uniaxial tension are given. A typical result giving the variation in radial strain, ϵ_r, and tangential strain, ϵ_θ, as a function of distance from the hole edge is presented in Figures 6.4 and 6.5.

6.8. Hsu-Forman Theory

The Hsu-Forman theory [21] of 1975 is basically the Nadai theory extended to account for work-hardening. The material behavior is represented by

$$\epsilon = \frac{\sigma}{E} \quad \text{for} \quad |\sigma| \le \sigma_o$$
$$\epsilon = \frac{\sigma}{E} \left|\frac{\sigma}{\sigma_o}\right|^{n-1} \quad \text{for} \quad |\sigma| \ge \sigma_o . \tag{6.22}$$

The 7075-T6 aluminum is adequately represented by $n = 15$, $\sigma_o = 78.2$ ksi (539 MPa). The assumptions are:

1) uniform pressure at the hole;

2) Mises-Hencky yield criterion;

3) Ramberg-Osgood representation of stress-strain curve.

The solution is developed in terms of a parameter a which varies between 90° and a_a. a_a corresponds to a radial expansion u_a and is equal to 134° for our case. The stresses, strains, and displacements are given in terms of a. There are a few easily-recognizible typographical errors in their paper. For the 0.006 inch radial expansion, the elastic-plastic boundary is found at $r_p = 2.01a$. The stresses and strains are plotted in Figures 6.4 and 6.5.

6.9. Potter-Ting-Grandt Theory

Potter and Ting [22] developed a solution to the general problem, and then Potter and Grandt [23] applied this solution to coldworked holes with an eye towards making it useful to designers. Their assumptions were:

1) uniform radial displacement at the hole;

2) Mises-Hencky yield criterion;

3) elastic-plastic material response.

Their work is similar to the earlier work of Nadai [4], except that they did not use a linearized yield criterion. The later work of Hsu-Forman contains their solution for loading as a special case. However, there are three important differences between the Potter-Grandt theory and these other two:

1) Potter-Grandt computed the yielding associated with unloading; they did not simply superpose an elastic solution. This changes the shape of the residual tangential stress curve near the hole edge (see Figure 6.2).

2) The geometry they considered was a finite ring of outer radius "b".

3) Their solution is not presented in closed form; the differential equation is solved numerically.

Nadai's theory (before linearization of the yield condition) shows that there is a limiting value of $r_p = 1.75a$ corresponding to the maximum allowable pressure. This restriction on the deformation shows up in the Potter-Grandt theory as a limitation on the allowable radial displacement. For the 7075-T6 material, this maximum radial displacement is 0.0053 inches, so the 0.006 inch radial expansion of the experiments is not permitted. Stresses and strains based on $u_a = 0.0053$ and a yield stress of 77.6 ksi have been provided by Major Potter and are depicted in Figures 6.2 and 6.3.

6.10. Discussion

The theories for predicting the stresses and strains around a cold-worked hole fall into two classes: those that allow workhardening (Figures 6.4 and 6.5) and those that do not (Figures 6.2 and 6.3). Within each class there is considerable variability as to the predicted response. All of the theories (except the finite-element one) considered are of the deformation, not incremental, type.

In the nonworkhardening theories, Carter-Hanagud account for the elastic deformation in computing their relation between u_a and r_p. This, plus the use of a different yield criterion (Tresca versus linearized Mises-

Hencky), causes their residual stresses to be considerably different from Nadai's. Potter-Ting-Grandt use still a different yield criterion (Mises-Hencky) and get a much smaller value of r_p. Within this class, the choice of yield criterion and decision whether to include elastic strain make a lot of difference. The Potter-Ting-Grandt theory is more complete because it accounts for elastic deformation, uses the nonlinear Mises-Hencky criterion, and computes yielding on unloading.

All of the workhardening theories account for the elastic deformation inside r_p. The assumptions that Swainger makes about the variation of stresses over the incremental plastic rings predicts results considerably different from the other two theories. The finite-element computation of Adler-Dupree suffers from an inability to compute (cheaply) values near the hole edge. However, it does compute yielding on unloading. The Hsu-Forman theory is the most general of all theories developed; furthermore, it is presented in a workable closed form that makes for economical computation.

In all of these theories, plane stress and small deformations are assumed. The strain computed at the hole edge are on the order of 0.1. This is certainly large enough to cause significant errors in these deformation theories ($\epsilon \ll 1$ is required for small deformations). Furthermore, the large deformations near the hole edge raise serious questions as to whether the state of stress remains plane there.

The assumption of elastic unloading is not correct; the residual stresses violate the yield criterion near the hole when this assumption is used. This difference may be significant, because in the Potter et al. theory it affects the residual tangential strain for approximately 0.5 mm from the hole edge. A complete theory, retaining the plane stress and small strain assumptions, would be the Hsu-Forman theory with yielding computed upon unloading.

As to experimental verification of any of these theories, it would be very difficult to match the boundary conditions at the expanding hole. Taylor did do this by pressing a rotating, slightly tapered mandrel into a very soft, thin sheet, but that is far removed from a practical coldworking process. Also, the higher coldworking levels of interest are really at the edge of or beyond the limits of the theories. Nevertheless, for modeling practical coldworking operations, theories of this type that accurately predict

the stress and strain are needed. The next section compares the residual strains predicted by these theories with those measured on specimens subjected to a particular coldworking process.

7. COMPARISON OF THEORIES WITH EXPERIMENTS

The experimental data used for comparison in this section is the average strain between the front and the back of the specimens. The front and back strains were plotted separately in section 5, as were values of standard deviations of the measurements. Using the average value near the hole edge must be done with care since the nature of the deformation is so different on the front versus the back. The average value is more useful for positions greater than 1 mm from the hole. Although it is always desirable to have more data, enough has been obtained to describe the residual strain field with confidence. The three theories used for comparison are those from section 6 that come closest to predicting the measured residual strain field for the particular expansion considered.

Figures 7.1 and 7.2 compare the theories and experiments. Comparisons should only be made away from the hole edge. The Adler-Dupree computation predicts higher radial and tangential strains than the other two theories (and a larger plastic zone). As the thickness of the specimen is reduced, the Adler-Dupree solution predicts the radial residual strain quite well for distances larger than 2 mm from the hole edge. This leads to two observations: the 1/4 inch (6.4 mm) specimen is not in a condition of plane stress, and the complicated deformation of the expanded hole looks like a uniform radial expansion if one moves far enough away from the hole. The difference in the Adler-Dupree solution from the other two is the inclusion of yielding in the unloading. Note how close together the Nadai and the Hsu-Forman theories are in spite of the fact that Nadai's theory is for a perfectly plastic material.

None of the theories agree with the residual tangential strain data. All of the data looks more or less the same away from the hole; there is not the clear-cut separation of the 1/4 inch (6.4 mm) specimen data from the other two. It is somewhat disturbing that the Adler-Dupree tangential strain prediction isn't in closer agreement. The Adler-Dupree results are different in the following ways: all other theories and all experimental results show the residual radial strain to be always larger than or equal to

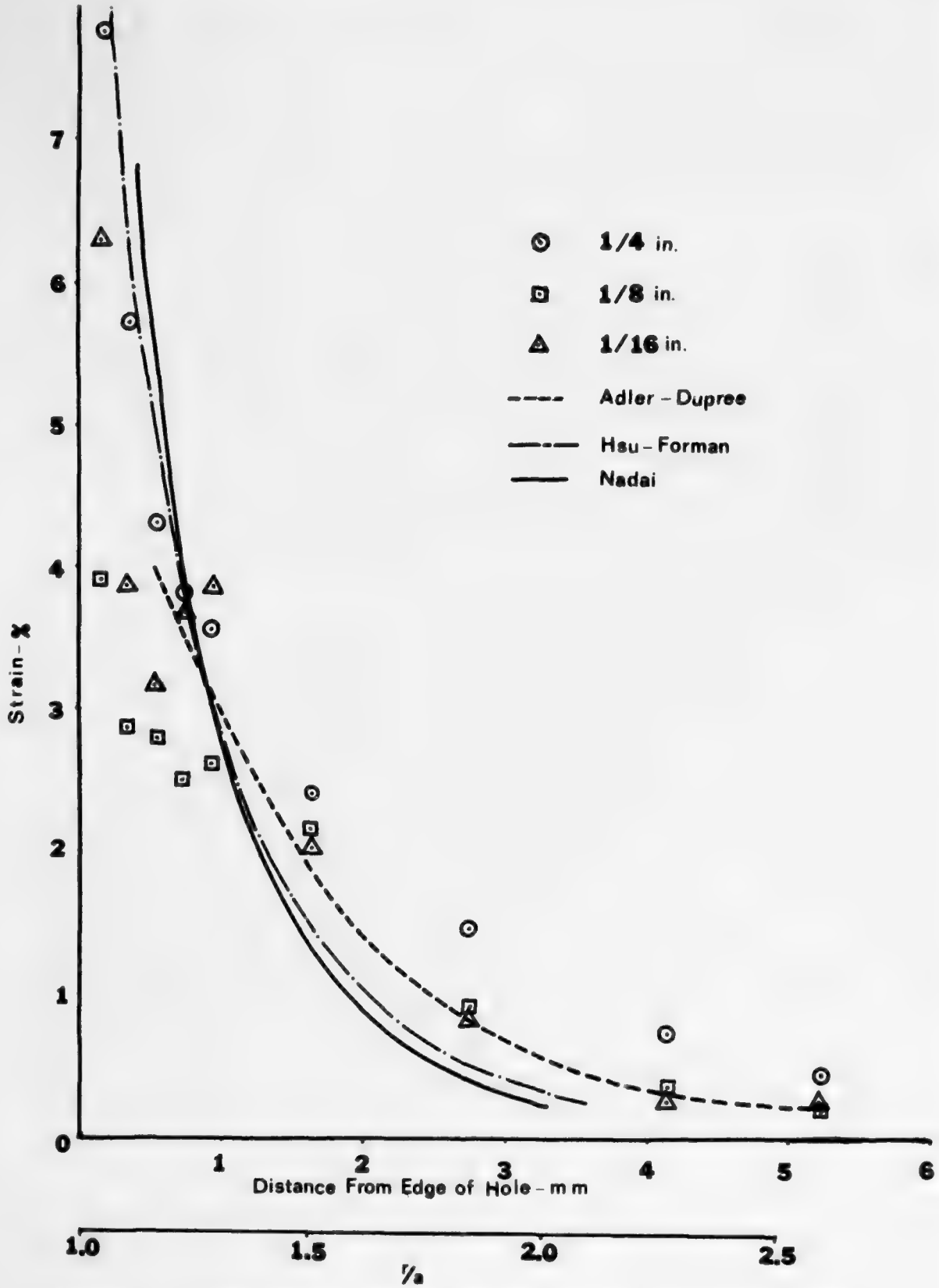

Figure 7.1 Comparison of average residual radial strains with three theories.

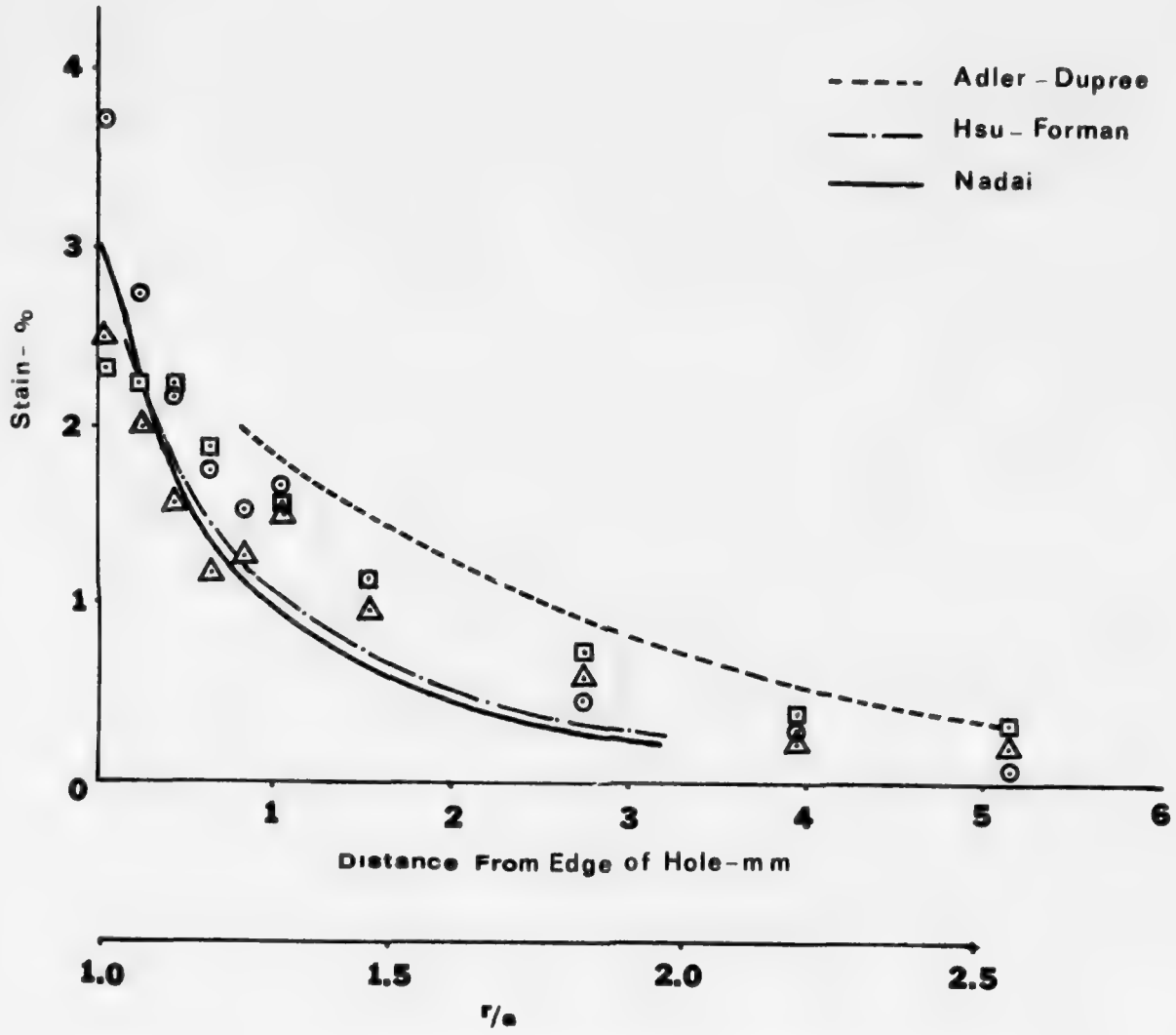

Figure 7.2 Comparison of average residual tangential strain with three theories.

the tangential; Adler and Dupree show the opposite for distances away from the hole. This can be readily seen by comparing residual strains in their Figure 2.11 for positions greater than about 0.25 inches along the axes. If the material in the plastic zone is incompressible, their result means that the specimen gets thinner away from the hole. Their computation for "mandrel in," i.e., the strains when the hole edge is held at the 0.006 inch (0.15 mm) shows the radial strain to be always larger; the change comes upon unloading.

At this level of expansion the residual strains away from the hole are not very sensitive to the amount of deformation at the hole. This is illustrated for radial strains by the experimental results of Figure 7.3 and by the Hsu-Forman theory in Figure 7.4. If one attempts to use strain measurements away from the hole to infer the strain at the hole, that is going to be difficult for large amounts of coldworking.

The region of interest is of course near or at the hole edge. This is where the stress concentration upon loading is largest and where the residual compressive stress in the tangential direction is largest (Potter et al. show it largest slightly away from the hole). Physically this deformation is very nonhomogeneous and variable through the specimen thickness. Measurements near the hole edge are going to have a lot of scatter. The best one can hope to do theoretically is to use the time-honored assumptions of homogeneity and isotropy to predict an average residual strain that agrees quantitatively with the average measured strain near the hole even though it varies through the thickness.

This particular coldworking process does not produce the uniform through-the-thickness radial expansion that the theories assume. However, one can conclude from Figure 7.1 that the finite-element technique does a fairly good job of predicting the residual strain (ignoring the tangential strain). It appears that the modeling of this coldworking process in terms of a uniform radial expansion is a reasonable one. If the Adler-Dupree computation used a finer mesh near the hole, one would expect even better agreement for the radial strain.

It must be pointed out that the large level of coldworking used is perhaps an unfair comparison for the theories. Lower levels of coldworking with the attendant smaller deformations would give the theories a better chance.

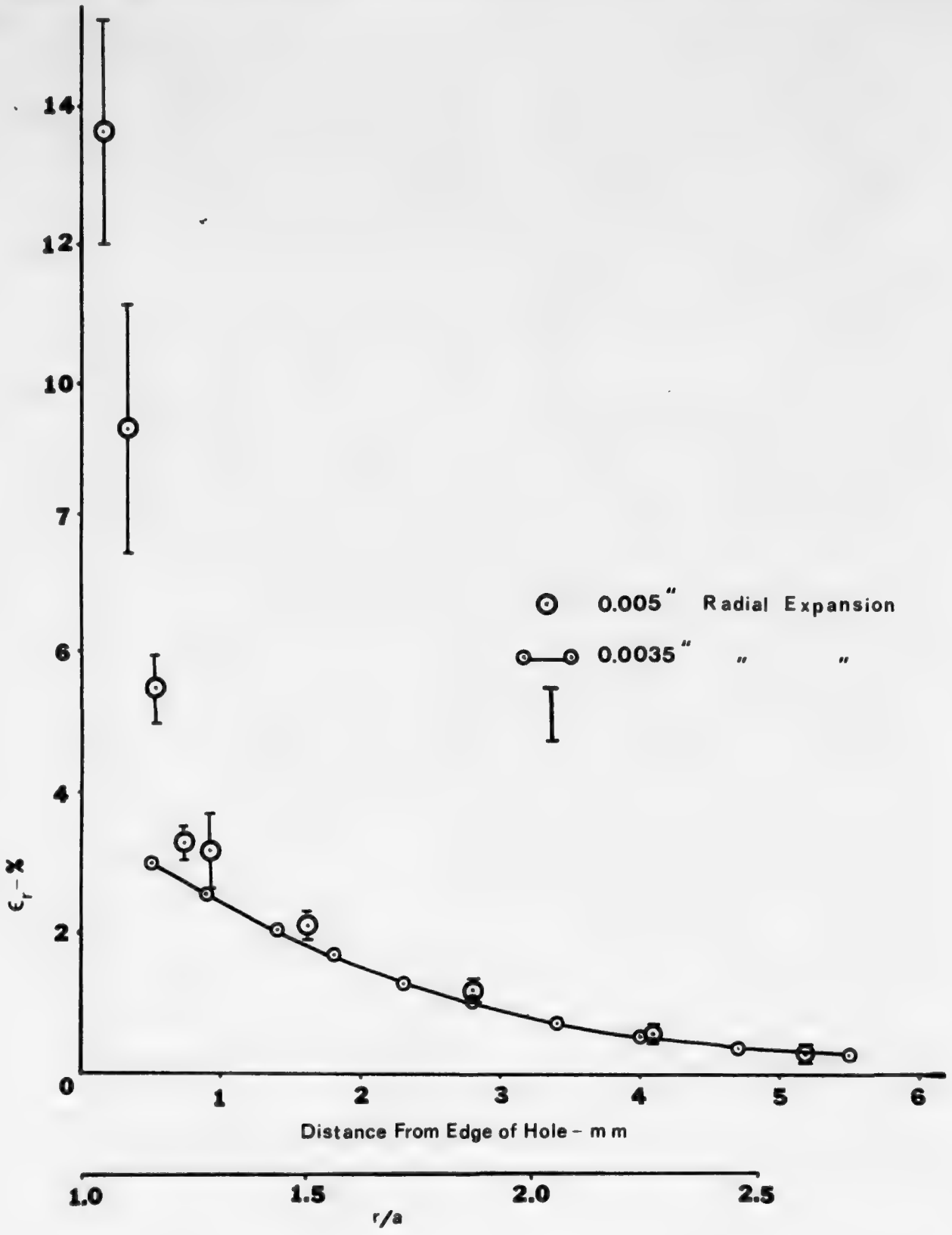

Figure 7.3 Residual radial strains for different diametral expansions of a 0.260 inch (6.6 mm) hole in a 1/4 inch (6.4 mm) plate.

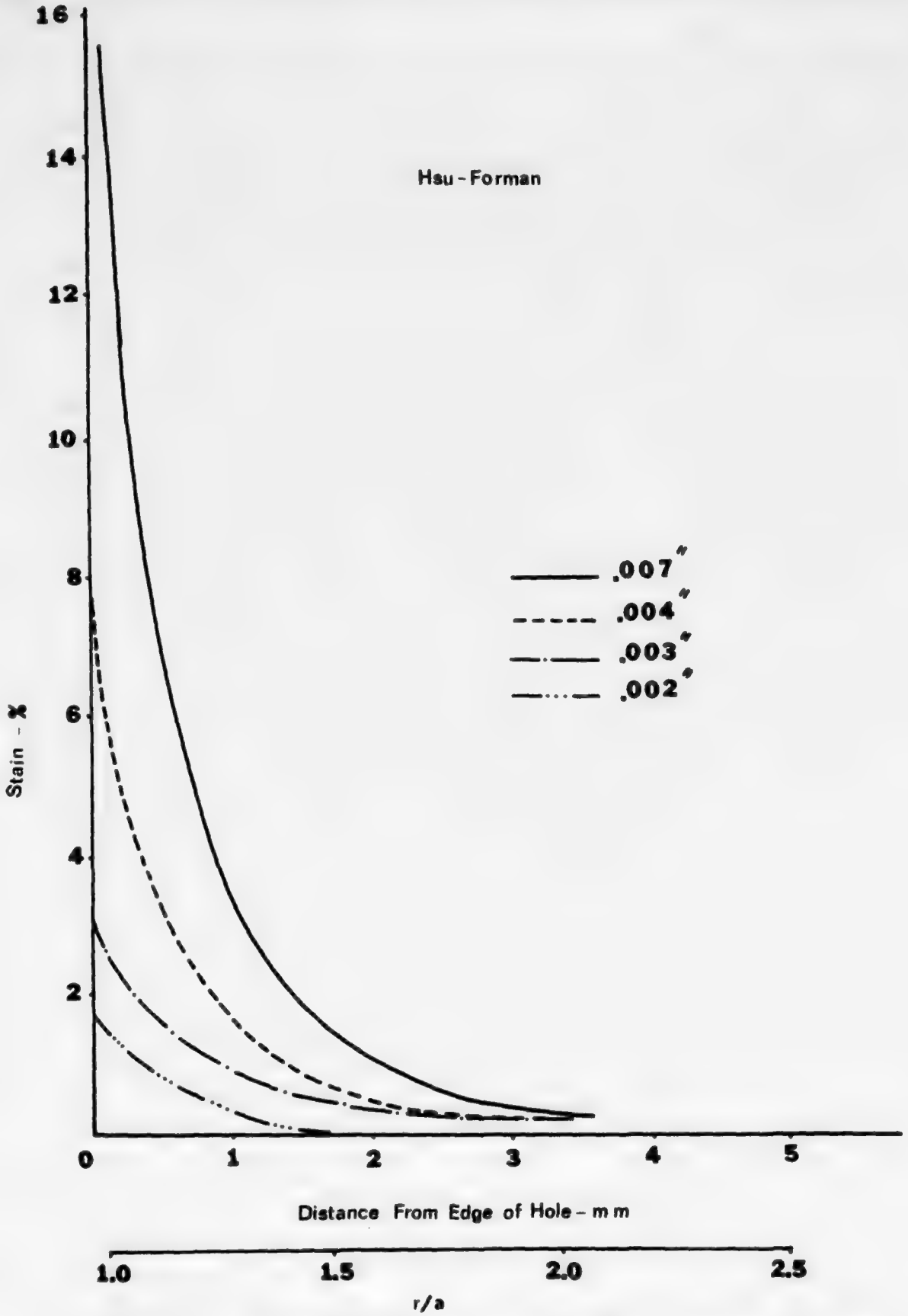

Figure 7.4 Residual radial strains for various diametral expansions of a 0.260 inch (6.6 mm) hole as predicted by the Hsu-Forman theory (21).

Though the Adler-Dupree computation gives the best agreement, it would be most useful to have a less expensive closed form solution. The Hsu-Forman theory with the addition of yielding on unloading or the Potter-Ting-Grandt theory with the addition of workhardening would appear to be the best choices. The next step in complication would be to include three-dimensional effects.

8. STRAINS DUE TO STATIC LOAD

Specimens of the three thicknesses were instrumented with 0.015 inch (0.4 mm) gage-length foil gages located approximately 0.5 mm from the edge of the hole. These tensile specimens were 18 inches (46 cm) with a 9 inch (23 cm) long test section that was 2.5 inch (6.4 mm) wide. The hole was, of course, located in the center of the test section. This specimen design is the same as that used by Adler and Dupree [3]. Specimens that were not coldworked were tested in addition to the coldworked ones. Before applying the foil gages to the coldworked specimens, the area around the hole on the front side was sanded flat with 400 grit sandpaper to permit good gage bonding. One gage was oriented to measure tangential strain on one side of the hole and one to measure radial strain on the other side. All the tangential gages were of the post-yield type, but some of the radial ones were previously available regular type gages; some of these broke at the higher strains. Several specimens broke in the grips because they were loaded to 68 ksi (470 MPa), which is very near the yield stress of the material.

Stress-strain data for a coldworked and noncoldworked 1/4 inch (6.4 mm) specimen upon loading and unloading are given in Figure 8.1. There is not a great deal of difference between the beahvior of the two specimens. Plotted on Figure 8.1 is the predicted behavior of the tangential strain from Figure 2.20 of Adler and Dupree's report [3]. Their data is taken from their plots of strain distribution as a function of applied load and thus is not very accurately presented. Their computations describe the behavior very well except for the plastic flow at the higher stresses. The strain predicted if the material were completely elastic is also plotted on Figure 8.1. The stress-strain behavior both measured and predicted by Adler-Dupree is elastic to approximately 50 ksi (340 MPa).

Similar data is presented for the 1/8 inch (3.2 mm) specimens in

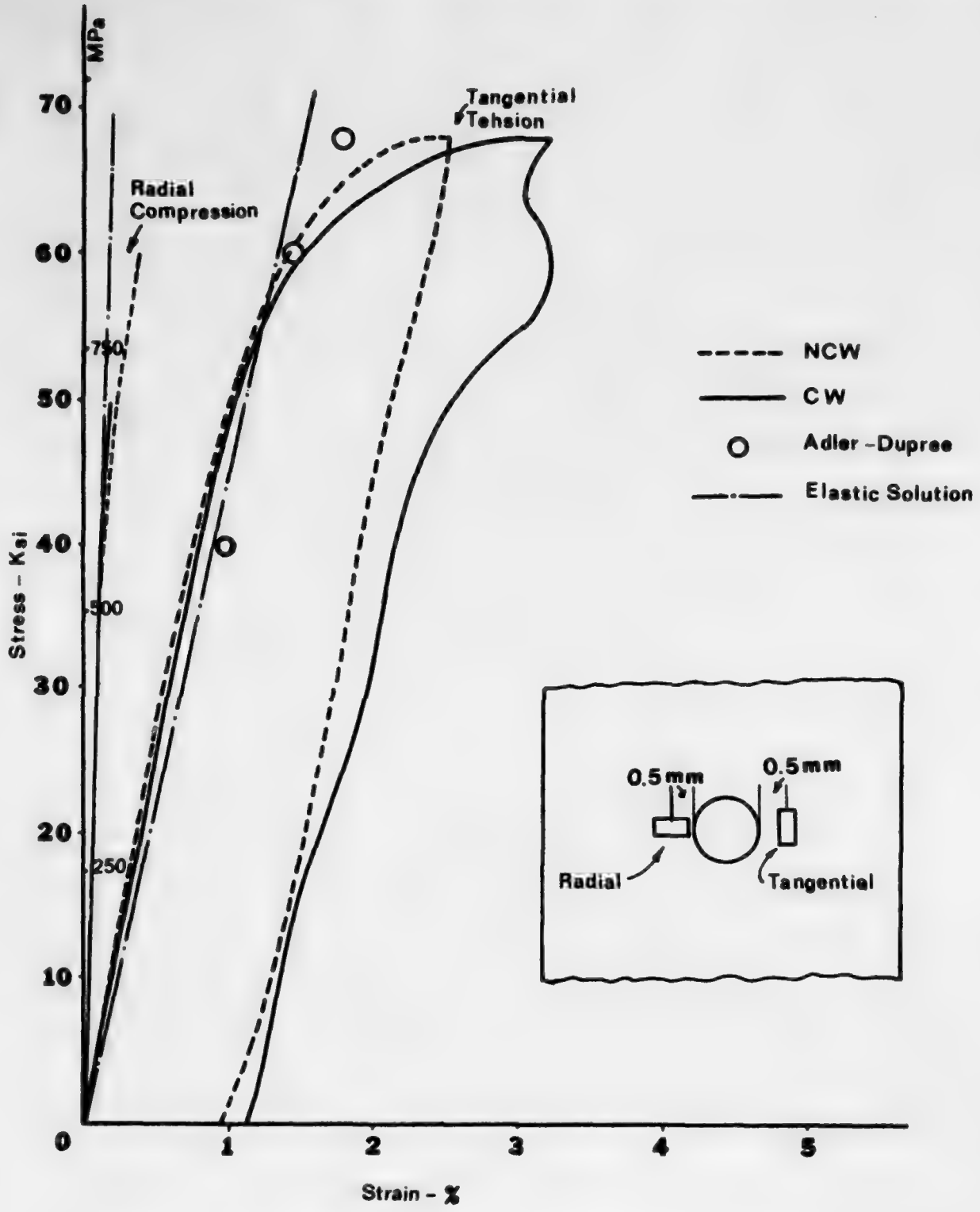

Figure 8.1 Strains near the hole as measured by foil gages on 1/4 inch (6.4 mm) tensile specimens.

Figure 8.2. The behavior of the noncoldworked specimen is very similar to Figure 8.1, but the coldworked specimen deforms quite differently. Remember that the coldworked 1/8 inch (3.2 mm) specimen showed a different residual strain pattern on the front surface.

Figure 8.3 gives the stress-strain data for the 1/16 inch (1.6 mm) specimens, both of which broke in the grips. It is interesting that the behavior of the two is so nearly the same even though the coldworked specimen had been buckled around the hole. This behavior is quite different from the previous two thicknesses, indicating that the three-dimensionality of the stress field in the others is important. The main difference is that this thinner specimen departs from elastic behavior at approximately 40 ksi (276 MPa). The elastic solution and Adler-Dupree's prediction could of course be superposed on Figures 8.2 and 8.3.

One must conclude from these results that coldworking the hole makes little difference in the static behavior away from the hole at the foil gage location. Note that the strains measured on the coldworked specimen have as their initial "zero" value the residual strain already existing in the material.

The 1/4 inch (6.4 mm) thick specimens were also instrumented with the same kind of foil gages at the top (and bottom) of the hole. The strains measured are shown in Figure 8.4. Note that the strain scale has been reduced by 10. The noncoldworked specimen shows some flow in the reverse direction for the radial strain, but the coldworked specimen shows large reverse flow for both radial and tangential strain. Adler and Dupree [3] in their Figure 2.21 predict that the tangential strain will be all compressive. Again, these strains are an order of magnitude smaller than the tangential strains on the side of the hole, but the large amount of flow indicates that the stresses there are quite large.

9. FATIGUE DATA

Some preliminary fatigue tests were run to examine the development and propagation of cracks around the coldworked holes. The available electrohydraulic test machine was limited to a maximum load of 5,000 lb (22,400N), so experiments had to be performed on the 1/16 inch (1.6 mm) specimens. All specimens were 18 inches (46 cm) long by 2.5 inches (6.4 cm) with a 9 inch (23 cm) test section. This is the same

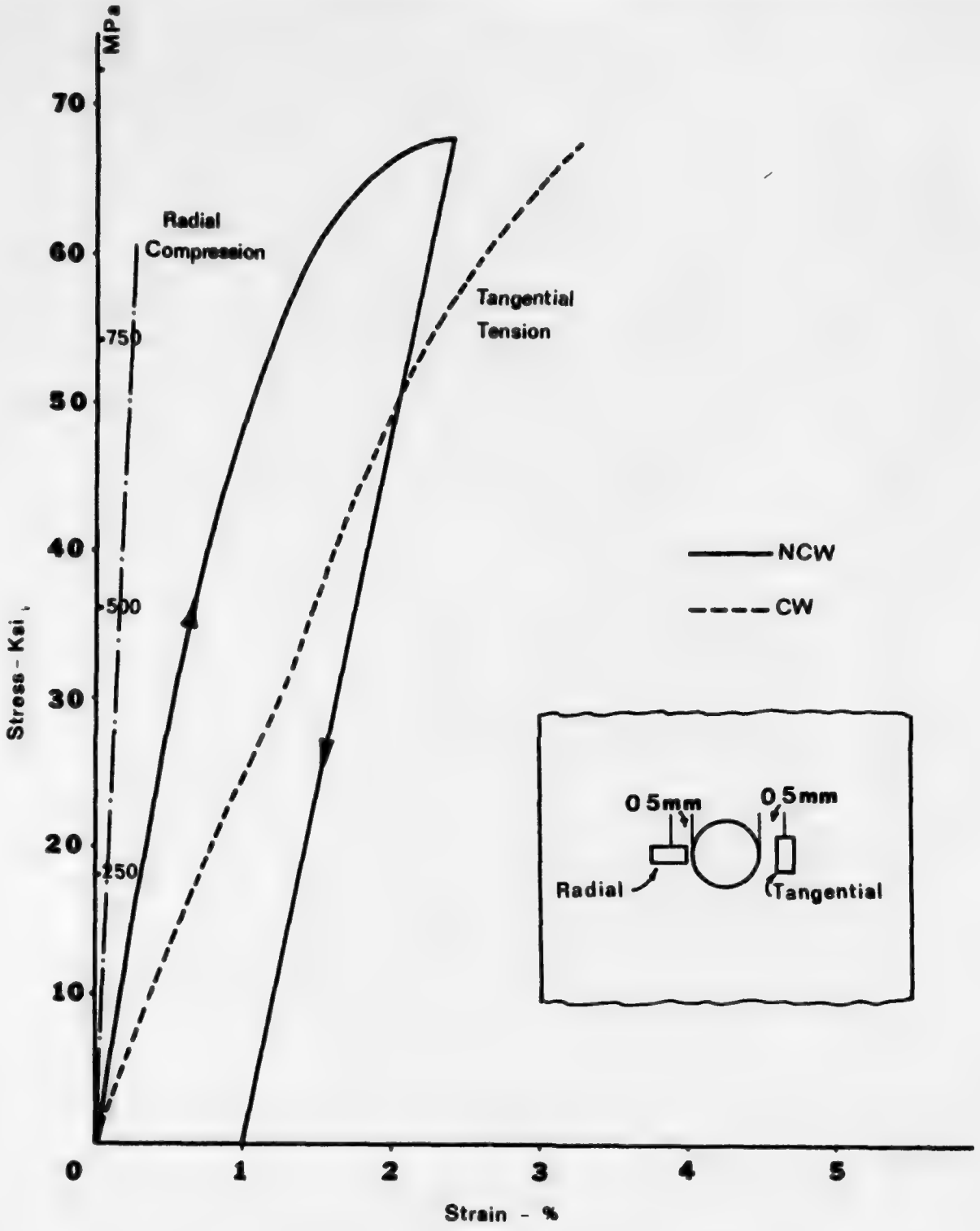

Figure 8.2 Strains near the hole as measured by foil gages on 1/8 inch (3.2 mm) tensile specimens.

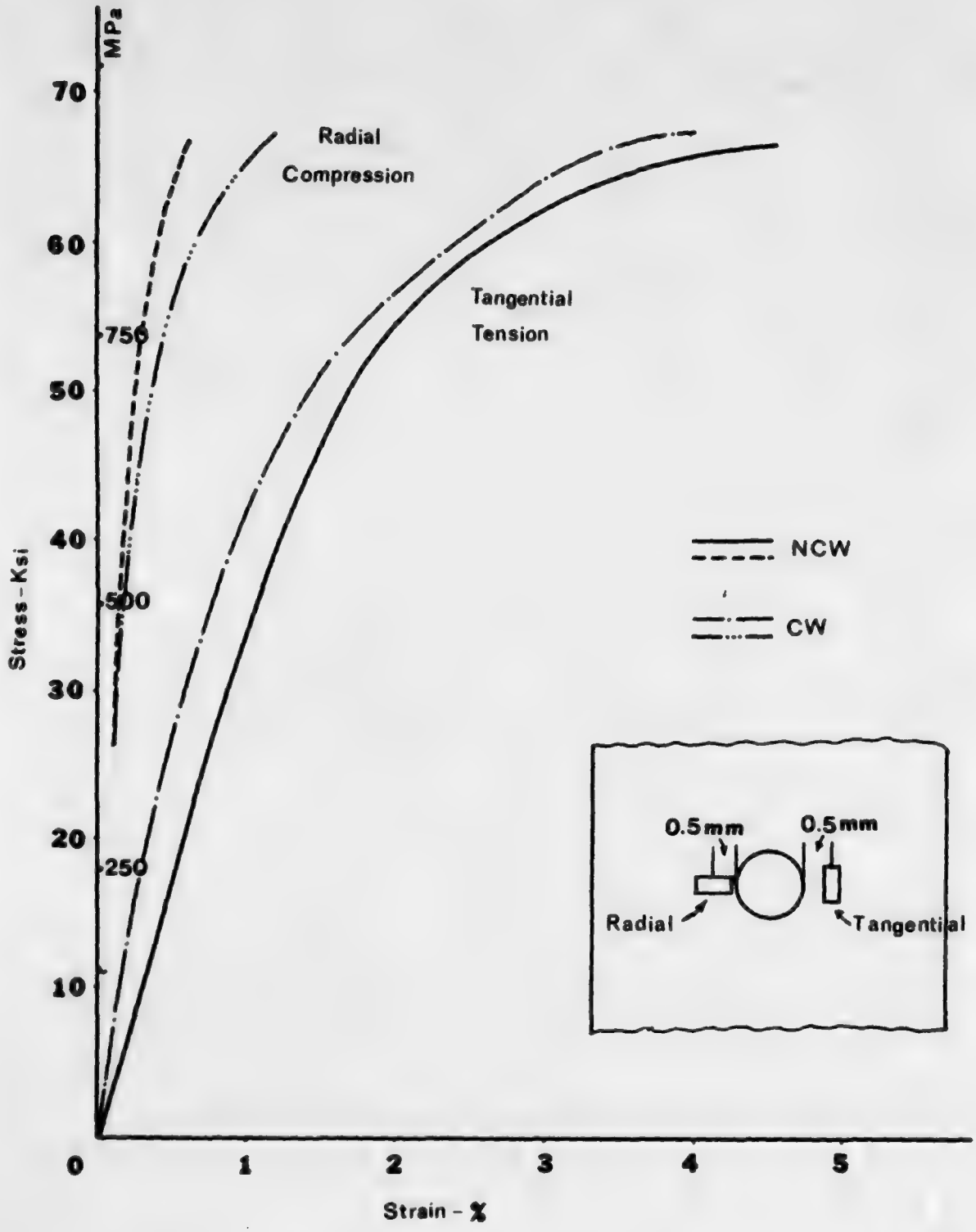

Figure 8.3 Strains near the hole as measured by foil gages on 1/16 inch (1.6 mm) tensile specimens.

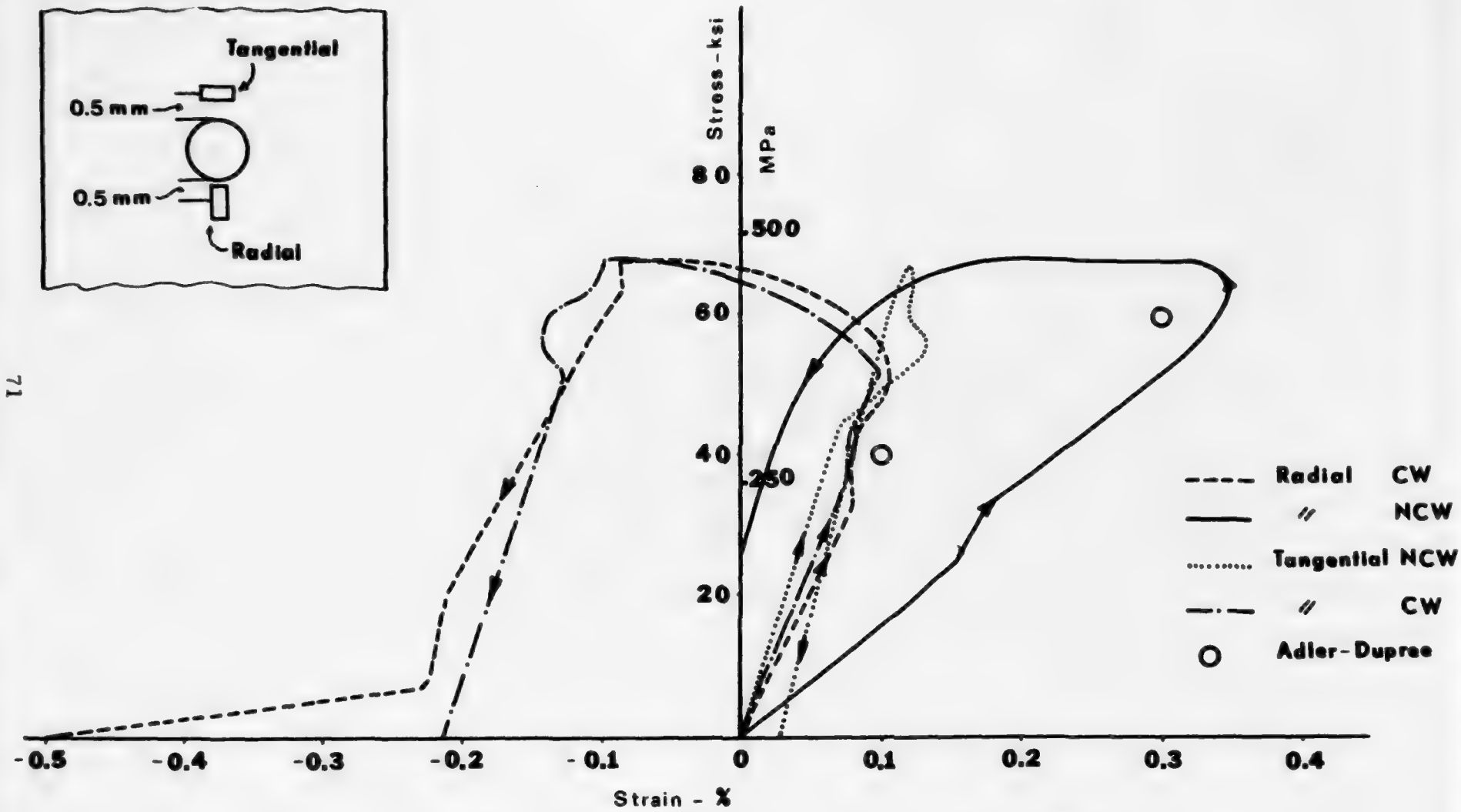

Figure 8.4 Strains measured by foil gages at the top and bottom of the hole in 1/4 inch (6.4 mm) tensile specimens.

configuration as tested by Adler and Dupree [3] except that the fillets reducing the grip ends to the test section are larger. All specimens were fatigue tested with a maximum stress of 30.7 ksi (212 MPa) and minimum stress of 3.1 ksi (21 MPa). From the loading experiments of the previous section one sees that this is near a stress level that would induce static yielding, i.e., these are basically low-cycle-fatigue tests. All tests were run at a loading frequency of 10 Hz. The specimens were fatigue loaded in increments of 2000 cycles until cracks were determined by examining the specimen out of the test machine under a microscope. After a crack (or cracks) had initiated, the specimen was cycled in increments of 1000 cycles.

Crack growth curves for three specimens are given in Figures 9.1 - 9.3. These specimens were all subjected to the same coldworking process on an originally 0.260 inch (6.6 mm) diameter hole (except for the specimen in Figure 3.2, whose original diameter was 0.263 inches (6.7 mm)). Several cracks appeared almost simultaneously in all specimens, and all continued to grow with fatigue loading. The cracks originated at the edge of the holes close to an imaginary line drawn through the center of the hole perpendicular to the load axis. All cracks started at between 6000 and 8000 cycles of loading.

Two specimens that had not been coldworked were fatigue tested under the same conditions. Their behavior is shown in Figure 9.4. On one specimen, cracks grew more or less equally from each side of the hole; on the other, only one crack grew. These cracks all grew exactly along a line perpendicular to the load axis. Note the larger horizontal scale in Figure 9.4.

The interesting result here is of course that the noncoldworked holes had greater fatigue life. The crack growth rate is roughly the same, but the coldworked holes develop cracks sooner. This is in direct contradiction to common experience with coldworking. In particular, Phillips [13] recorded increasing fatigue life with increasing amounts of interference--roughly a factor of 10 for maximum interference over the noncoldworked hole. But those were 0.375 inch (9.5 mm) holes in 0.25 inch (6.4 mm) thick specimens. In a comparison of specimen thickness effects, all 0.375 inch (9.5 mm) holes were coldworked to 0.019 inch (0.48 mm)--equivalent to a 0.013 inch (0.33 mm) expansion on a 0.26 inch (6.4 mm) hole which

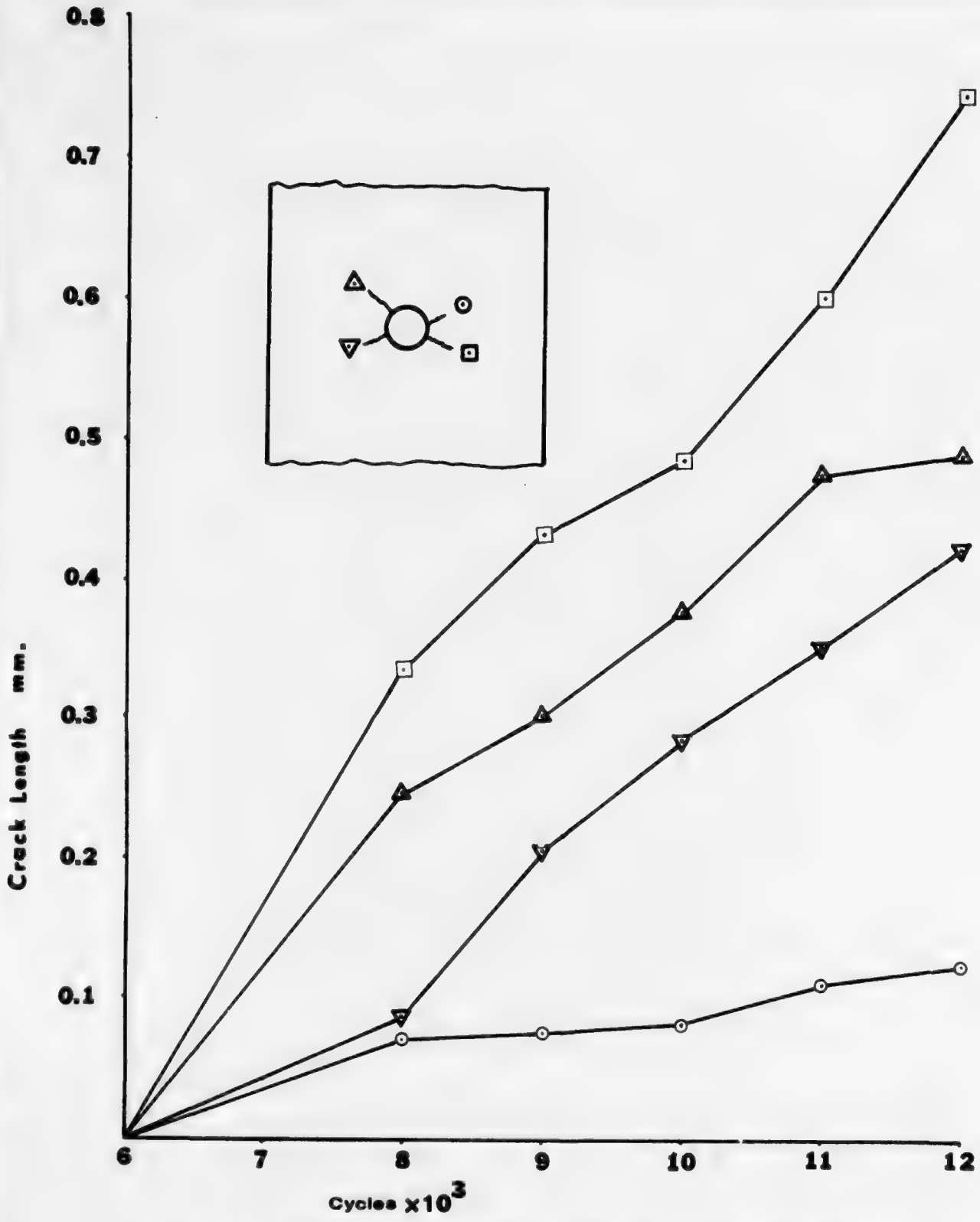

Figure 9.1 Growth curves for cracks emanating from coldworked holes in 1/16 inch (1.6 mm) specimens.

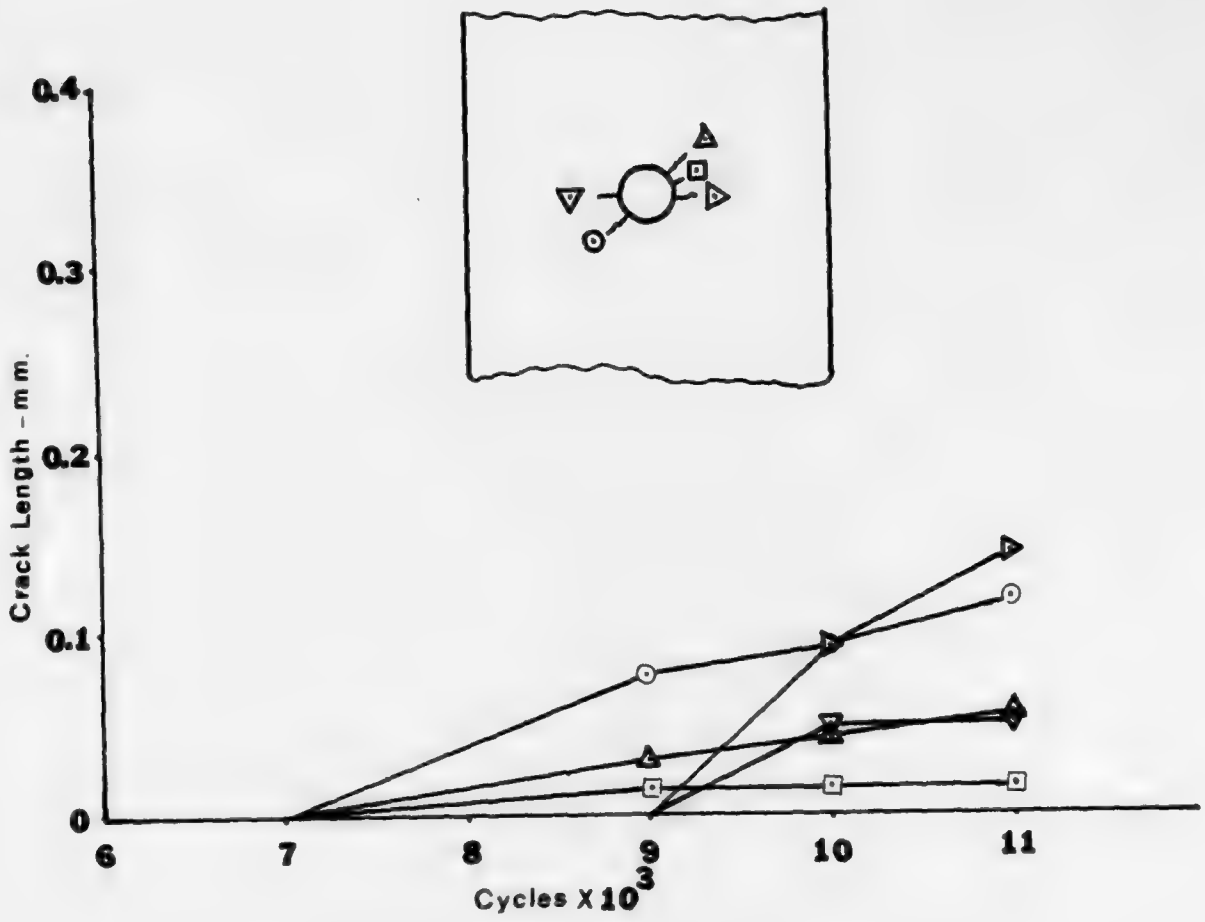

Figure 9.2 Growth curves for cracks emanating from coldworked holes in 1/16 inch (1.6 mm) specimens.

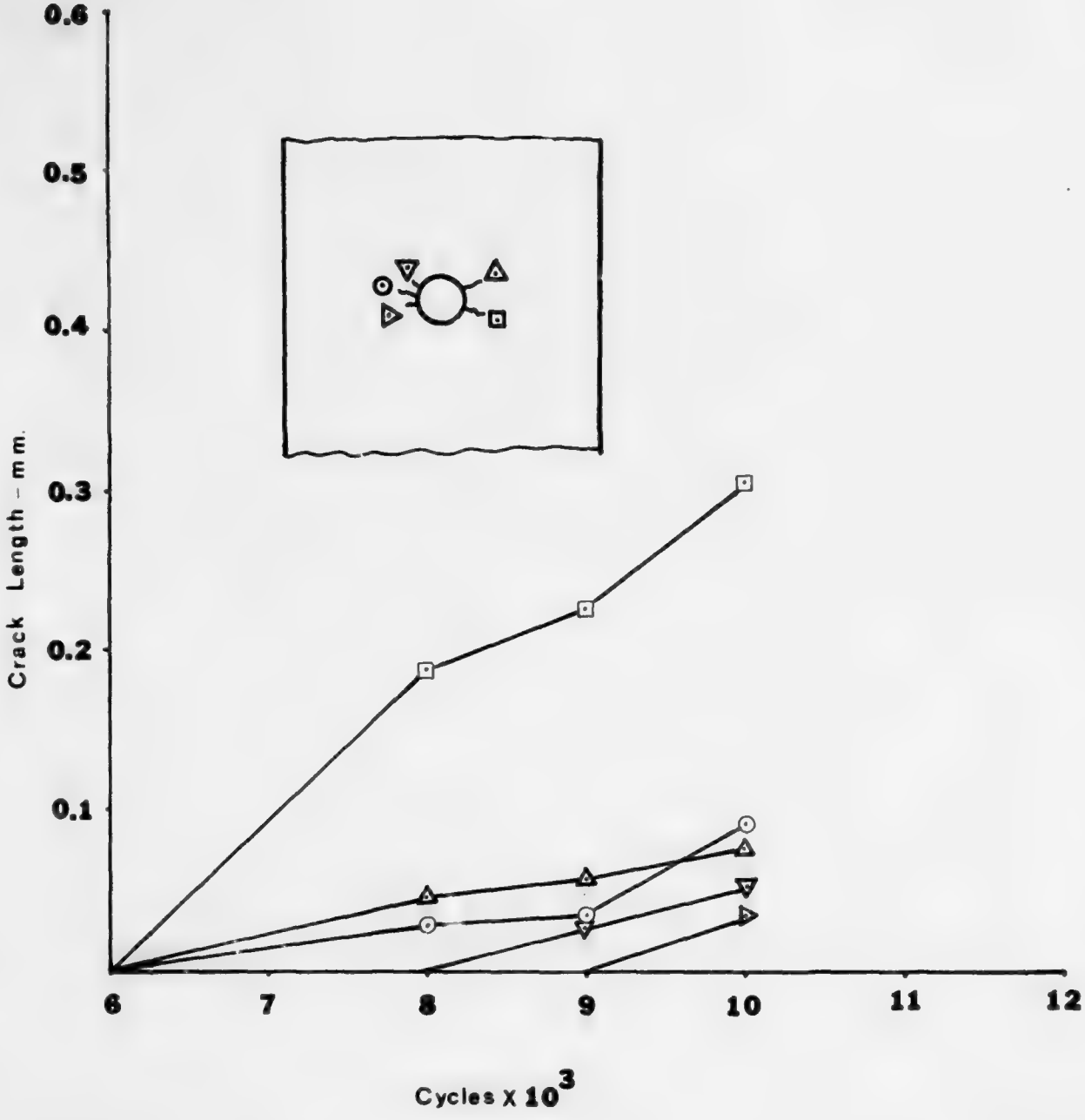

Figure 9.3 Growth curves for cracks emanating from coldworked holes in 1/16 inch (1.6 mm) specimens.

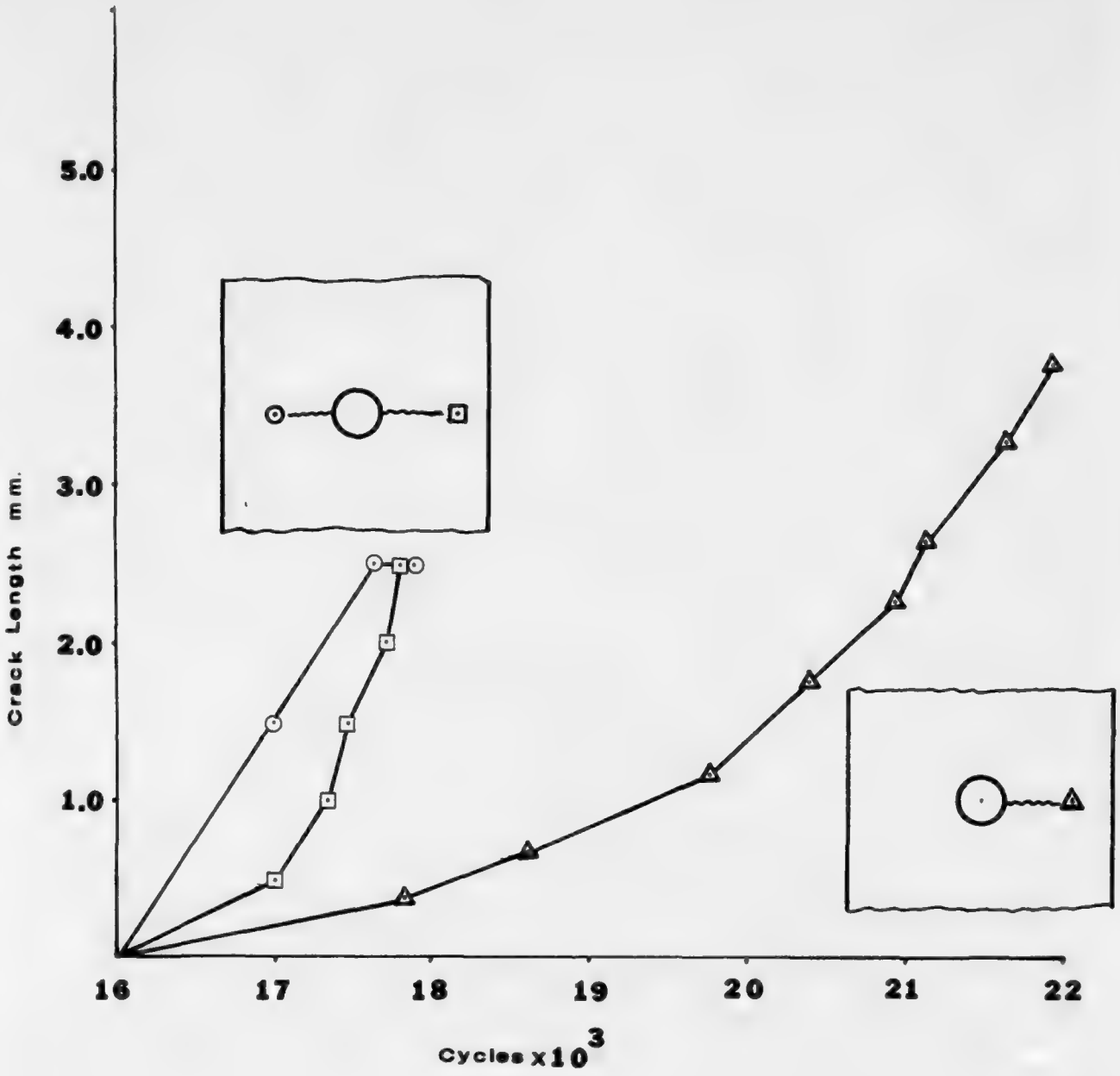

Figure 9.4 Growth curves for cracks emanating from non-coldworked holes in 1/16 inch (1.6 mm) specimens.

is very near to the 0.012 inch (0.30 mm) value used in this report. The larger thickness gave a life to failure of approximately 400,000 cycles, while the thinner specimens lasted only to approximately 40,000 cycles. Their stress levels were 30 ksi (207 MPa) and their material was 2024-T851 aluminum. Their results are consistent with ours--the ratio of hole diameter to specimen thickness is important.

10. CONCLUSIONS

Laboratory specimens can be prepared and tested with satisfactory control of the original hole size and the coldworking procedure. In other words, the results obtained from two specimens subjected to the same treatment are nearly identical. One can then examine the effects of various parameters (such as specimen thickness) with confidence.

Only one amount of radial expansion and hole size [0.006 inches (0.15 mm) and 0.26 inches (6.60 mm)] and one type of mandrel was used in this experimental study because those were used by Adler-Dupree [3]. These parameters are good choices for 1/4 inch (6.4 mm) thick specimens, but not for the thinner ones. The 1/8 inch (3.2 mm) specimens do not expand vertically on the free surface as they should, and the 1/16 inch (1/6 mm) specimens tend to buckle around the hole. A more complete study should consider the effects of various levels of coldwork.

The strains around a coldworked hole are symmetric about a vertical axis through the hole. However, near the edge of the hole the strain is large (several percent), increases sharply, and becomes very inhomogeneous. Because of these difficulties, the measurement of indentations nominally 200 microns apart with a microscope and the moiré method are the two most suitable strain measuring techniques. The strain near the hole is the most critical because that is where fatigue cracks start. Therefore, that strain must be measured and either the largest value, or the average value, used in comparison with theories.

An industrial coldworking process (J. O. King, Inc.) was used for expanding the holes. A sleeve with a lip was inserted into the hole, a tapered mandrel pulled through the hole, and (to compare with theories) the sleeve then removed. This process generates a strain distribution that varies through the thickness of the specimen near the hole. The deformation near the hole is not plane stress; the strain on the surface opposite

the sleeve lip is different than on the surface with the sleeve lip. This industrial process does not produce the uniform radial expansion of the hole edge that all theories assume. The shearing deformation associated with the pulling of the mandrel and the removal of the sleeve is important. However, away from the hole edge after the strains have dropped to two percent or less, the deformation is similar to that caused by a plane stress radial expansion of the hole.

The Adler-Dupree finite-element computation makes the best prediction of the residual radial strain around the hole based on comparisons of strains at locations greater than 1 mm from the hole's edge. The analytical theories predict strains that are smaller away from the hole and too large at the edge of the hole. None of the theories predicts the tangential strain very well. The thinner specimens agree better with the theories than do the 1/4 inch (6.4 mm) specimens, indicating that plane stress is too restrictive as assumption for a hole-diameter-to-thickness ratio of one. Of the various analytical theories considered, the Hsu-Forman [21] and Potter-Ting-Grandt [22, 23] ones are the best.

Experimental evidence shows that the deformation of the elastic-plastic boundary is of the form that would be produced by a uniform radial expansion of the hole. The strains there are equal and opposite in sign and do not vary through the thickness. It is quite possible that a theory would correctly predict the location of this boundary over a range of parameters (e. g., amount of coldworking, material, etc.) and yet not predict the average strain at the hole edge. For large coldworking levels, the location of this boundary does not vary much with amount of coldwork; the evaluation of theories must take this into account.

Only the Adler-Dupree finite-element approach can compute the strains around a coldworked hole subjected to remote loads, and in limited comparisons it indicates the correct trends. Fatigue tests were restricted to 1/16 inch (1.6 mm) thick specimens, and the size of hole and amount of coldwork damage the hole and reduce the fatigue life rather than entrance it.

This experimental study has evaluated and developed strain measuring and specimen preparation techniques for studying the deformation around coldworked holes. Experimental information about the nature of the strain field around a hole that is coldworked by an industrial process has been generated and compared with existing elastoplastic theories. The

primary conclusion is that the theories (which assume a state of plane stress) do not accurately predict the strains near the hold edge, but do a reasonable job of predicting the strains away from the hole, at least for this particular industrial process. The strains near the hole are large and inhomogeneous, which makes their measurement and their comparison with continuum theories difficult. A limitation of this experimental work is that only one coldworking level was studied; future research should be directed toward varying this as well as other parameters.

11. REFERENCES

1. Grandt, A.F., Jr., "Stress intensity factors for some thru-cracked fastener holes," accepted for publication in Intl. J. of Fracture.

2. Wood, H.A., "The use of fracture mechanics principles in the design and analysis of damage tolerant aircraft structures," Fracture Mechanics of Aircraft Structures, AGARD-AG-176, edited by H. Liebowitz (January 1974).

3. Adler, W.F., and D.M. Dupree, "Stress analysis of coldworked fastener holes," AFML-TR-74-44, Air Force Materials Laboratory, Wright-Patterson Air Force Base (July 1974).

4. Nadai, A., "Theory of the expanding of boiler and condenser tube joints through rolling," Trans. ASME 65, 865-880 (November 1943).

5. Allen, M., and J.A. Ellis, "Stress and strain distribution in the vicinity of interference fit fasteners," AFFDL-TR-72-153, Air Force Dynamics Laboratory, Wright-Patterson Air Force Base (January 1973).

6. Carey, R.P., "Experimental determinations of strain fields resulting from interference fit tapered pins," ARL/SM 377, Aeronautical Research Laboratories, Melbourne, Australia (June 1972).

7. Ford, S.C., et al., "Interference-fit fastener investigation," AFFDL-TR-75-93, Air Force Flight Dynamics Laboratory, Wright-Patterson Air Force Base (September 1975).

8. Liu, H.W., and J.S. Ke, "Moiré method," Experimental Techniques in Fracture Mechanics, Vol. 2, Iowa State University Press, Ames, Iowa, 1975.

9. Sharpe, W.N., Jr., and A.F. Grandt, Jr., "A laser interferometric technique for crack surface displacement measurement," Proc. 20th Intl. Instrumentation Symp. of the Instrument Soc. of America (1974).

10. Adams, F.A., and G.E. Maddux, "On Speckle diffraction interferometry for measuring whole field displacements and strains," AFFCL-TR-73-123, Air Force Flight Dynamics Laboratory, Wright-Patterson Air Force Base (December 1973).

11. Lee, T.C., C. Mylonas, and J. Duffy, "Thickness effects in birefringent coatings with radial symmetry," Experimental Mechanics 1, 134-142 (1961).

12. Zandman, F., S.S. Redner, and E.I. Reigner, "Reinforcing effect of birefringent coatings," Experimental Mechanics 2, 55-64 (1962).

13. Phillips, J. L., "Sleeve coldworking fastener holes," AFML-TR-74-10, Vol. 1, Air Force Materials Laboratory, Wright-Patterson Air Force Base (February 1974).

14. Little, R. W., Elasticity, Prentice-Hall, Inc., Englewood Cliffs, New Jersey, 1973.

15. Taylor, G. I., "The formation and enlargement of a circular hole in a thin plastic sheet," Quar. J. Mech. and Appl. Math., Series 7, 1, 103-124 (1948).

16. Swainger, K. H., "Compatibility of stress and strain in yielded metals," Phil. Mag., Series 7, 36, 443-473 (1945).

17. Nadai, A., Theory of Flow and Fracture of Solids, McGraw-Hill Book Co., Hightstown, New Jersey, 1950.

18. Alexander, J. M., and H. Ford, "On expanding a hole from zero radius in a thin infinite plate," Proc. Royal Soc., Series A, 226, 543-561 (1954).

19. Mangasarian, O. L., "Stresses in the plastic range around a normally loaded circular hole in an infinite sheet," J. Appl. Mech. 27, 65-73 (1960).

20. Carter, A. E., and S. Hanagud, "Stress corrosion susceptibility of stress-coined fastener holes in aircraft structures," AIAA Journal 13: 7, 858-863 (1975).

21. Hsu, Y. C., and R. G. Forman, "Elastic-plastic analysis of an infinite sheet having a circular hole under pressure," J. Appl. Mech. 42: 2, 347-352 (1975).

22. Potter, R. M., and T. W. Ting, "The problem of forced fittings," Arc. Rational Mech. and Anal. 58: 1, 77-94 (1975).

23. Potter, R. M., and A. F. Grandt, Jr., "An analysis of residual stresses and displacements due to radial expansion of fastener holes," preliminary draft.